

THE ROLE OF INTERFERON GAMMA AND CTLA4 IN MELANOCYTE
AND MELANOMA BIOLOGY

A Dissertation
Submitted to
the Temple University Graduate Board

In Partial Fulfillment
of the Requirements for the Degree
DOCTOR OF PHILOSOPHY

by
Xuan Mo
December 2018

Examining Committee Members:

M. Raza Zaidi, PhD, Fels Institute for Cancer Research and Molecular Biology
Jonathan Soboloff, PhD, Medical Genetics and Molecular Biochemistry
Italo Tempera, PhD, Fels Institute for Cancer Research and Molecular Biology
Ana M. Gamero, PhD, Medical Genetics and Molecular Biochemistry
Glenn F. Rall, PhD, External Member, Fox Chase Cancer Center

ABSTRACT

Ultraviolet radiation (UVR) stimulates melanogenesis in melanocytes, primarily via release of alpha-melanocyte stimulating hormone from keratinocytes. UVR also induced an inflammatory response in the skin in which Interferon-gamma (IFN γ) cytokine plays an important orchestrating role. Here we report that recombinant IFN γ induces a temporal increase of melanogenesis in mouse melanoma cells. IFN γ elevates expression of microphthalmia-associated transcription factor (Mitf), which is the master regulator of melanogenesis by initiating transcription of melanogenic enzymes, tyrosinase (*Tyr*), tyrosinase-related protein 1 (*Tyrp1*) and dopachrome tautomerase (*Dct*). Interestingly, tyrosinase protein, but not mRNA expression, accumulated in response to IFN γ treatment and was consistent with tyrosinase activity. In addition, glycosidase digestion showed that IFN γ induced ER-resistant, fully mature tyrosinase via post-transcriptional mechanisms, rather than increased *de novo* synthesis or early processing in the ER. Most strikingly, IFN γ mediated alkalization of melanosomes by elevating Oca2 expression, which leads to facilitate melanosome maturation and sequential accumulation of mature tyrosinase. Both Jak1/Jak2 inhibitor Ruxolitinib and knockout of Stat1 mediated by CRISPR-CAS9 blocked the IFN γ -induced Mitf, tyrosinase, Oca2 expressions and melanin biosynthesis. Our data reveals that IFN γ -Jak1/2-Stat1 axis regulates melanogenesis by inducing maturation of melanosomes and accumulation of mature tyrosinase via post-translational mechanisms.

CTLA4 is a cell surface receptor on T cells that functions as an immune checkpoint molecule to enforce tolerance to cognate antigens. Anti-CTLA4 immunotherapy is highly effective at reactivating T cell responses against melanoma, which is postulated to be due to targeting CTLA4 on T cells. Here we report that CTLA4 is also highly expressed by

most human melanoma cell lines, as well as in normal human melanocytes. Interferon-gamma (IFN γ) signaling activated the expression of the human CTLA4 gene in a melanocyte and melanoma cell-specific manner. Mechanistically, IFN γ activated CTLA4 expression through JAK1/2-dependent phosphorylation of STAT1, which bound a specific gamma-activated sequence (GAS) site on the CTLA4 promoter, thereby licensing CBP/p300-mediated histone acetylation and local chromatin opening. In melanoma cell lines, elevated baseline expression relied upon constitutive activation of the MAPK pathway. Notably, RNA-seq analyses of melanoma specimens obtained from patients who had received anti-CTLA4 immunotherapy (ipilimumab) showed upregulation of an IFN γ - response gene expression signature, including CTLA4 itself, which correlated significantly with durable response.

We also show that ectopic expression of Ctla4 in mouse melanoma cells promotes tumor growth in immunocompetent mice. Ctla4-enhanced melanomagenesis is blocked in immunodeficient NSG mice. In addition, ligation of CD86 (one of Ctla4 ligands) in T cells inhibits CD8 T cells proliferation *in vitro*. Expression of Ctla4 in melanoma cells are resistant to CD8 T cell cytotoxicity *in vitro*. Our data demonstrates and highlights the novel and unrecognized functions of CTLA4 in melanoma cells that aids their survival, immunoevasion and tumorigenic capabilities.

Taken together, these findings have potential implications for the conventional and prototypical roles of the IFN γ signaling pathway and CTLA4 in tumor immunosurveillance and tumor immunoevasion. More importantly, our results raise the possibility that CTLA4 targeting on melanoma cells may contribute to the clinical immunobiology of anti-CTLA4 responses.

TABLE OF CONTENTS

	Page
ABSTRACT.....	ii
LIST OF FIGURES	ix
 CHAPTER	
1. INTRODUCTION.....	1
The Biology of IFNs	1
IFN γ -producing Cells.....	1
JAK-STAT Signaling Pathway.....	2
The Biological Function of IFN γ	3
The Role of IFN γ Promoting Antitumor Innate and Adaptive Immunity.....	3
Antitumor Effects of IFN γ	4
Administration of Recombinant IFN γ for Cancer Treatment	5
The Role of IFN γ in Cancer Immunoediting	5
Dark Side of IFN γ in Mediating Cancer Immuno evasion	6
The Biology of CTLA4.....	8
UV Irradiation-induced Skin Pigmentation	10
The Signaling Pathway of α MSH.....	10
The Biosynthesis of Tyrosinase	11
The pH of Melanosomes.....	11
Regulation of Melanosomal Ionic Equilibrium	12
Project Aims.....	13

2. INTERFERON-GAMMA REGULATES MELANOGENESIS IN	
MOUSE MELANOMA CELLS	16
Materials and Methods.....	16
Cell Culture.....	16
Cytokines Treatment.....	16
Quantitative Real-time PCR	17
Ruxolitinib Treatment.....	18
Melanin Content Assay.....	18
Melanosomal pH Measurement	18
Tyrosinase Activity Assay	19
Glycosidase Digestion	19
Cycloheximide Pulse-chase Assay	20
Western blotting.....	20
CRISPR-Cas9 Mediated Knockout of Stat1 and Stat3	21
Statistical Analysis.....	21
Results	22
Recombinant IFN γ Induces a Temporal Increase of Melanogenesis	
in Mouse Melanoma Cells	22
IFN γ Increases Mitf Expression in Melanoma Cells	25
Tyrosinase Protein Accumulates in Response to IFN γ Treatment	
and is Consistent with Tyrosinase Activity	26
Accumulation of ER-Resistant, Fully Mature and Prolonged Half-	
life of Tyrosinase in Response to IFN γ Treatment	32

IFN γ Mediates Alkalization of Melanosomes by Elevating Oca2	
Expression.....	35
Jak-Stat1 Axis Mediates IFN γ -induced Melanogenesis	40
3. INTERFERON GAMMA SIGNALING IN MELANOCYTES AND	
MELANOMA CELLS REGULATES EXPRESSION OF CTLA4.....	44
Materials and Methods.....	44
Cell Culture.....	44
IFN γ Treatment	45
Cytokines Treatment.....	45
Quantitative RT-PCR.....	45
Immunofluorescence Staining	46
Flow Cytometry	47
Ruxolitinib Treatment.....	47
Western blotting.....	48
siRNA-mediated Knockdown.....	49
Plasmid Construction	49
Luciferase Reporter Assay	50
Chromatin Immunoprecipitation (ChIP) Assays	50
CBP Inhibitor Treatment.....	51
MAPK Pathway Inhibitor Treatment.....	52
CCLE Analysis	52
RNA-seq Data of Ipilimumab-treated Melanoma Patients.....	52
Statistical Analysis.....	53

Results	54
CTLA4 is Overexpressed in Human Melanoma Cells	54
IFN γ Activates Expression of CTLA4 in Melanocytes and Melanoma Cells	58
IFN γ Induces CTLA4 Expression via STAT1-mediated Canonical Signaling	61
CTLA4 Promoter is Transcriptionally Active in Melanocytes and Melanoma Cells	65
IFN γ Signaling Recruits the Transcriptional Machinery to the CTLA4 Promoter	70
IFN γ Signaling Induces Histone Acetylation at CTLA4 Promoter	73
Overexpression of CTLA4 in Melanoma Cell Lines is Regulated by MAPK Pathway	76
IFN γ - induced Gene Signature in Melanoma Correlates with Response to Ipilimumab	79
 4. THE ROLE OF CTLA4 IN MEDIATING MELANOMA IMMUNOEVASION	 83
Materials and Methods.....	83
Cell Culture.....	83
Mouse Imaging and Quantification of Bioluminescent Signal.....	83
Histology.....	84
Lentivirus Production and Transduction.....	84
Flow Cytometry	84

CD8+ T Cell Isolation, Activation and Culture in Vitro	85
CFSE Labeling.....	85
Co-culture Assay.....	86
Results	87
Ctla4 Expression Enhances Melanomagenesis in Vivo.....	87
Ctla4-enhanced Melanomagenesis is Mediated by Inhibition of the Immune System	93
Ligation of CD86 in T Cells Inhibits CD8 T Cells Proliferation in Vitro, but not CD80 Ligation.....	96
Expression of Ctla4 in Melanoma Cells is Resistant to CD8 T Cell Cytotoxicity in Vitro.....	99
5. DISCUSSION	103
Part I: Interferon Gamma Regulates Melanogenesis in Mouse Melanoma Cells	102
Clinical Implication	106
Part II: The Role of Interferon Gamma-induced CTLA4 in Tumor Immuno evasion.....	107
Clinical Implication	107
New Mechanism of Anti-CTLA4 Immunotherapy.....	113
Biomarkers for Anti-CTLA4 Immunotherapy.....	113
Combination Therapy of MAPKi and Anti-CTLA4 Antibody.....	115
REFERENCE CITED	117

LIST OF FIGURES

Figure	Page
1. Effects of Type I and Type II Interferon on melanogenesis.....	23
2. Effects of cytokines on Mitf expression	28
3. Effects of cytokines on expression of melanogenesis-related genes and tyrosinase activity	30
4. Tyrosinase processing, maturation and degradation in B16N after IFN γ treatment	34
5. IFN γ regulates Oca2 expression and melanosomal pH	38
6. Jak1/2-Stat1 mediates IFN γ -induced melanogenesis	42
7. CTLA4 is highly overexpressed in human melanoma cells	56
8. IFN γ induces CTLA4 expression in human primary melanocytes and melanoma cell lines	59
9. IFN γ -induced CTLA4 expression is mediated by JAK-STAT1 pathway	63
10. Promoter analysis of human <i>CTLA4</i>	69
11. IFN γ /pSTAT1-mediated recruitment of CBP/p300 to the <i>CTLA4</i> promoter and accompanied acetylation of histone 3 (H3) and histone 4 (H4).....	72
12. IFN γ signaling induces histone acetylation at CTLA4 promoter	74
13. MAPK pathway regulates basal CTLA4 expression in human melanoma cells	77
14. Relationship between CTLA4 expression in melanoma cells and response to anti-CTLA4 immunotherapy	81
15. Effects of ectopic expression of Ctl4 in melanomagenesis of B2905A	90

16. Effects of ectopic expression of Ctl4 in melanomagenesis of B16N	92
17. Role of the immune system in Ctl4-enhanced melanomagenesis	94
18. The role of CD80 and CD86 in regulation of the activation and proliferation of CD8 T cells	97
19. Role of Ctl4 in inhibition of CD8 T cell cytotoxicity	100

CHAPTER 1

INTRODUCTION

The Biology of IFNs

Interferons (IFNs) are a family of cytokines that elicit important functions, including induction of antiviral and antibacterial immunity and immunomodulatory properties. IFNs were originally described as proteins that are capable of ‘interfering’ with viral replication via the activation of gene transcription programs. The IFNs include three main classes: type I IFNs, type II IFNs and type III IFNs, which are classified by distinct structure homology, genetic loci, binding receptors and downstream genes. Type I IFNs are a large subgroup containing numerous members including: IFN α , IFN β , IFN δ , IFN ϵ , IFN κ , IFN τ and IFN ω (1). All type I IFNs are clustered on the same chromosome with similar structural homologues, and binds to type I IFN receptors (2). In contrast, IFN γ is the only type II interferon. IFN γ does not share structural homology with type I IFNs and binds to type II IFN receptors (3). Type III IFNs were recently identified as IFN-like molecules with antiviral properties but are structurally different from both type I and type II IFNs (4). These cytokines also have distinct cellular signaling intermediates, compared to type I and type II IFNs.

IFN γ -producing Cells

IFN α and IFN β , the major members in type I IFNs, are ubiquitously expressed in almost all nucleated cells (5). In contrast, IFN γ is more predominantly secreted by immune lineage cells such as natural killer (NK) cells, natural killer T (NKT) cells,

activated CD8 cytotoxic T cells, CD4 T helper type I cells (Th1) and $\gamma\delta$ T cells (6). B cells, antigen presenting cells (APCs), macrophages and mucosal epithelial have been shown to produce IFN γ under certain physiological circumstances (7).

JAK-STAT Signaling Pathway

IFN γ receptors, IFN γ R1 and IFN γ R2, transduce IFN γ signaling from the extracellular environment to the cellular signaling machinery. IFN γ R1 is constitutively and ubiquitously expressed on the surface of almost all cells. In contrast, the expression of IFN γ R2 is tightly regulated, which dictates the IFN γ -responsiveness (8). The IFN γ R1 is associated with one member of the Janus activated kinase (JAK) family, JAK1, whereas IFN γ R2 is associated with JAK2. The canonical IFN γ signaling is mediated by JAK/STAT (signal transducer and activator of transcription) pathway. The receptors are rearranged and dimerized upon binding of IFN γ , followed by the autophosphorylation and activation of receptor-associated JAK1 and JAK2. The activated JAKs phosphorylate the tyrosine residue at position 701 (Tyr701) in STAT1, leading to the formation and activation of STAT1-STAT1 homodimers (9). The STAT1 homodimers translocate to nucleus and bind to the IFN- γ -activated site (GAS) element, which initiates transcription of IFN γ -stimulated genes mediated varied biological responses. The serine residue at position 727 (Ser727) in STAT1 is also phosphorylated by the activated JAKs. Such phosphorylation is important for maintaining its full transcriptional capability, but not required for the dimerization and translocation of STAT1 (10). Ser 727 phosphorylation in STAT1 is essential for recruitment of co-activators, such as histone acetyltransferases

CBP (cAMP-responsive-element-binding protein (CREB)-binding protein) and p300, to enhance transcription of IFN γ target genes (11). Among other STATs, STAT3 has been reported to be activated by IFN γ in melanocytes and melanoma cells (12, 13).

The Biological Function of IFN γ

IFN γ is well known to be an important cytokine for induction and modulation of innate and adaptive immunity to fight against viral infection, certain types of bacterial infections and tumor development. Mice deficient in IFN γ and IFN γ -receptor 1 are more susceptible to infections and tumor formation (14-16). The production of IFN γ is tightly controlled and remains localized in inflammatory tissues without systemic effects to minimize tissue damage. Also, aberrant IFN γ is associated with autoimmune diseases (17).

The Role of IFN γ in Promoting Antitumor Innate and Adaptive Immunity

IFN γ plays an important role in orchestrating antitumor immunity to control and eliminate tumor growth. IFN γ is critical for initiating, activating and maintaining anti-tumor functions of immune cells such as NK cells, CD4 T helper cells and CD8 cytotoxic cells. For instance, NK cells, considered as cytotoxic lymphocytes of the innate immune system, play a critical role in tumor surveillance. NK cells are capable of recognizing and eliminating abnormal cells lacking major histocompatibility complex (MHC) expression (18). IFN γ has demonstrated to enhance NK cell-mediated cytotoxic lysis of tumor cells (19, 20). Additionally, Takeda et al. have showed that IFN γ -secreted NK cells are

essential in eradicating lung nodules of B16 melanoma cells inoculated into syngeneic C57BL/6 mice (21).

CD4⁺ and CD8⁺ T cells are the two major types of lymphocytes in development of anti-tumor immunity. IFN γ is essential for polarizing antigen-specific CD4 Th1 cells. IFN γ -producing Th1 cells recruit macrophages and NK cells to the tumor microenvironment (22). Importantly, these cells are critical for activation of anti-tumor CD8 cytotoxic T cells in tumor microenvironments (23). Antigen-specific CD8 cytotoxic T cells are the most dominant and powerful killer of tumor cells. IFN γ enhances CD8 T cell expansion, migration and cytotoxic functions (24, 25). These findings demonstrate the importance of IFN γ in orchestrating anti-tumor immunity to limit tumor growth.

Antitumor Effects of IFN γ

IFN γ has been shown to modulate proliferation and apoptosis of tumor cells by, induce cell cycle arrest and enhance tumor antigen presentation. IFN γ induces cell cycle arrest through activation of p21 and p27 mediated by STAT1 pathway in multiple tumor cell lines (26, 27). IFN γ also induces apoptosis and cell death via increased the production of nitric oxide (NO) and reactive oxygen species (ROS) (28). Moreover, IFN γ upregulates expression of MHC class I molecules (29), expression of the peptide transporter subunits (TAPs) (30), formation of immunoproteasomes (31), and production of peptide-loaded MHC II molecules (32), all of which are critical for presenting tumor antigens and recognition by the immune system.

Administration of Recombinant IFN γ for Cancer Treatment

Considering the important roles of IFN γ in initiating anti-tumor immunity and eliminating tumor cells, administration of recombinant IFN γ had been proposed to treat cancer patients as an immunotherapy agent. A phase IIb clinical trial of metastatic melanoma showed that patients administered with IFN γ via i.v. infusion three times per week for at least 8 weeks, had minimal efficacy (33). Another randomized trial of high-risk melanoma patients received daily subcutaneous injections of IFN γ as adjuvant treatment after tumor resection and showed no efficacy in improving disease-free survival and overall survival. Unfortunately, more than 97% patients experienced toxicities (34, 35). Additionally, other clinical trials using IFN γ alone or in combination with standard care in patients with either ovarian (36), bladder or colon cancer (37), did not show any clinical benefit. The failures of IFN γ therapy in multiple types of cancer suggest that the role IFN γ in the tumor microenvironment is sophisticated with additional effects besides its anti-tumor properties. Taken together, clinical administration of IFN γ , as an immunomodulatory agent, should be thoroughly evaluated and designed.

The Role of IFN γ in Cancer Immunoediting

Cancer development is a complicated multi-step process. Transformation of normal cells is the initial step, resulting from abnormal genetic and epigenetic alterations, in combination with environmental factors. However, the growth advantage of transformed cells is not sufficient for tumor formation. To eventually establish clinically apparent bulk tumors, those transformed cells need to develop multiple strategies to

evade from immune attacks. The crosstalk and battles between transformed cells and the immune system during cancer development are called cancer immunoediting (38-41). It consists of three phases: elimination, equilibrium and escape (40). During the elimination phase, the majority of transformed cells will be eliminated by the host immune system via both innate and adaptive immunity. The ‘leftover’ transformed cells that are capable of surviving and proliferating such attacks, will reshape the immune system, which is termed ‘equilibrium’. The highly immunogenic transformed cells will be eliminated by the immune system as a result of cancer immunoediting. The poorly immunogenic transformed cells are selected, which results in aggressive proliferation and eventually dominating in tumor bulk in the presence of IFN γ in tumor microenvironment.

Dark Side of IFN γ in Mediating Cancer Immunoavoidance

IFN γ has been shown to play an anti-tumor role in the elimination and equilibrium phases of immunoediting by enhancing innate and adaptive immunity (38). Cancer immunoavoidance refers to the ability of tumor cells to escape adaptive anti-tumor immunity (42). Accumulating evidence demonstrates that IFN γ plays a pro-tumor role in the escape phase via numerous mechanisms.

Suppression of NK cell and CD8 cytotoxic T cell-mediated immune responses enable tumor cells to escape anti-tumor immunity. IFN γ activates the expression of non-classical MHC I class molecules, such as HLA-E and HLA-G to protect tumor cells from NK cell-mediated cytotoxicity via binding to inhibitory receptors expressed on NK cells to inhibit its functions (20, 43).

Another well-studied pathway that mediates cancer immunoevasion is the Programmed Cell Death 1 (PD1) pathway. PD1 is the major inhibitory receptor expressed on T cells. The ligation of PD1 to its ligands Programmed Cell Death 1 Ligand (PDL1 or PDL2) expressed on tumor cells leads to T cell dysfunction, apoptosis and exhaustion (44, 45). Disruption of this pathway with antibodies targeting either PD1 or PD-L1 restores T cell function in the tumor microenvironment, resulting in control of tumor growth. Anti-PD1 and anti-PDL1 antibody therapies have been successfully used in clinics for treatment of multiple cancer types, including melanoma, nonsquamous non-small cell lung cancer, small cell lung cancer, head and neck squamous cell carcinoma, classical Hodgkin lymphoma, primary mediastinal large B-cell lymphoma and urothelial carcinoma (42, 46-49). Interestingly, patients with higher PDL1 expression in tumors have better response and survival (50, 51). IFN γ is well-documented to induce PD-L1 and PD-L2 expression in various types of cells, including tumor cells, enabling them to escape T cell attacks. PD1:PD-L1/PD-L2 pathway is used by normal cells to minimize the possibility of chronic autoimmune inflammation by limiting activated immune response (52). However, tumor cells hijack this intrinsic mechanism to evade IFN γ -induced anti-tumor adaptive immunity.

IFN γ has shown to promote an immunosuppressive tumor microenvironment (42). For instance, indoleamine 2, 3-dioxygenase (IDO) aids tumor immune escape via suppression of anti-tumor immunity by various mechanisms (53). IFN γ has been shown to upregulate IDO expression in melanoma cells, to create an immunosuppressive microenvironment, leading to tumor growth (54, 55).

Are tumor cells able to escape the immune system by losing responsiveness to IFN γ ? Indeed, Sucker et al. have recently showed that inactivating mutations in JAK1 and JAK2 protect melanoma cells from anti-tumor immunity (56). Survival analysis on melanoma cohort from The Cancer Genome Atlas database showed that the patients with loss of either *IFNGR1*, *IFNGR2*, *IRF-1* or *JAK2* had worse survival than those without the mutations (57).

Despite IFN γ being well-recognized and well-characterized roles in orchestrating anti-tumor immunity, this evidence highlights its pro-tumorigenic role in tumor development, especially in mediating tumor immunoevasion. Thus, it is critical to further investigate and identify new immunoevasion pathways mediated by IFN γ . Considering the enormous success of checkpoint blockades in cancer treatments, we believe that identification of new targets mediating IFN γ -induced immunoevasion is certainly significant. It can potentially revolutionize cancer treatment and benefit more cancer patients from immunotherapy.

The Biology of CTLA4

Cytotoxic T lymphocyte antigen 4 (CTLA4/CD152) was originally identified as a homodimeric glycoprotein of the Ig family expressed on the surface of activated T cells and played an important role in the negative and homeostatic regulation of T cells activation and function. The germline *Ctla4*-knockout (*Ctla4*-KO) mice develop lymphoproliferative disorder, autoimmune diseases and die from fatal multi-organ tissue destruction by ~3 to 4 weeks of age (58).

T cells require two simultaneous signals from antigen presenting cells (APC) for optimal activation: T cell receptor (TCR) interaction with a peptide antigen presented by the major histocompatibility complex (MHC) class I molecules, and the engagement of T cell costimulatory molecules, e.g. CD28, with those of APCs, e.g. B7-1 and B7-2 (CD80 and CD86, respectively) (59). However, a number of coinhibitory molecules limit T cell activity in order to prevent tissue damage due to immune over-activation (59). Rapid elevation of CTLA4 on activated T cells interrupt co-stimulation signals by competitively binding to CD28 ligands, B7 with a higher affinity. The ligation of CTLA4:B7 causes T cell deactivation and anergy, leading to cell cycle arrest and inhibition of cytokine production. In addition, CTLA4 is constitutively and highly expressed on the surface of regulatory T cells, which inhibits effector T cells and APCs in tumor microenvironments (60).

Anti-CTLA4 monoclonal antibody (Ipilimumab) therapy functions by increasing the activity of the tumor antigen-specific CTLs (59). Therapeutic management of melanoma is the best characterized application of anti-CTLA4 immunotherapy, albeit with limited response rates (61). Since CTLA4 is expressed predominantly by the T cell lineage, the therapeutic action of Ipilimumab is conventionally thought to be antagonistic to either the CTLs themselves or the immunosuppressive regulatory T cell subtype (T_{reg}) which limits the activity of T cells (62). Notably, however, CTLA4 expression has also been reported in some non-lymphoid cell lineages such as tumor cells, which highlights the potential of CTLA4 as a therapeutic target beyond the T cell compartment (63, 64).

There is evidence suggesting that CTLA4 is expressed on melanoma cells and may be involved in tumor immune escape (65-68).

UV Irradiation-induced Skin Pigmentation

Melanin, the major contributor of skin pigmentation, is synthesized in lysosome-related cellular organelles called melanosomes within epidermal melanocytes.

Melanosomes are then transported to adjacent keratinocytes leading to skin pigmentation, which plays a key physiological defense against UV irradiation (69). Inflammatory cytokines secreted by keratinocytes and infiltrated lymphocytes in the skin microenvironment after UV irradiation or other dermatological damages, have been implicated in regulating proliferation, differentiation and melanogenesis of melanocytes via direct or indirect mechanisms (13, 70). The most well-known and potent inducer of melanogenesis is α -melanocyte-stimulating hormone (α MSH), which is synthesized in keratinocytes exposed to UV irradiation and secreted into epidermal microenvironments to stimulate melanogenesis of the adjacent melanocytes.

The Signaling Pathway of α MSH

α MSH activates microphthalmia-associated transcription factor (*MITF*), a key regulator of melanin production. MITF initiates transcription of melanogenic-associated enzymes including tyrosinase (*TYR*), tyrosinase related protein 1 (*TYRP1*) and DOPAchrome tautomerase (*DCT*) (71, 72). Tyrosinase catalyzes the tyrosine oxidation to dopaquinone, which is the first and rate-limiting step of melanogenesis (73). Thus, TYR is considered as the most important enzyme in melanin synthesis. TYRP1 and DCT are

involved in later steps of melanin synthesis and also play important role in regulating the melanogenic apparatus (74).

The Biosynthesis of Tyrosinase

Tyrosinase is a type I membrane-bound glycoprotein with a native molecular weight of 58 Kd (75). Nascent protein is co-translationally translocated into endoplasmic reticulum (ER) lumen, and undergoes initial asparagine-linked (N-linked) glycosylation. It is the most important post-translational modification, as inhibition of glycosylation with tunicamycin or glucosamine abolishes TYR maturation, trafficking and its enzymatic activity (76, 77). Also, mutations of this N-linked glycosylation sites cause hypopigmentation phenotype by obstructing tyrosinase maturation (78). The core-glycosylated TYR (~70kD) is transported to the cis-Golgi network (TGN) undergoing further modifications of additional mannose residues after passing the quality control in the ER. Matured TYR (~ 80kD) is then transported out of the TGN to melanosomes where melanin synthesis occurs (76). Aberrant disruption of tyrosinase trafficking also affects melanin production. Regulation of melanogenesis via alteration of tyrosinase occurs at both transcriptional and post-transcriptional levels.

The pH of Melanosomes

The pH of melanosomes is another important factor in controlling melanosome maturation and the rate of melanogenesis (79, 80). Melanosome maturation is classified by four stages with distinct morphologies and melanin content. Intraluminal fibrils are formed in melanosomes at stage I and II that are acidic and unpigmented. Pmel17 is an

important protein in formation of these fibrils. Stage III and Stage IV melanosomes have melanin deposits (81). Vacuolar (H⁺) ATPase (V-ATPase) regulates endosomal compartments including melanosomes by pumping protons into the lumen resulting in endosomal acidification (82). Treatment of cultured melanocyte and melanoma cells with bafilomycin A1, a vacuolar-type H⁺-ATPases inhibitor, increases melanosomal pH and increases melanin synthesis (83, 84). In addition, acidic melanosomal pH accelerates tyrosinase degradation (85). This suggests that the optimal pH for tyrosinase activity is nearly neutral (85, 86). Moreover, melanosomal pH controls melanosome maturation rate and regulates the processing and trafficking of tyrosinase (79, 87).

Regulation of Melanosomal Ionic Equilibrium

OCA2, *SLC45A2* and *SLC24A5* are part of the solute carrier family of membrane transporters that have been reported to regulate melanosomal pH by changing electric and ionic equilibrium. Mutations and SNPs in these genes cause different pigmentation phenotypes (72). Oculocutaneous albinism type 2 (*OCA2*) is a melanosome-specific transmembrane protein. Mutations in *OCA2* causes the most common form of albinism in humans (88, 89). Additionally, *Oca2* (pink-eyed dilution protein, *p*)-deficient mice lose fur pigmentation (90). The *SLC45A2* is also called membrane-associated transporter protein (MATP). Mutations of *SLC45A2* causes Oculocutaneous albinism type 4 (*OCA4*) (91). It has been show that *SLC45A2* serves as an H⁺/ sucrose transporter and can increase melanosomal pH (92). *SLC24A5* is Na⁺/Ca²⁺/K⁺ exchange channel has also been shown to modulate pH in melanosome (93). Mutations in *SLC24A5* are strongly associated with non-syndromic oculocutaneous albinism in human (94)

Project Aims

In order to uncover the molecular mechanisms underlying ultraviolet radiation (UVR)-induced melanomagenesis, we previously investigated the genomic response of melanocytes to UVR *in vivo* (95). We showed that in addition to damaging DNA, UVR alters gene expression in exposed melanocytes that drives their interactions with elements of the microenvironment to remodel damaged skin and escape destruction. These results implicated a UVR-induced pro-tumorigenic inflammatory cascade, whereby UVB directly upregulated melanocytic expression of ligands to the chemokine receptor CCR2, which recruited macrophages into the neonatal skin microenvironment. A subset of these macrophages produced IFN γ , which elicited a positive feedback type activation of expression in stimulated melanocytes of a putative “survival signature,” consisting of genes involved in immunoevasive mechanisms (95).

Intriguingly, CTLA4 was the highest upregulated gene prominently clustered among this IFN γ -induced gene expression signature (95), prompting us to hypothesize that CTLA4 is a novel direct downstream target gene regulated by the IFN γ -induced signaling pathway in melanocytes and melanoma cells.

What could be the possible role of CTLA4 expression in melanocytes and melanoma cells? We asked whether melanocytic CTLA4 expression can protect these cells from T cell-mediated cytotoxicity. CTLA4 is a key negative regulator of anti-tumor activity of cytotoxic T-lymphocytes (CTLs) via suppression of CD28-B7 costimulation, contributing to T-cell tolerance and anergy. We posited that CTLA4 expressed on melanocytic cells might directly inhibit CTLs via interaction with the B7 ligands

expressed on CD8 T cells, which would lead to melanocyte/melanoma cell-mediated CTL inactivation and anergy leading to immunoevasion. Thus, we hypothesize that CTLA4 expression in melanocytes and melanoma cells has a novel immunoevasive function that enhances tumorigenesis.

The most accepted mechanism of anti-CTLA4 monoclonal antibody therapy is blockade of CTLA4 ligation which increases the activity of the tumor antigen-specific CTLs. Corollary to this potential novel CTLA4 function in melanoma cells, a provocative possibility is that the melanoma cells themselves may also be the targets of the anti-CTLA4 immunotherapy. If this turns out to be the case, then it is plausible that CTLA4 expression on melanoma cells may be a predictive biomarker for response to Ipilimumab, which currently shows dismal response rates. Potentially, the results will be informative with high clinical relevance for single agent as well as combination immunotherapy regimens.

α MSH is the most well-known hyperpigmentation inducer in response to UV irradiation. Considering the recruitment of IFN γ -producing macrophages to neonatal mouse skin after UVB irradiation, we asked whether IFN γ induced melanin synthesis in melanocytes and melanoma cells. In our preliminary experiments, we observed an increasing melanin synthesis in mouse melanoma cells cultured with mouse IFN γ *in vitro*. Therefore, we hypothesize that IFN γ signaling regulates melanogenesis.

We addressed these questions through the following aims:

Aim 1. To assess the effect of IFN γ in melanogenesis, and its potential molecular mechanism

Aim 2. To determine whether CTLA4 is a downstream gene of IFN γ signaling pathway

Aim 3. To delineate the role of IFN γ -induced CTLA4 expression in melanoma immunoevasion

CHAPTER 2
INTERFERON-GAMMA REGULATES MELANOGENESIS IN MOUSE
MELANOMA CELLS

Materials and Methods

Cell Culture

Mouse melanoma cell lines B16 and B16N (a subclone cell line of B16 generated at National Cancer Institute) were cultured in Dulbecco's Modified Eagle Medium (DMEM) supplemented with 5-10% fetal bovine serum (FBS), L-alanyl-L-Glutamine (2 mM) and Gentamycin (50 µg/ml) at 5% CO₂.

Cytokines Treatment

Mouse recombinant IFN-gamma (with BSA carrier) was purchased from Cell Signaling Technology (catalog #5222). The concentration used was 10 ng/ml, otherwise the concentrations are indicated within the figure. According to MSDS provided by the manufacturer, the bioactivity was determined in a virus protection assay. The ED₅₀ of each lot is between 30-150 pg/ml. The conversion of 10ng/ml to biological activity is 67 U/ml-330 U/ml.

Mouse IFN alpha 2 recombinant protein was purchased from Affymetrix eBioscience (catalog #14-8312). The concentration used was 10 ng/ml, otherwise the concentrations are indicated within the figure. The conversion of 10 ng/ml to biological activity is 100 U/ml according to the MSDS provided by the manufacturer.

α MSH was purchased from SIGMA-ALDRICH (catalog #581-05-5). The concentration we used 10 nM.

Quantitative Real-time PCR

Total cellular RNA was extracted using the Trizol method (Life Technologies) and RNeasy Mini Kit (QIAGEN). RNA was used to generate cDNA by GoTaq 2-step RT system (QIAGEN). RT-qPCR analysis of mouse *Tyr*, *Tyrp1*, *Dct*, *Mitf-M*, *Oca2* and *18s rRNA* (reference gene) were measured by ABI StepOnePlus PCR system. The $\Delta\Delta C_T$ method was used to calculate relative expression levels. The sequence of primers for amplification of different genes were: *Mitf-M* (Forward 5'-GCCTTGTTTATGGTGCCTTC-3', Reverse 5'-GTCCTCCTCCCTCTACTTTCTGT-3'); *Dct* (Forward 5'-CTTCCTAACCGCAGAGCAAC-3', Reverse 5'-CAGGTAGGAGCATGCTAGGC-3'); *Tyrp1* (Forward 5'-TCTCTTCGGGCAATTAACAG-3', Reverse: 5'-GGGGAGGACGTTGTAAGATT-3'); *Oca2* (Forward 5'-GGAGGTAATGGGACACTTATCG-3', Reverse: 5'-ACATGAGCATCACAGGGAAG-3'); *Slc45a2* (Forward 5'-GGAGTTGAGGTCGGATGTTG-3', Reverse 5'-GCCAAAGAGCAAATATCCCATG-3'); *18s rRNA* (Forward 5'-CTTAGAGGGACAAGTGGCG-3', Reverse 5'-ACGCTGAGCCAGTCAGTGTA-3').

Ruxolitinib Treatment

B16 cells were pretreated with ruxolitinib (2 μ M, Selleckchem) for 4 h and cultured in the presence or absence of indicated cytokines for 2 d. The cells were collected to assess melanin content after cultured with regular medium for another 2 d.

Melanin Content Assay

B16 and B16N cells were collected after treatment of different cytokines for indicated time points. The pellets were lysed in NP-40 lysis buffer with protease inhibitors. Melanin was separated from lysates by centrifugation for 15 min then dissolved in 1 M NaOH at 100 °C. The melanin content was determined by measuring the absorbance of the dissolved melanin containing solution at 490nm. Synthesis melanin standards (SIGMA) curve was also generated to calculate the melanin contents of each sample. Protein concentrations of each sample were measured with the Bio-Rad Protein Assay following manufacturer's protocol. The melanin content was obtained by normalization of melanin amount to protein input.

Melanosomal pH Measurement

B16 and B16N cells cultured on cover slips were treated with indicated cytokines for 4 d then incubated with LysoSensor Green DND-189 (Invitrogen) at a final concentration at 1 μ M in regular DMEM medium at 37 °C for 1 h. Cells were washed twice before fixed with 4% fresh paraformaldehyde in PBS and permeabilized with 0.01% Triton X-100, 22.52 mg/ml glycine and 1% BSA in PBS for 30 min, following of incubation of anti-PEP1 antibody (1:500) or anti-Gp100 antibody (EP4863(2), 1:200,

Abcam) at room temperature for 2 h. Cells were then incubated with Alexa Fluor 594–conjugated goat anti-rabbit secondary antibody (1:400, Life Technology) for 30 min at room temperature. After washing thoroughly, the cover slips were mounted with VECTASHIELD mounting medium with DAPI (Vector Laboratories Inc) and imaged with Leica TCS SP8 Confocal microscope at the specified magnification at the same day.

Tyrosinase Activity Assay

The tyrosinase activity was determined by measuring the rate of oxidation of 3, 4-Dihydroxy-L-phenylalanine (L-DOPA, SIGMA). B16N cells were cultured with indicated cytokines for 4 d then collected cell pellets. The pellets was washed with ice-cold PBS, then lysed in 0.1 M phosphate buffer (pH 6.8) containing 1% Triton X-100 and 1x Halt Protease inhibitor cocktail. The lysates were centrifuged at 13,000 g at 4 °C for 10 min. The tyrosinase containing lysates were incubated with the same amount of 3 mg/ml L-DOPA solutions that were dissolved in 0.1 M phosphate buffer (pH 6.8) at 37 °C. The absorbance at 490nm was measured for at least 2 h and the tyrosinase activity was calculated as OD490 absorbance value/min/mg of protein of lysate used.

Glycosidase Digestion

B16N cells were cultured in medium containing indicated cytokines for 4 d and collected for lysates. We treated 20 µg of protein lysates with either Endo H (New England Biolabs) or PNGase F for 1 h at 37 °C, followed standard protocol provided by the manufacturer. The same amount of protein digestion products were subjected to Western blot analysis by using 10% Mini-Protean TGX gel system (Bio-Rad) and

probing with a-PEP7h' antibody (1:5000) or GAPDH-HRP (D16H11, 1:5000, Cell Signaling Technology).

Cycloheximide Pulse-chase Assay

For cycloheximide chase analysis, B16N cells was treated with indicated cytokines for 4 d, then were cultured with medium containing 50 μ M of cycloheximide (Sigma) for 3 h, 6 h. Protein lysates were collected for analysis of tyrosinase abundance by Western blot.

Western blotting

Cells were lysed in Pierce RIPA buffer (Thermo Scientific) containing 1x Halt protease inhibitor cocktail (100X, Thermo Scientific) and 1x Halt phosphatase inhibitor cocktail (100X, Thermo Scientific) and the protein concentration was measured with the Bio-Rad Protein Assay following manufacturer's protocol. The same amounts of protein extracts were subjected to polyacrylamide gel electrophoresis using the 4%-20% Mini-Protean TGX gel system (Bio-Rad), transferred to PVDF (0.45 μ m pore size, Millipore) membranes, and immunoblotted using antibodies that specifically recognize Tyrosinase (a-PEP7h', 1:5000), Tyrp1 (a-PEP1, 1:5000), Dct (a-PEP8, 1:5000) and Mitf (D5G7V, 1:1000, Cell Signaling Technology), p-Stat2 (a gift from Dr. Ana M. Gamero), p-Creb (87G3, 1:1000, Cell Signaling Technology), Creb (48H2, 1:1000, Cell Signaling Technology), p-Erk (D13.14.4E, 1:2000, Cell Signaling Technology), Erk (137F5, 1:1000, Cell Signaling Technology), GAPDH-HRP (D16H11, 1:1000, Cell Signaling Technology), The secondary antibodies used for detection were HRP-conjugated goat

anti-mouse and goat anti-rabbit IgG (1:5000, Thermo Scientific). The blots were incubated with Luminata Western HRP substrate (Millipore) for 5 min. Band intensities of Tiff images were quantified by using Image J software.

CRISPR-Cas9 Mediated Knockout of Stat1 and Stat3

We designed two gRNAs targeting different exons for *Stat1* and *Stat3* locus by online CRISPR Design Tool. Plasmid construction and molecular cloning were done by following the previously published protocol (96).

Statistical Analysis

All graphs were generated by GraphPad Prism. To analyze statistical difference between two groups, two-tailed unpaired Student's t-test was used. For gene expression correlation analyses, the Pearson correlation coefficient was used in GraphPad Prism. P value <0.05 was considered as statistically significant.

Results

Recombinant IFN γ Induces a Temporal Increase of Melanogenesis in Mouse Melanoma Cells

To evaluate effect of IFN γ in melanin synthesis, mouse melanoma B16 and B16N cells were cultured continuously in medium containing either IFN γ (10 ng/ml), type I interferon IFN α 2 (10 ng/ml), or α MSH (10 nM) as a positive control for indicated time points (Fig. 1A), and then total melanin content was assessed. Treatment of B16 and B16N cells with IFN γ for at least 3 days profoundly increased melanin synthesis visualized in the cell pellets (Fig. 1B, C) and measured in the melanin content assay (Fig. 1D, E). However, type I interferon IFN α 2, failed to increase melanin content in these two cell lines. As expected, treatment of α MSH elicited a rapid upregulation of melanin synthesis, as early as 1 d (Fig. 1B, C) with a greater production of melanin (Fig. 1D, E) than IFN γ treatment. This suggests that IFN γ increases melanogenesis via different mechanisms compared to α MSH.

To evaluate if continuous IFN γ signaling is necessary for inducing melanin synthesis, we treated B16 cells with IFN γ for shorter time periods (as indicated in Fig. 1F), then measured melanin content at 4 d. Surprisingly, a visible elevation in melanin content was apparent in B16 cells by exposing to IFN γ as short as 1 d (Fig. 1G) demonstrating the potency of IFN γ in inducing melanin synthesis without changing the proliferation. Therefore, IFN γ -induced melanogenesis is strongly time-dependent rather than requiring continuous exposure via an indirect modulation of cellular processes.

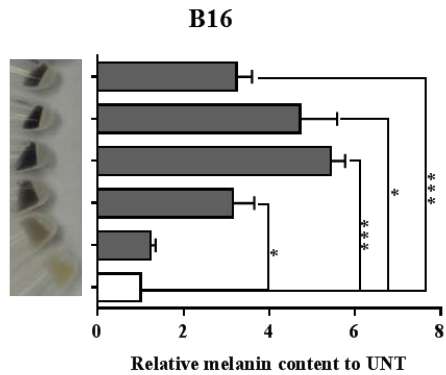
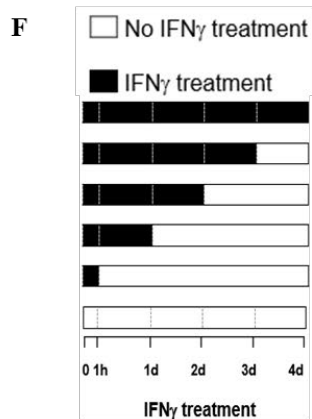
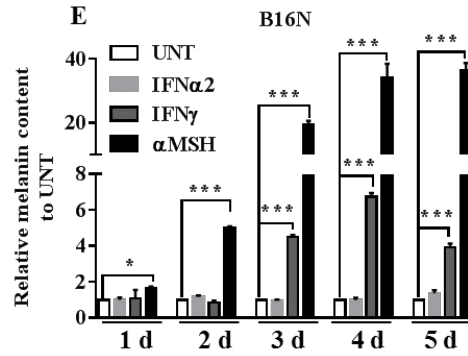
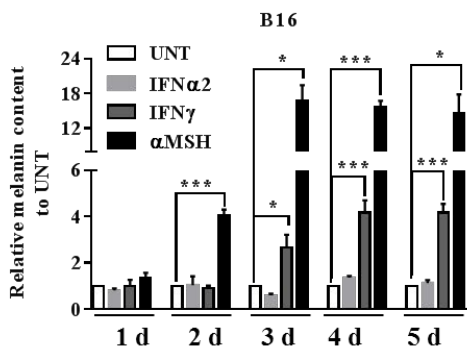
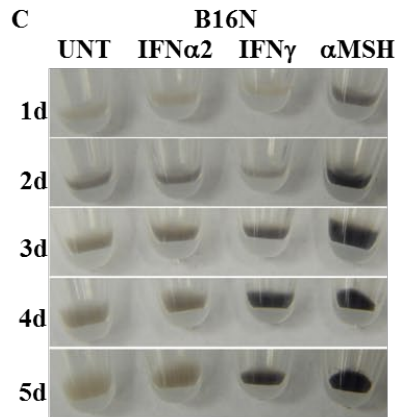
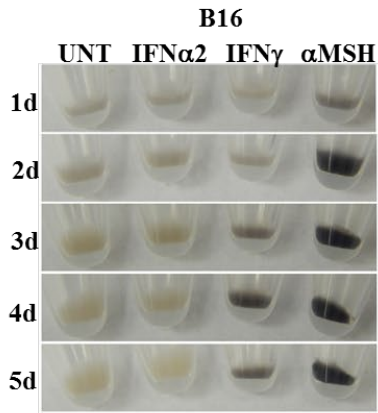


Figure 1. Effects of Type I and Type II Interferon on melanogenesis. **A**, Schematic description of cytokine treatment schedule. **B, C** Photos of cell pellets of B16 and B16N collected after different cytokine treatments for indicated time points. Images are representative of at least 3 independent experiments. **D, E** Quantification of melanin content in melanoma cells treated with or without these cytokines. The melanin content of each samples are normalized with protein concentrations. **F**, Left panel, schematic of IFN γ treatment schedule; Middle panel, representative image of B16 cells corresponding to indicated treatments in left panel; Right panel, melanin content quantification. All graphed data are presented as the mean \pm SEM of three biological replicates, relative to UNT group of each indicated time points. *P<0.05; **P<0.01; ***P<0.001.

IFN γ Increases Mitf Expression in Melanoma Cells

Mitf acts as a master regulator of melanogenesis, but is also important for the survival of pigmented cells (97). Mitf has multiple distinct isoforms derived from unique alternative-splicing. Mitf-M isoform exclusively expressed in melanocyte/melanoma cells (98). To exam the effects of cytokines on Mitf-M expression, we measured mRNA expression and protein level by qRT-PCR and Western blot, respectively. IFN γ treatment decreased the mRNA of *Mitf* after 2 h in B16N cells (Fig. 2A), and it was consistent with a rapid decreasing Mitf protein expression less than 24 h (Fig. 2B, line 1, 6-8). Activation of Cre-binding protein (Creb) by phosphorylation is important for initiating and maintaining expression of *Mitf* (99). In contrast to fast activation of Creb by α MSH treatment, IFN γ induced a decrease in the amount of p-Creb and may explain the rapid degradation of Mitf (Fig. 2B, lane1, 6-8). Surprisingly, we observed increasing mRNA expression of Mitf (Fig. 2A), and protein levels by treatment of IFN γ for 1 d (Fig. 2B, lane1, 9; Fig. 2C, lane 1, 3, 5, 7). This suggests reduction of p-Creb mediated by IFN γ is transient. The activation of extracellular regulated protein kinase (Erk) has shown to phosphorylate Mitf, enhancing its transcriptional abilities. Indeed, accumulation of Erk phosphorylation form (higher molecular weight band) was observed after IFN γ treatment. This indicates activation of Erk by IFN γ treatment is partially responsible for upregulation of Mitf after treatment of IFN γ for 1 d (Fig. 2B, lane 1, 9). However, the prolonged treatment of IFN γ and α MSH (4 d) reduced Mitf expression when melanin synthesis occurred (Fig. 2C, lane 9-16). It has been shown that Mitf expression balances differentiation and survival in melanocytes and melanoma cells. Low levels of Mitf is

essential for survival of melanoma cells, whereas high expression drive melanocyte differentiation (100). Additionally, it has been reported that production of melanin is toxic to melanoma cell growth (101). This indicates that melanoma cells overcome the cytotoxic effect of increasing melanin synthesis via downregulation of Mitf.

Taken together, IFN γ treatment increases Mitf expression after 1 d, which potentially mediates melanin synthesis.

Tyrosinase Protein Accumulates in Response to IFN γ Treatment and is Consistent with Tyrosinase Activity

To evaluate whether transcription of *Tyr*, *Tyrp1* and *Dct* correlate with upregulation of Mitf expression, the mRNA levels were determined in B16N cells treated with IFN γ for either 2 h, 1 d, 2 d or 4 d. Interestingly, none of the *Tyr*, *Tyrp1*, *Dct* transcripts were up-regulated by treatment of IFN γ at any time point tested (Fig. 3A, B, C), despite increased Mitf protein after 1d treatment with IFN γ (Fig. 2B). Protein levels of Tyr and Tyrp1 decreased by treatment of IFN γ for 4-24h (Fig. 3D), as melanin production did not increase during this time. Unexpectedly, only the Tyr protein level significantly increased at 4 d by treatment of IFN γ , but not levels of Tyrp1 and Dct (Fig. 3E, F, G). The increasing Tyr protein level was in accordance with increasing melanin content. We confirmed this by measuring tyrosinase activity, which is a more sensitive indicator of melanogenesis than measurement of total melanin content (102). Treatment of B16N with IFN γ for 4 d profoundly increased Tyr activity (Fig. 3H) and closely correlated with melanin content and Tyr protein level. Therefore, IFN γ -induced

melanogenesis is not dependent on upregulation of Mitf or mRNA level of *Tyr*, but due to post-transcriptional modulations that account for the changes of Tyr protein abundance.

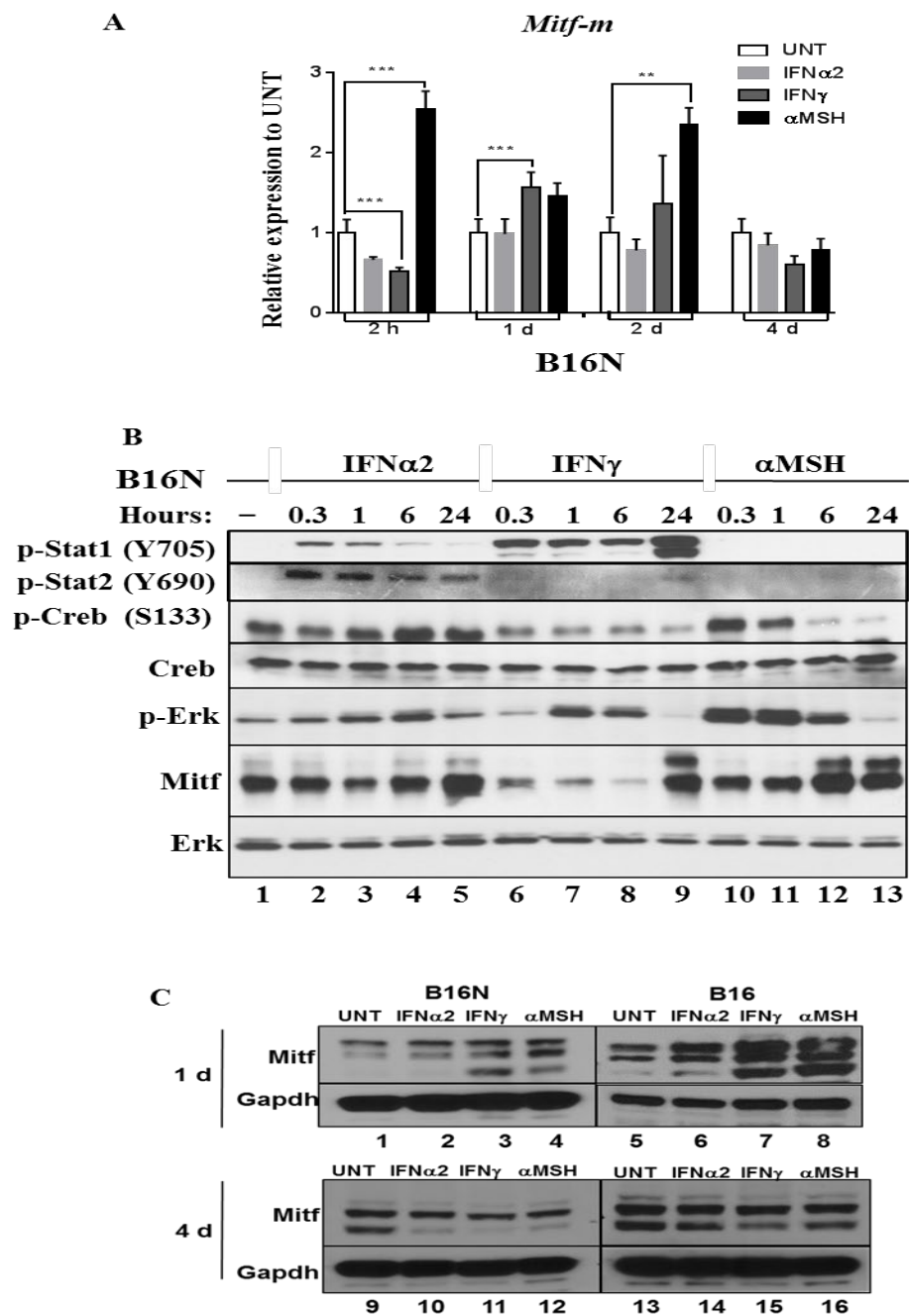


Figure 2. Effects of cytokines on *Mitf* expression. **A**, qRT-PCR analysis of mRNA expression of *Mitf-M* in B16N cells cultured in the presence or absence of cytokines for indicated time points. Data is presented as mean \pm SEM of three biological replicates. **B**,

Western blot analysis of expressions of p-Stat1 (Y705), p-Stat2 (Y690), p-Creb (S133), Creb, p-Erk, Erk and Mitf in B16N cells treated with cytokines for indicated time points. C, Western blot analysis of expressions of Mitf and Gapdh in B16N and B16 cells treated with indicated cytokines for either 1 d or 4 d. Immunoblotting images are representative of 2 independent experiments. **P<0.01; ***P<0.01.

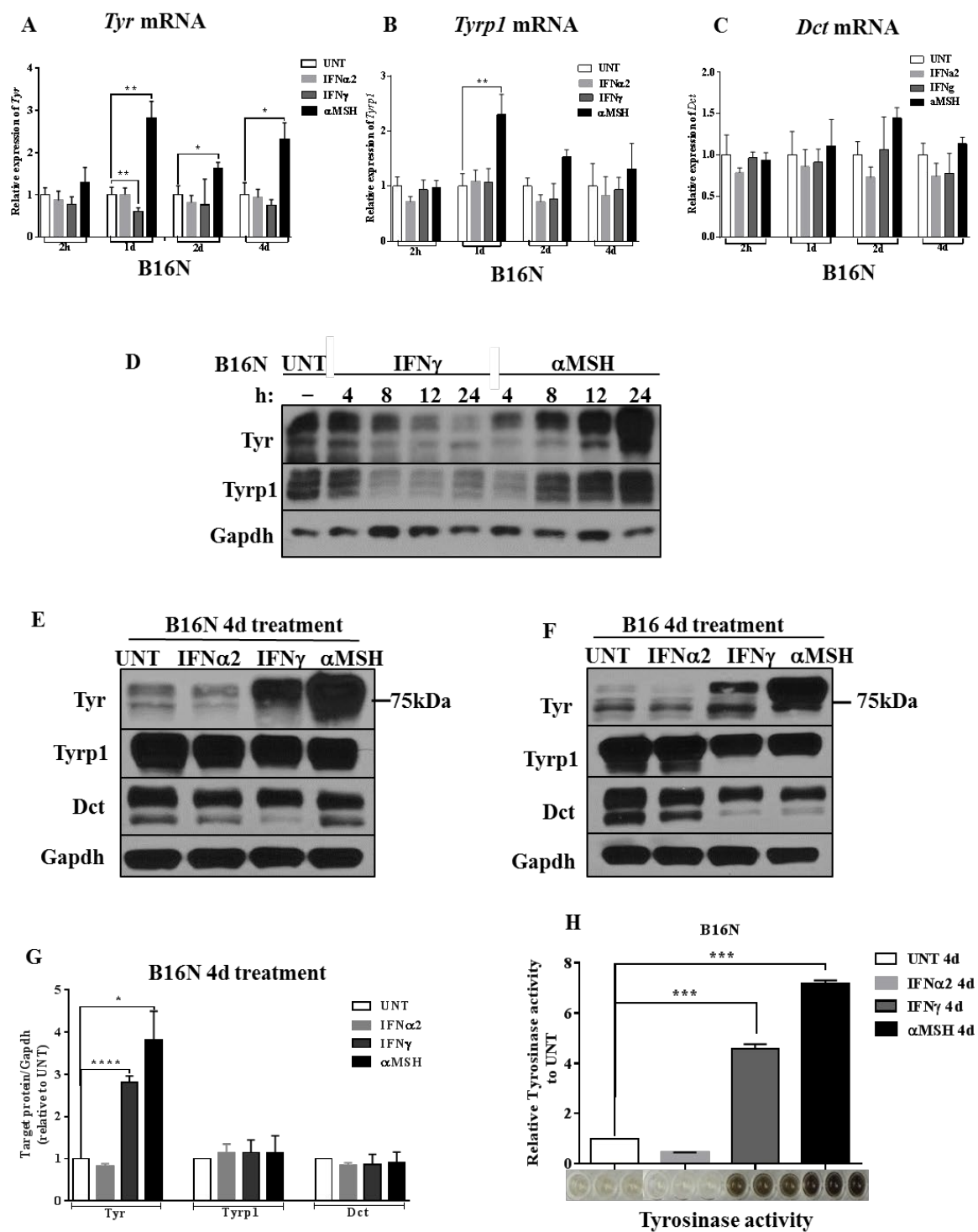


Figure 3. Effects of cytokines on expression of melanogenesis-related genes and tyrosinase activity. A-C, qRT-PCR analysis of mRNA expression of *Tyr*, *Tyrp1* and *Dct*

in B16N cells cultured in the presence or absence of cytokines for indicated time points. Data is presented as mean±SEM of three biological replicates. **D**, Western blot analysis of expressions of Tyr and Tyrp1 in B16N cells treated with or without either IFN γ or α MSH for indicated time points. **E-F**, Western blot analysis of expressions of Tyr, Tyrp1 and Dct in B16N (**E**) and B16 (**F**) cells treated with indicated cytokines for 4 d. **G**, Quantification of protein abundances in **E**, based on band intensities of Tiff images were quantified by Image J. Gapdh was used as a loading control to calculate the fold changes, normalized to control group. The histogram represents as mean±SEM of three independent experiments. Immunoblotting images are representative of 2 independent experiments in **F**. **H**, Tyrosinase activity in B16N cells in response to 4 d treatment of cytokines by measuring the oxidation of L-DOPA for 2 h. The histogram represents as mean±SEM of three biological samples, relative to UNT group. The representative images of color of the L-DOPA conversion for 2 h are shown at the bottom. *P<0.05; **P<0.01; ***P<0.001; ****P<0.0001.

Accumulation of ER-Resistant, Fully Mature and Prolonged Half-life of Tyrosinase in Response to IFN γ Treatment

Western blot of Tyr showed that IFN γ treatment for 4 d led to a remarkable increase in abundance of mature Tyr that appeared mostly as a ~75-80 KDa band (Fig. 3E, F). The elevation of mature Tyr by IFN γ was potentially mediated by the post-translational mechanisms. Thus, we utilized glycosidase digestion to evaluate the post-translational modification of Tyr following cytokine treatments. Endoglycosidase H (Endo H) cleaves early, less processed mannose added to Tyr in the ER, as Endo H-sensitive (immature form) Tyr, but not those exit the TGN, which are known as Endo H-resistant (fully mature form) Tyr (103). Another enzyme used for glycosidase digestion, N-Glycosidase F (PNGase F) cleaves all N-linked oligosaccharides from glycoproteins. The glycosidase digestion revealed that the majority of tyrosinase extracted from IFN γ -treated B16N was the Endo H-resistant, Golgi processed, fully mature (Fig. 4A, ~75kD band in lane 6), whereas, tyrosinase in either untreated or IFN α 2-treated B16N was largely Endo H-sensitive, ER-retained immature protein (Fig. 4A, ~58kD bands in line 4, 5 respectively). In addition, PNGase F digestion showed that the total amount of de-glycosylated Tyr (~58kD) significantly increases after IFN γ treatment (Fig. 4A, lanes 7-9). Next, we assessed the degradation rate of Tyr by cycloheximide pulse-chase assay in B16N cell treated with different cytokines for 4 d. Cycloheximide pulse-chase assay showed that half-life of Tyr in untreated cells was around 3 h to 4 h (Fig. 4B, lane 1-3; Fig. 4C), as reported before (77, 104). The half-life of Tyr was significantly prolonged in IFN γ -treated cells (Fig. 4B, lane 7-9; Fig. 4C). In contrast, pre-treatment of IFN α 2 did not alter the degradation rate of Tyr (Fig. 4B, lane 4-6; Fig. 4C). Intriguingly, there was

less ER-sensitive Tyr in IFN γ -treated B16N, suggesting it did not increase *de novo* synthesis of Tyr or early processing in the ER, which was consistent with the mRNA expression of *Tyr*. Therefore, our findings suggest that IFN γ enhances the processing and trafficking of tyrosinase, which results in accumulation of mature form Tyr with a prolonged half-life, leading to increasing melanin synthesis.

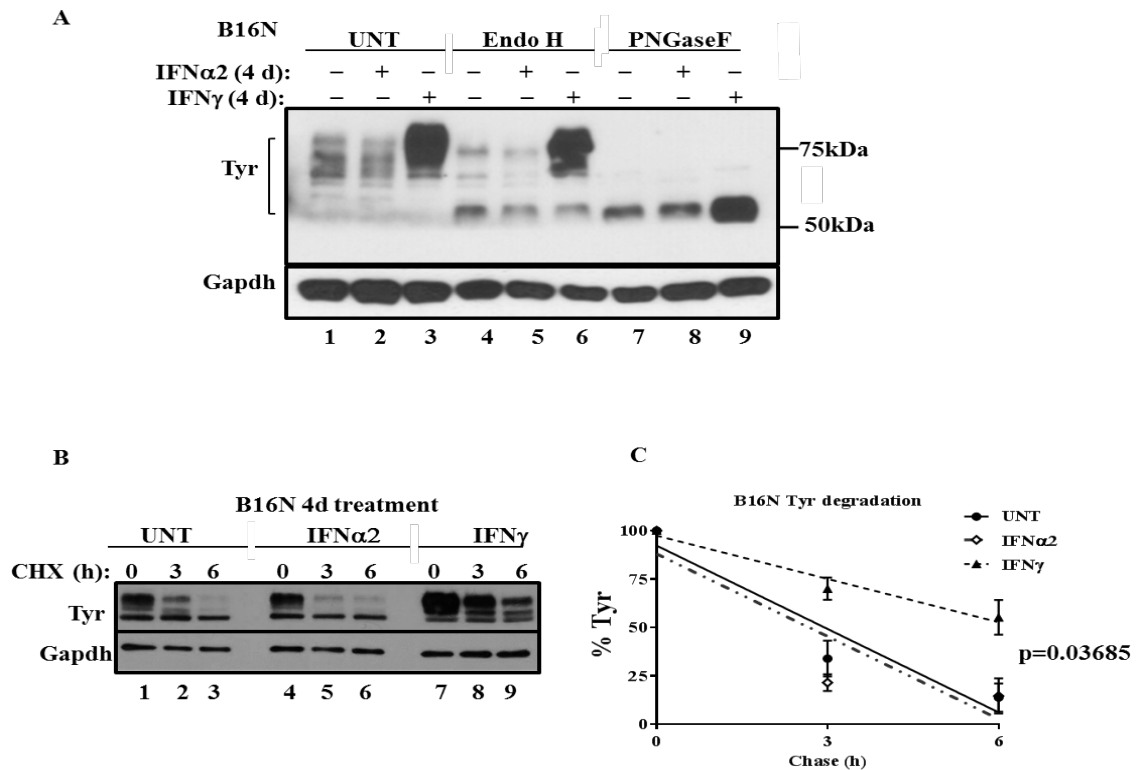
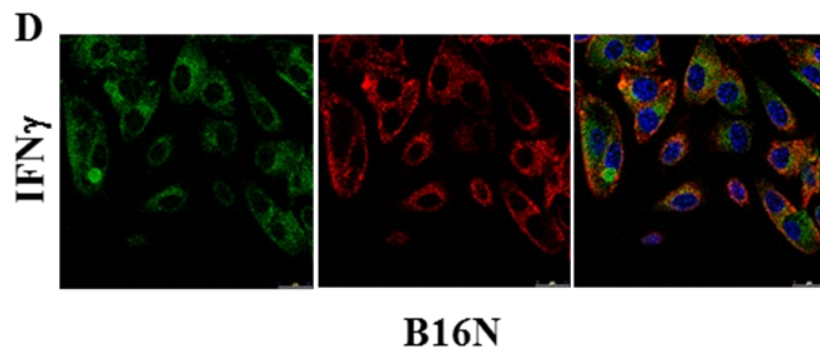
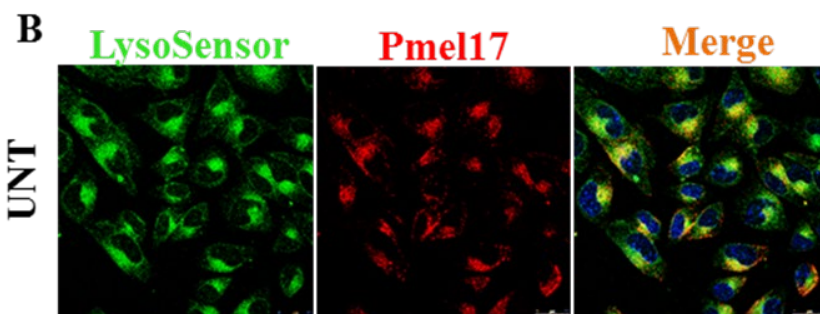
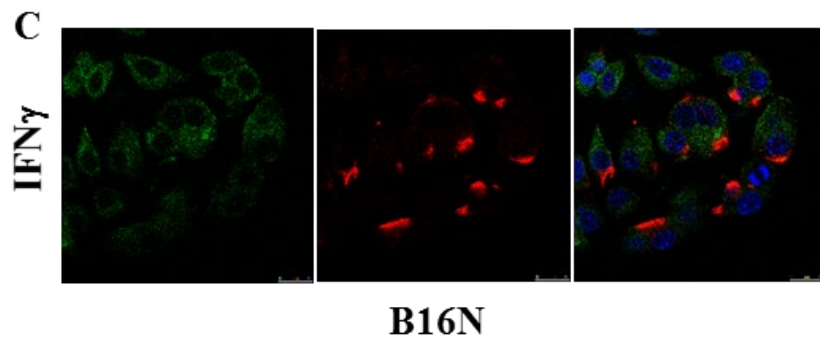
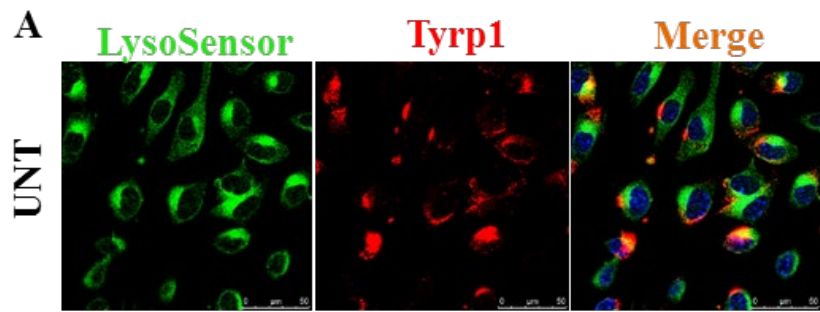


Figure 4. Tyrosinase processing, maturation and degradation in B16N after IFN γ treatment. **A**, Cell lysates obtained from B16N cells in the presence or absence of either IFN α 2 or IFN γ for 4 d were subsequently incubated with Endo H or PNGase F. Western blot of Tyr and Gapdh to access the glycosidase digestion. Tyrosinase is range from 58 to 80 KDa. **B**, B16N cells were cultured with IFN α 2 or IFN γ for 4 d, then treated with 50uM cycloheximide for either 3 h or 6 h, in following of Western blot analysis of Tyr abundance. Immunoblotting images are representative of 3 independent experiments. **C**, Relative band densities of tyrosinase within chasing time of 6 h in B. The curve represents as mean \pm SEM of three independent experiments. Y axis, the percentage of tyrosinase is relative to the starting point and normalized with Gapdh. Linear regression and statistics are performed in Prism 6.

IFN γ Mediates Alkalization of Melanosomes by Elevating Oca2 Expression

Neutral pH in melanosome is essential for maintaining and regulating tyrosinase activity (105, 106). In addition, Melanosomal pH has been shown to regulate the processing and trafficking of tyrosinase (87). Neutralization of intracellular pH resulted in enhancing trafficking of tyrosinase to stage II melanosomes by treatment of proton pump inhibitors (87). To assess the effect of IFN γ in regulating melanosomal pH, we stained B16N with LysoSensor-Green dye that became more fluorescent in acidic organelles, and co-stained with melanosome markers either Tyrp1 (red) or Pmel17 (red). The melanosomal protein Pmel17 serves as the structural foundation of fibrils in stage I and II melanosomes that are acidic and unpigmented, whereas Tyrp1 is only transported to in stage III and stage IV pigment producing mature melanosomes (81). Indeed, the melanosomes localized at the distal portion of the dendrites were positive for Tyrp1 and did not stain with LysoSensor (Fig. 5A), confirming that the lumen of mature melanosomes is not acidic. In contrast, the stage I and II melanosomes positive for Pmel17 were also co-stained with LysoSensor (in yellow), which suggests the early stage of melanosomes are acid (Fig. 5B). B16N cells lost co-localization of melanosome markers with LysoSensor (decrease in yellow fluorescence), especially in stage I and stage II melanosomes labeled with Pmel17 (Fig. 5C, D) upon IFN γ treatment. It reveals that melanosomes are dramatically alkalized upon IFN γ treatment, especially those early stages, immature melanosomes. To evaluate if IFN γ -downregulated V-ATPases explained alkalization, we analyzed RNAseq data collected from B16 and B16N cells treated with or without IFN γ for 2 d. Surprisingly, IFN γ upregulated a majority V-

ATPases. Thus, we tested whether the expression of ion channels shown to regulate pH in melanosomes were regulated by IFN γ . The expression of *Slc45a2* (Fig.5D) and *Slc24a5* (data not shown) were not increased by IFN γ . However, the expression of *Oca2* was upregulated by treatment of IFN γ for 2 d IFN γ treatment before increasing melanin synthesis occurred (Fig. 5C). *Oca2* is critical for melanin synthesis by alkalizing melanosomal pH and modulating trafficking and maturation of tyrosinase. Bellono *et al.* used direct patch-clamp of skin to demonstrate OCA2 is a chloride-selective anion channel that regulates melanin synthesis by increasing melanosomal pH (107). In addition, ectopic expression of *Oca2* in *Oca2*-null murine melanocyte rescues melanin production and induces higher level of mature Tyr protein (108). Most importantly, overexpression of *Oca2* in B16-F1 cells with intact melanogenic machinery elevates melanin production by ~75% (109). Upregulation of *Oca2* by IFN γ treatment mediated the alkalization of melanosomes. Alkalization of early stages of melanosomes might facilitate trafficking of tyrosinase to melanosomes, resulted in increasing melanin production. Interestingly, we only observed increasing *Oca2* expression following upregulation of *Mitf*. This suggested *Mitf* might be a transcriptional factor regulating of *Oca2* transcription. Indeed, we found that *OCA2* expression was closely correlated with *MITF* and *TYR* expression, but not *DCT* expression (Fig. 5E-G) by analyzing microarray data of 62 melanoma cell lines in CCLE database.



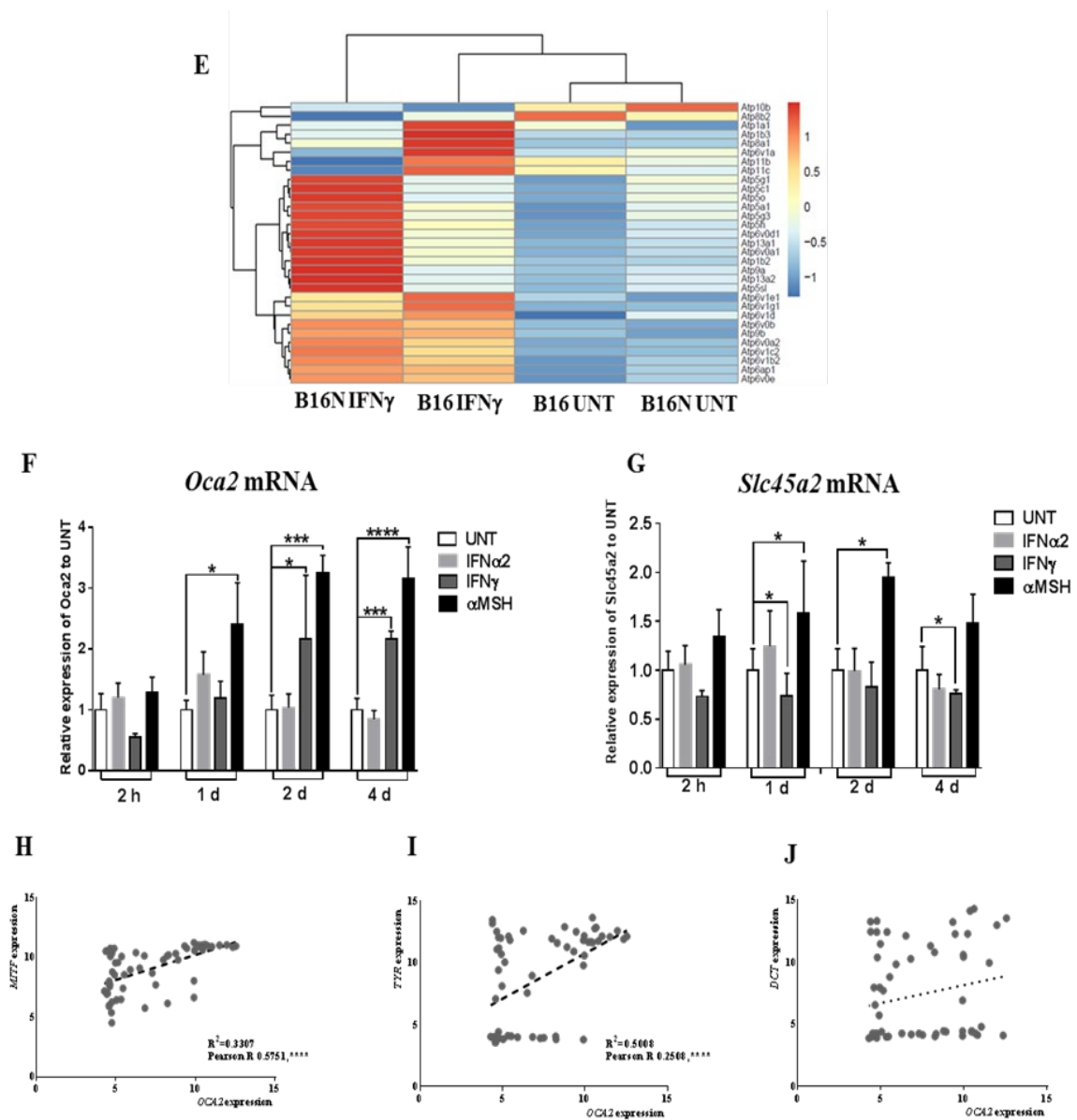


Figure 5. IFN γ regulates *Oca2* expression and melanosomal pH. A-D, Confocal photomicrographs of lysoSensor (Green) and Tyrp1/Pmel17 immunostaining (Red) in B16N treated with or without IFN γ . Blue, DAPI. Scale bar is shown in images. E, RNAseq analysis of B16 and B16N cells treated with or without IFN γ for 2 d. The genes of vacuolar-type H⁺-ATPase family that were significantly changed in response to IFN γ

treatment were used to generate the heatmap. **F-G**, qRT-PCR analysis of mRNA expression of *Oca2* and *Slc45a2* in B16N cells cultured in the presence or absence of cytokines for indicated time. The histogram data are presented as mean±SEM of three biological replicates. **H-J**, Correlation of *CTLA4* expression with *Mitf*, *Tyr* and *Dct* expression. X, Y axis, FPKM values of indicated genes. Spearman correlation coefficients (R2), Pearson correlation R, and P values are listed. *P < 0.05; ***P < 0.001; ****P < 0.0001.

Jak-Stat1 Axis Mediates IFN γ -induced Melanogenesis

JAK-STAT cascade is the major mediator for IFN γ -dependent signaling. However, accumulating evidence suggests that there are several other IFN γ -regulated signaling pathways operating independently of the JAK-STAT pathway to maximize the IFN γ effect (3). To delineate the signaling cascades that is responsible for IFN γ -induced melanogenesis, we treated B16 cells with IFN γ in the presence or absence of Jak1/2 inhibitor, ruxolitinib. Ruxolitinib treatment completely blocked IFN γ -induced pigmentation but did not affect the α MSH-induced melanogenesis (Fig. 6A). Stat1 is the major transcription factor in mediating IFN γ signaling. Accumulating evidence suggests that Stat3 is also activated directly upon IFN γ treatment (110, 111) and Stat3 activity is important in maintaining melanogenesis in B16 cell (12). Indeed, both of pStat1 (Y701), pStat1 (S727) and pStat3 (Y705) were robustly activated in response to IFN γ by Western blot. (Fig. 6B). To evaluate which transcriptional factor mediates melanogenesis, we generated multiple clones of either Stat1 or Stat3 knockout mediated by CRISPR-Cas9 in B16N cells (Fig. 6C). Activation of pStat3 was still observed in the Stat1-KO clones. Interestingly, upregulation of Stat3 protein by IFN γ was impaired by loss of Stat1 (Fig. 6C). Cell pellets showed that IFN γ failed to increase both of melanin synthesis and tyrosinase activity in Stat1-KO clones, but not in Stat3-KO clones (Fig. 6D, E). Upregulation of Mitf and mature tyrosinase by IFN γ treatment were blocked in Stat1-KO clones as well (Fig. 6F). The expression of Tyrp1 was not altered by either Stat1 KO or Stat3 KO (Fig. 6G). Upregulation of Oca2 by treatment of IFN γ was blocked by Stat1

knockout (Fig. 6H). This indicates that Jak1/2-Stat1 axis mediates IFN γ -induced melanogenesis alone, and is independent on the Stat3 signaling axis.

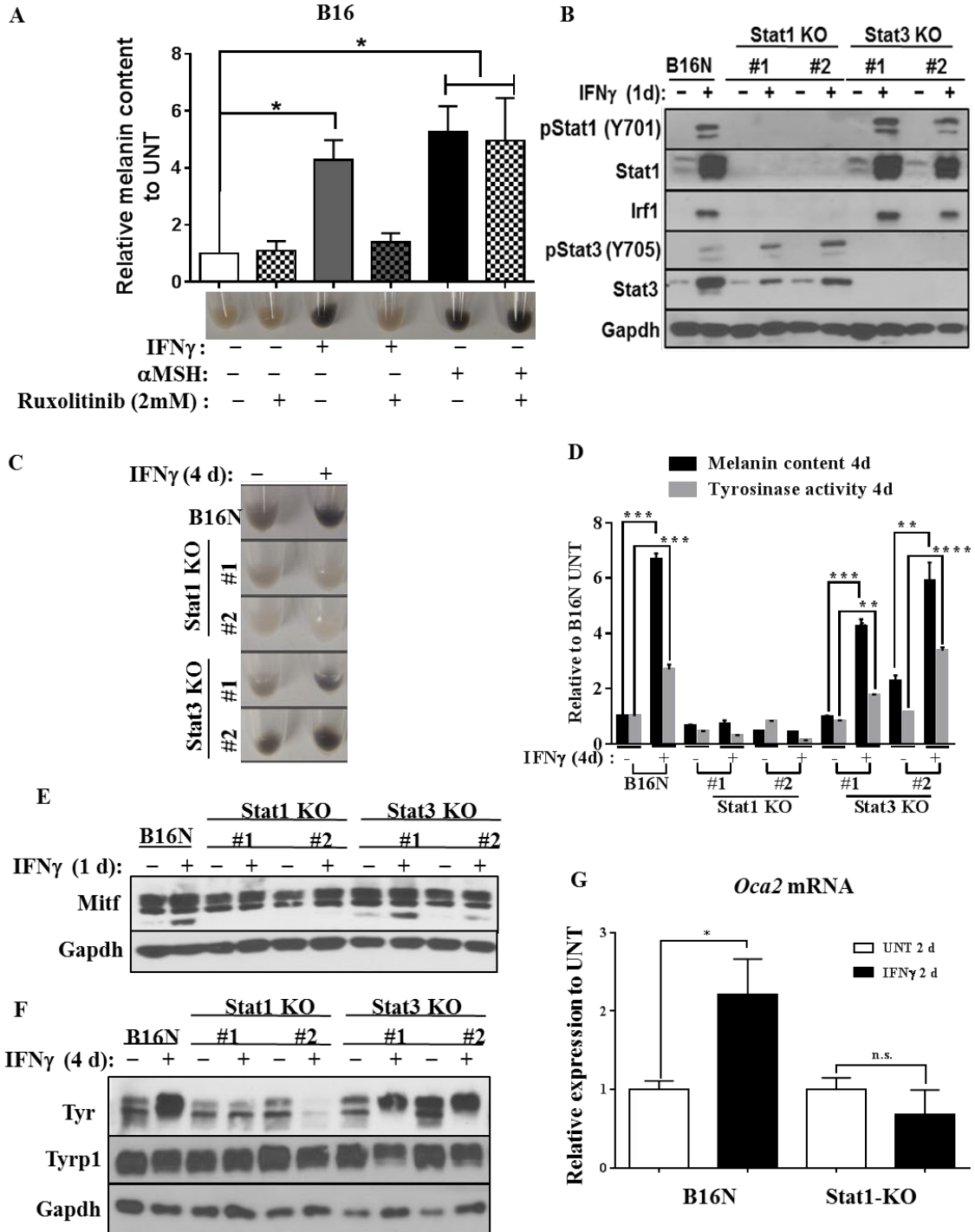


Figure 6. Jak1/2-Stat1 mediates IFN γ -induced melanogenesis. A, Melanin content in B16 cells cultured with either IFN γ or α MSH in the presence or absence of ruxolitinib (2

μM). **B**, Western blot of pStat1 (Y701), Stat1, Irf1, pStat3 (Y705), Stat3 and Gapdh expressions in parental B16N cells and Stat-KO clones in response to IFN γ treatment. **C**, Photos of cell pellets of B16N and Stat-KO clones collected after 4 d treatment of IFN γ . **D**, Melanin content and tyrosinase activity were measured in B16N and Stat-KO clones in response to IFN γ for 4 d. **E-F**, Western blot analysis of expressions of Mitf, Tyr and Tyrp1 in B16N and Stat-KO cells treated with or without IFN γ for 1 d (E) or 4 d (F). **G**, qRT-PCR analysis of *Oca2* expression in B16N cells cultured with or without IFN γ for 2 d. Immunoblotting images are representative of two independent experiments in B and E&F, respectively. Data is presented as mean \pm SEM of three biological replicates in D and G. *P<0.05; **P<0.01; ***P<0.01; ****P<0.0001.

CHAPTER 3
INTERFERON GAMMA SIGNALING IN MELANOCYTES AND MELANOMA
CELLS REGULATES EXPRESSION OF CTLA4

Materials and Methods

Cell Culture

The human primary neonatal foreskin melanocytes: HEMn-LP (from lightly pigmented donor), HEMn-MP (from moderately pigmented donor) and HEMn-DP (from darkly pigmented donor) were cultured at 37°C in medium 254 supplemented with HMGS-2 (PMA-free) and Gentamycin (50 µg/ml) with 5% CO₂. The human epidermal neonatal keratinocytes (HEKn) were cultured at 37°C in EpiLife medium supplemented with HKGS and Gentamycin (50 µg/ml) with 5% CO₂. All cells, media and supplements listed above were purchase from Life Technology.

The human melanoma cell line Hs 936.T was purchased from ATCC; the human melanoma cell lines A2058 and COLO679 were obtained from Dr. Glenn Merlino (NCI); the human melanoma cell lines WM983(B), 451 Lu, WM3918 and WM3912 were obtained from Dr. Meenhard Herlyn (Wistar Inst); the human melanoma cell line UACC1273 was obtained from Dr. Ashani Weeraratna (Wistar Inst); the human colon carcinoma cell lines RKO and HCT116 were obtained from Dr. Jean-Pierre Issa (Temple Univ); the human embryonic kidney cell line HEK293 and the human osteosarcoma cell line U-2 OS were obtained from Dr. Richard Pomerantz (Temple); The human fibroblast cell line FS2, the human hepatocellular carcinoma cell line FOCUS, the human ovarian

adenocarcinoma cell lines SK-OV-3 and OVCAR429, the human ovarian teratocarcinoma cell line PA-1, the human prostate carcinoma cell lines HTB-81 and PC-3, the human osteosarcoma cell line MG63, the human breast adenocarcinoma cell lines MCF7 and MDA-MB-231, the human acute lymphoblastic leukemia cell line CEM, the human Burkitt's Lymphoma Daudi, and the human lung carcinoma cell line A549 were obtained from Dr. Raghbir Athwal (Temple). All tumor cell lines were cultured at 37°C in Dulbecco's Modified Eagle Medium (DMEM) supplemented with 10% fetal bovine serum (FBS), L-alanyl-L-Glutamine (2 mM) and Gentamycin (50 µg/ml) at 5% CO₂. DMEM, FBS and L-alanyl-L-Glutamine were purchased from Corning, Cellgro.

IFN γ Treatment

Human recombinant IFN γ (with BSA carrier) was purchased from Cell Signaling Technology (catalog #8901). The concentration used was 10ng/ml except Fig. 2B, where the concentrations are indicated within the figure. According to MSDS provided by the manufacturer, the bioactivity of h-IFN γ was determined in a virus protection assay. The ED₅₀ of each lot is between 0.3-1.2 ng/ml. The conversion of 10ng/ml to biological activity is 8.33 U/ml-33.33 U/ml.

Quantitative RT-PCR

qRT-PCR analysis was performed to quantitatively measure the mRNA abundance. Total cellular RNA was extracted using the Trizol method (Life Technologies) and RNeasy Mini Kit (QIAGEN). RNA concentration was determined by Nanodrop. cDNA was generated by GoTaq 2-step RT system (QIAGEN). qRT-PCR

analysis of human *CTLA4*, *IRF1*, *GAPDH*, *NR4A3*, *STAT1*, *PSMB9* and *TAPI* were performed with the Power SYBR-Green PCR Master Mix (Fisher Scientific) and the ABI StepOnePlus PCR system. *18s rRNA* was used as the reference gene. The $\Delta\Delta CT$ method was used to calculate relative expression levels. The sequence of primers for amplification of different genes were: Human *CTLA4* (Forward 5'-AGCCAGGTGACTGAAGTCTG-3', Reverse 5'-CATAAATCTGGGTTCCGTTG-3'); Human *IRF1* (Forward 5'-AGTGATCTGTACAACCTTCCAGG-3', Reverse 5'-CCTTCCTCATCCTCATCTGTTG-3'); Human *GAPDH* (Forward 5'-CTTTGTCAAGCTCATTTCTGG -3', Reverse 5'-TCTTCCTCTTGTGCTCTTGC -3'); Human *NR4R3* (Forward 5'-AGTGTCTCAGTGTTGGAATGG-3', Reverse: 5'-AGGAGAAGGTGGAGAGGG-3'); Human *STAT1* (Forward 5'-TGAACCTACCCAGAATGCCC -3', Reverse 5'-CAGACTCTCCGCAACTATAGTG -3'); Human *PSMB9* (Forward 5'-GAGAGGACTTGTCTGCACATC-3', Reverse 5'-GCATCCACATAACCATAGATAAAGG-3'); Human *TAPI* (Forward 5'-AGAAGGTGGGAAAATGGTACC-3', Reverse: 5'-GTTGGCAAAGCTTCGAACTG-3'); *18s rRNA* (Forward 5'-CTTAGAGGGACAAGTGGCG-3', Reverse 5'-ACGCTGAGCCAGTCAGTGTA-3').

Immunofluorescence Staining

Human melanocytes and melanoma cells were fixed with 4% PFA for 10 min and permeabilized with 0.25% Triton X-100 in PBS, then incubated with a blocking buffer (1% BSA, 22.52 mg/ml glycine in PBST) for 30 min at room temperature, which was followed by overnight incubation with mouse anti-human-CTLA4 (1:100, BNI3, BD

Biosciences) antibody at 4°C. The control groups were only incubated with antibody dilution buffer (1% BSA in PBST). After washing, the fixed cells on cover slips were incubated with Alexa Fluor 488–conjugated goat anti-mouse secondary antibody (1:400, Life Technology) for 1h at room temperature. The cover slips were mounted with VECTASHIELD mounting medium with DAPI (Vector Laboratories Inc) overnight and imaged with Leica TCS SP8 Confocal microscope at the specified magnification.

Flow Cytometry

For intracellular staining, human melanocytes and melanoma cells were fixed and permeabilized by BD Fixation/Permeabilization Solution Kit, followed by manufacture's protocol. Cells were then stained with a mouse anti-human CTLA4-PE (BD Biosciences, cat#555853) or isotype control anti-mouse IgG-PE (BD Biosciences, cat#554648) for 30 min at 4°C. Cells were then washed and analyzed on a BD FACSCalibur. The data were analyzed using FlowJo software.

Ruxolitinib Treatment

HEMn-MP cells were seeded into 60mm dishes at 5×10^5 per dish. After one day, these cells were pretreated with Ruxolitinib (5 μ M, Selleckchem) for 4h, then cultured in the presence or absence of r IFN γ for indicated time periods. The cells were harvested to assess *CTLA4* and *IRF1* mRNA expression by qRT-PCR. Hs 936.T, A2058, and WM983(B) cells were seeded into 60mm dishes at 5×10^5 per dish. After one day, these cells were treated with ruxolitinib (5 μ M) for 1 day and harvested to assess *CTLA4*, *IRF1*, *STAT1*, *TAP1* and *PSMB9* expression by qRT-PCR.

Western blotting

Human melanocytes and melanoma cells were lysed in Pierce RIPA buffer (Thermo Scientific) containing 1x Halt protease inhibitor cocktail (100X, Thermo Scientific) and 1x Halt phosphatase inhibitor cocktail (100X, Thermo Scientific) and the protein concentration was measured with the Bio-Rad Protein Assay following manufacturer's protocol. The same amounts of protein extracts were subjected to polyacrylamide gel electrophoresis using the 4%-20% Mini-Protean TGX gel system (Bio-Rad), transferred to PVDF (0.45 um pore size, Millipore) membranes, and immunoblotted using antibodies that specifically recognize STAT1 (1:1000, Cell Signaling Technology), pSTAT1 (Y701, 58D6, 1:1000, Cell Signaling Technology), pSTAT1 (Y727, D3B7, 1:2000, Cell Signaling Technology), STAT3 (124H6, 1:1000, Cell Signaling Technology), pSTAT3 (Y705, D3A7, 1:2000, Cell Signaling Technology), GAPDH-HRP (D16H11, 1:1000, Cell Signaling Technology), IRF1 (D5E4, 1:1000, Cell Signaling Technology), Histone 3 (#ab1791, 1:3000, Abcam), Histone 4 (#39269, 1:1000, Active Motif), pan-acetyl-Histone 3 (#06-599, 1:10,000, Millipore), pan-acetyl-Histone 4 (#06-866, 1:5000, Millipore). The secondary antibodies used for detection were HRP-conjugated goat anti-mouse and goat anti-rabbit IgG (1:5000, Thermo Scientific). The blots were incubated with Luminata Western HRP substrate (Millipore) for 5 min. Band intensities of Tiff images were quantified by using Image J software.

siRNA-mediated Knockdown

UACC1273 melanoma cells were transfected with indicated siRNAs (10 pM) or scramble (Scr) siRNA (10 pM) with Lipofectamine RNAiMAX Reagent (Invitrogen) according to the manufacturer's protocol. Transfection efficiency was assessed by measuring the amounts of the proteins of interest. The siRNAs are listed below: Scramble siRNA (Scr, Silencer® Select Negative Control No. 1 siRNA, Catalog number: 4390843, Ambion); STAT1 siRNA S1-1, sense, 5'-CGGUUGAACCCUACACGAATT-3', ID:s278, Ambion; STAT1 siRNA S1-2, sense, 5'-CCUACGAACAUGACCCUAUTT - 3', ID:s277, Ambion; STAT3 siRNA S3-1, sense, 5'- GCACCUUCCUGCUAAGAUUtt- 3', ID:s745, Ambion; STAT3 siRNA S3-2, sense, 5'-GCCUCAAGAUUGACCUAGATT -3', ID:s743, Ambion; IRF1 siRNA IRF1-1, sense, 5'- GCAGAUUAAUCCAACCAATT -3', ID:s7502, Ambion; IRF1 siRNA IRF1-2, sense, 5'- CCUCUGAAGCUACAACAGATT-3', ID:s7501, Ambion. All siRNAs were purchased from Thermo Scientific.

Plasmid Construction

The 1021-base pair (bp) segment of *CTLA4* promoter luciferase construct containing four putative GAS sites was synthesized and cloned into a firefly luciferase vector (pGL4.20_luc2/Puro, Promega) by Genescript gene synthesis and cloning service. Site-directed mutagenesis was performed by QuikChange II site-directed Mutagenesis Kit (Agilent Technologies) and generated mutants with deletion of each putative GAS sites by manufacture's protocol. Human CTLA4 ORF cDNA vector was purchased from Origene.

Luciferase Reporter Assay

HEMn-MP cells were transiently transfected with different *CTLA4* promoter firefly luciferase reporter constructs with Nucleofector Kits for Human Melanocytes (NHEM-neo) following manufacturer's protocol. The cells were also co-transfected with a Renilla luciferase vector (pGL4.74_hRluc/TK, Promega) using Nucleofector I device. Two days after transfection, the cells were treated with IFN γ , or mock-treated, for 7 days, then were harvested and analyzed. The luciferase activity of each samples was measured with the Dual-Luciferase Reporter Assay System (Promega) with a Promega Glomax detection system according to the manufacturer's protocol.

Chromatin Immunoprecipitation (ChIP) Assays

Chromatin immunoprecipitation (ChIP) was performed with the modified protocol provided by Upstate Biotechnology with minor modifications (112). Briefly, HEMn-MP cells were cultured in the presence or absence of 10 ng/ml rIFN γ for 7 days, then fixed in 1% formaldehyde for 15 min, and neutralized by addition of 0.125 M glycine (pH 7.0) for 5 min. Cells were lysed in 100 μ L SDS lysis buffer containing proteinase and phosphatase inhibitors per 1×10^6 cells and then sonicated using a sonic dismembrator (Fisher Scientific) to shear chromatin into 200-300 bp DNA fragments. The chromatin fragments were subjected to immunoprecipitation with the following antibodies: Rabbit IgG (5 μ g, Millipore), STAT1 (1:50, Cell Signaling Technology), pSTAT1 (Y701, 58D6, 1:100, Cell Signaling Technology), Histone 3 (#ab1791, 5 μ g, Abcam), Histone 4 (62-141-13, 5 μ g, Millipore), pan-acetylated-Histone 3 (5 μ g,

Millipore), pan-acetylated-Histone 4 (5 µg, Millipore), CBP (D6C5, 1:25, Cell Signaling Technology), and RNA polymerase II (8WG16, 5 µg, Millipore). The coimmunoprecipitated DNA was purified with GeneJET PCR Purification Kit (Thermo Scientific). Occupancy of the promoter and other regulatory regions was measured by qRT-PCR with the following primer sets by using 1/100 of the ChIP DNA. The base pair location is in reference to transcription start site (TSS) of CTLA4: R1 (-885bp to -736bp) Forward 5'-ATTCAATCCTAAGTGCACAGAATTC-3', Reverse 5'-TGTAGACAGGACCAATGATCTAAC-3'; R2 (-576bp to -480bp) Forward 5'-TTGTCTCTGTTGAGTTAAGGC-3', Reverse 5'-CACAAGAAATAAACTGAAAATAGGCG-3'; R3 (-319bp to -240bp) Forward 5'-GCTCAGAAAGTTAGCAGCCTAGTAG-3', Reverse 5'-CAATCTTCTGGGCATCCTTAACC-3'; R4 (+530bp to +621bp) Forward 5'-CAGGCAATTCAGACCCTTCTATG-3', Reverse 5'-CCTGAAACCCAGCTCAAATG-3'.

CBP Inhibitor Treatment

HEMn-DP and UACC1273 were seeded into 60mm dishes at 5×10^5 cells per dish. After one day, these cells were pretreated with SGC-CBP30 (5 µM or 10 µM, Selleckchem) or PF-CBP1 (10 µM or 20 µM, Selleckchem) for 4h, then cultured in the presence or absence of rIFN γ for indicated time periods. The cells were harvested to assess *CTLA4* and *IRF1* mRNA expression by qRT-PCR analysis, and p-STAT1 (Y701), STAT1, IRF1 and GAPDH protein expression by western blot.

MAPK Pathway Inhibitor Treatment

A2058, WM983(B), UACC1273, Hs 936.T, SK-MEL-2, WM3912 and WM3918 cells were seeded into 60mm dishes at 5×10^5 cells per dish. After one day, these cells were treated with either BRAFV600E inhibitor Vemurafenib (10 μ M, Selleckchem) or MEK inhibitor PD0325901 (5 μ M, Selleckchem) for 1 d and then harvested to assess *CTLA4* mRNA expression by qRT-PCR analysis.

CCLC Analysis

The Cancer Cell Line Encyclopedia (CCLE) mRNA data were downloaded from the CCLE website (<http://www.broadinstitute.org/ccle>) from the file *CTLA4_file6805.gct*. The figure was generated by GraphPad Prism. RMA gene expression values of cell lines were used to generate the figure.

RNA-seq Data of Ipilimumab-treated Melanoma Patients

Ipilimumab-treated melanoma patients were described previously (113, 114). RNA-seq data on tumors collected pre- and post-treatment were downloaded from dbGaP (phs001038). Cluster analysis is performed on anti-CTLA4 treated melanoma patients using Heat Mapper. Average linkage clustering method and Euclidean distance measurement method are applied in the hierarchical clustering (115).

Statistical Analysis

All experiments were performed in triplicate and data are presented as mean±SEM, and graphs were prepared with GraphPad Prism. To analyze statistical difference between two groups, two-tailed unpaired Student's t-test was used. Comparisons involving multiple groups were assessed by one-way ANOVA with post-hoc Tukey analysis. For survival analysis, Kaplan-Meier plots and log-rank tests were performed to determine the significance of differences in cumulative survival. For gene expression correlation analyses, the Pearson correlation coefficient was used. P value <0.05 was considered as statistically significant.

Results

CTLA4 is Overexpressed in Human Melanoma Cells

We had previously found CTLA4 to be highly expressed in mouse melanoma allograft tumors with distinct expression in melanoma cells (95). We therefore analyzed the Broad-Novartis Cancer Cell Line Encyclopedia (CCLE) database for CTLA4 expression in its large panel of approximately 1000 cell lines of a variety of human cancer types, including 62 melanoma cell lines (115, 116). Human melanoma cell lines exhibited the greatest mean CTLA4 expression among all the cancer cell types (Fig. 7A). In fact, this mean expression was even greater than that of 180 of the hematologic and lymphoid cancer cell lines, with the difference being statistically significant (Fig. 7A). This prompted us to validate the mRNA expression of CTLA4 in human primary melanocytes and melanoma cells. Three different primary human epidermal melanocyte (HEMn) cell populations, but not human epidermal keratinocytes (HEKn), exhibited low but readily detectable expression of CTLA4 tested by quantitative RT-PCR (qRT-PCR) (Fig. 7B). On the other hand, all of the 13 human melanoma cell lines expressed CTLA4 at ~30-10,000-fold greater levels than HEMn cells (Fig. 7B).

Flow cytometric analysis failed to detect cell surface expression of CTLA4 in HEMn and melanoma cell lines. This is in accord with previously published expression pattern of CTLA4 seen in T cells, where it is also rarely expressed on the membrane and gets rapidly internalized into cytoplasm via clathrin-mediated endocytosis (117). Intracellular immunostaining readily detected CTLA4 protein expression in melanoma cells, but the expression in HEMn cells was barely detectable by flow cytometry (Fig.

7C). On the other hand, immunofluorescence staining of HEMn cells showed very low levels of diffuse punctate localization throughout cytoplasm, but not on the cell surface, which is consistent with endosomal/lysosomal vesicular localization within cytoplasm (Fig. 7D). Human melanoma cell lines showed much greater cytoplasmic punctate localization, but a large majority of the overexpressed CTLA4 protein was observed to be localized in perinuclear areas, presumably in the trans-Golgi network (Fig. 7D), as previously reported in T cells (118-120). As a positive control for the specificity of anti-CTLA4 antibody, we ectopically expressed human CTLA4 in HEK293T cells, which do not express endogenous CTLA4. The mouse anti-human-CTLA4 antibody (clone BNI3) readily and specifically detected CTLA4 in the ectopic CTLA4-expressing cells by both flow analysis of intracellular immunostaining and immunofluorescence, but not in the untransfected control HEK293T cells (Fig. 7C,D).

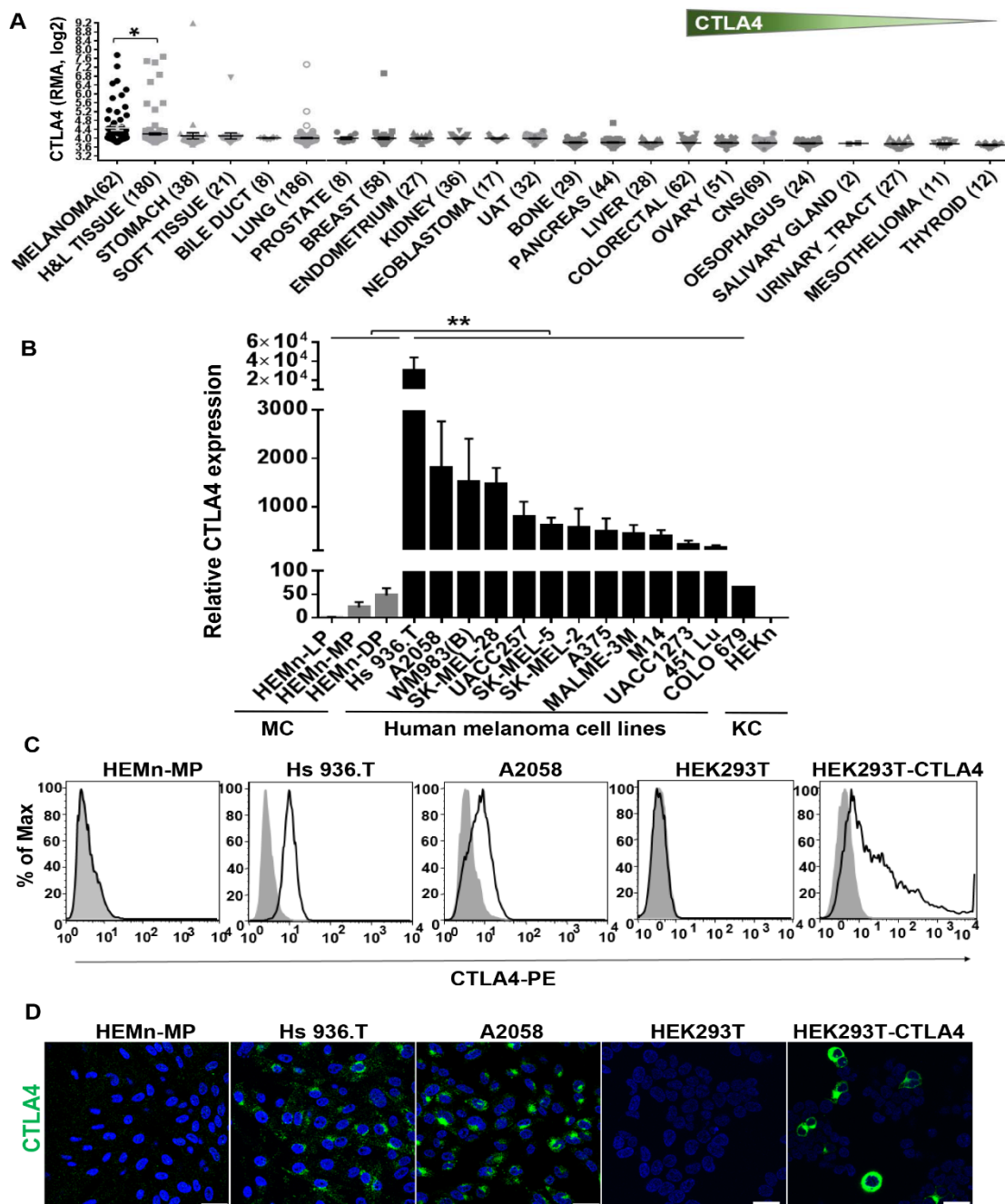


Figure 7. CTLA4 is highly overexpressed in human melanoma cells. A, CTLA4 mRNA expression pattern across different types of cancer cell lines in the Cancer Cell Line Encyclopedia (CCLE) database. Sample numbers (n) are indicated in parentheses.

H&L, hematopoietic and lymphoid tumor cell lines; UAT, upper aerodigestive tract tumor cell lines; CNS, central nervous system tumor cell lines. Each dot represents one tumor cell line. * $p < 0.05$. Unpaired t-test with Welch's correction. Y axis, RMA (Robust Multi-Array Average) was used to normalize the expression data and then converted to \log_2 . B, CTLA4 mRNA expression in human primary melanocytes (MC), human melanoma cells, and human primary keratinocyte (KC) was determined by qRT-PCR, and plotted relative to HEMn-LP melanocytes. Data presented as mean \pm SEM of three to six independent experiments. C, Total CTLA4 protein expression in fixed and permeabilized human melanocytes, melanoma cell lines, HEK293T and CTLA4-overexpressing HEK293T cells stained with either mouse anti-human CTLA4-PE (BNI3) or isotype-PE control antibody, were analyzed by flow cytometry. D, Confocal photomicrographs of CTLA4 immunostaining (green) in melanocytes, melanoma cell lines, HEK293T and CTLA4-overexpressed HEK293T cells. Blue, DAPI. Images are representative of 3-5 independent experiments. Scale bar=25 μ m.

IFN γ Activates Expression of CTLA4 in Melanocytes and Melanoma Cells

Since we had identified *CTLA4* to be the highest upregulated gene in the context of UVB-mediated IFN γ -induced gene expression signature in melanocytes (95), we postulated that *CTLA4* might be regulated by the IFN γ signaling pathway in melanocytes and melanoma cells. Indeed, we found that treatment of HEMn cells with relatively low concentrations of recombinant IFN γ (1-10 ng/ml; 1.3-13.3 U/ml) robustly activated the expression of CTLA4, with a plateau of response reached between 10 ng/ml and 100 ng/ml concentrations (Fig. 8A,B). This IFN γ -mediated induction of expression was statistically significant within 30 min, and continually increased in extent to approximately 200-fold by 3 wk timepoint (Fig. 8A). IFN γ treatment also increased CTLA4 in human melanoma cells at both mRNA and protein levels, albeit to a lesser degree (<4-fold change) than in HEMn, presumably due to the already relatively high baseline expression in these cells (Fig. 8C). Flow cytometric analysis also showed robust and statistically significant induction of intracellular CTLA4 protein expression by IFN γ in melanocytes and melanoma cells (Fig. 8D,E). However, the IFN γ -mediated induction of CTLA4 expression was restricted to the melanocytes and melanoma cells, as neither the other primary or normal cells, i.e. keratinocytes, human embryonic kidney cells, and fibroblasts, nor several non-melanoma solid tumor cell lines expressed CTLA4 before or after IFN γ treatment (Fig. 8F). Immunofluorescence analysis readily showed upregulation of CTLA4 in the HEMn-MP melanocytes and UACC1273 melanoma cells (Fig. 8G). Once again, the CTLA4 expression was absent from the cell membrane, but

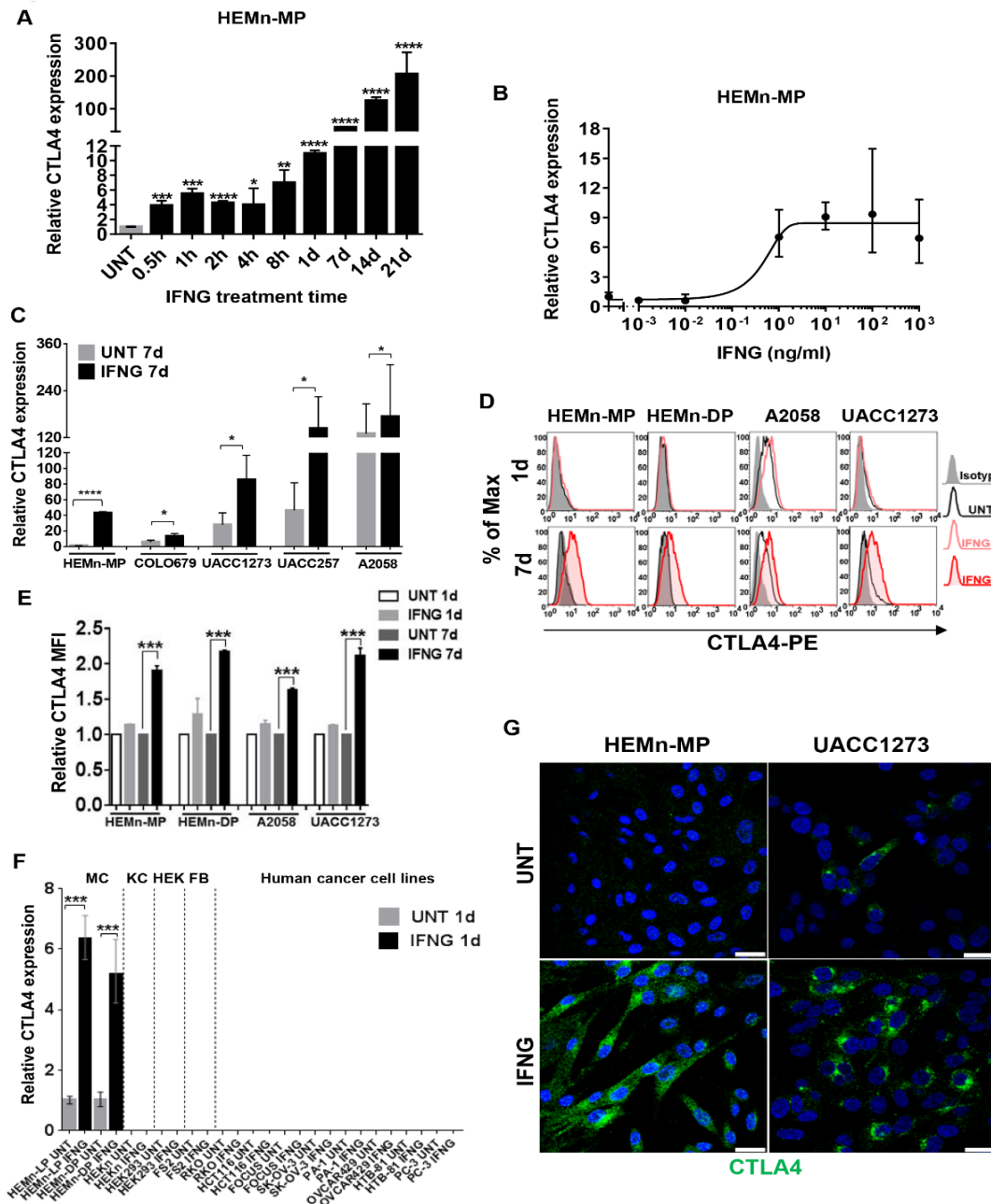


Figure 8. IFN γ induces CTLA4 expression in human primary melanocytes and melanoma cell lines. **A**, qRT-PCR analysis of CTLA4 mRNA expression in HEMn-MP cells cultured in the presence or absence of 10 ng/ml IFN γ is shown at indicated time points. **B**, qRT-PCR analysis of CTLA4 mRNA expression in HEMn-MP cells cultured

in the presence or absence of indicated concentrations of IFN γ for 1d. **C**, qRT-PCR analysis of CTLA4 mRNA expression in cells that were cultured for 7 days in the presence or absence of 10 ng/ml IFN γ . **D**, Total CTLA4 protein expression in fixed and permeabilized human melanocytes and melanoma cell lines cultured in the presence or absence of 10 ng/ml IFN γ for either 1d or 7d, immunostained with either mouse anti-human CTLA4-PE (BNI3) or isotype-PE control antibody, and analyzed by flow cytometry. Data are representative of at least three independent experiments. **E**, Histogram representing the average MFI \pm SEM of three independent experiments. Y axis, fold-change of CTLA4 MFI is compared to the untreated (UNT) group. **F**, qRT-PCR analysis of CTLA4 expression in human primary neonatal melanocytes (MC); human epidermal neonatal keratinocytes (KC); human embryonic kidney cells (HEK); human fibroblast cell line (FB); and the indicated human solid cancer cell lines. RKO/HCT116, human colon carcinoma cell lines; FOCUS, human hepatocellular carcinoma; SK-OV-3/OVCAR429, human ovarian adenocarcinoma cell lines; PA-1, human ovarian teratocarcinoma cell line; HTB-81/PC-3, human prostate carcinoma cell lines. **G**, Confocal photomicrographs of CTLA4 immunostaining (green) in HEMn-MP and UACC1273 cells that were cultured in presence or absence of 10 ng/ml recombinant IFN γ for 7d. Blue, DAPI. Images are representative of three independent experiments. Scale bar=25 μ m. All graphed data are presented as mean \pm SEM of three biological replicates. *P<0.05; **P<0.01; ***P<0.001; ****P<0.0001.

was diffusely spread throughout cytoplasm in the distinct punctate pattern, with dominant trans-Golgi network localization (Fig. 8G).

IFN γ Induces CTLA4 Expression via STAT1-mediated Canonical Signaling

The canonical IFN γ cytokine signaling downstream of the IFN γ receptors is mediated by activation of Janus Kinases 1 and 2 (JAK1/2), which phosphorylate the Signal Transducer and Activator of Transcription 1 (STAT1) transcription factor prompting its homodimerization (110). The phosphorylated STAT1 (pSTAT1) homodimers then shuttle to the nucleus and activate transcription of genes whose promoters harbor the IFN-gamma-activated sequence (GAS) DNA-binding motif(s) (110). One of the classical primary response genes activated by IFN γ signaling is the one that encodes the transcription factor Interferon Regulatory Factor 1 (IRF1), which subsequently transcribes numerous secondary IFN γ -response genes (121). Additionally, IFN γ signaling also results in phosphorylation of transcription factor STAT3 in a cell type-specific and context-dependent manner (122). We sought to delineate the role of the canonical IFN γ signaling and the specific downstream transcription factor (s) responsible for the activation of CTLA4 expression in melanocytes and melanoma cells.

We started by testing the ability of JAK1/2 inhibitor drug ruxolitinib (123) to block IFN γ -induced CTLA4 expression in melanocytes. Indeed, ruxolitinib (5 μ M) completely inhibited activation of CTLA4 in response to IFN γ treatment of HEMn-MP melanocytes (Fig. 9A). The induction of IRF1 expression by IFN γ treatment was also completely abolished, indicating blockade of the IFN γ signaling pathway (Fig. 9B).

IFN γ treatment of HEMn cells robustly increased phosphorylation of STAT1 at both tyrosine 701 (pSTAT1-Y701) and serine 727 (pSTAT1-S727), both of which are important for pSTAT1-mediated transcriptional activation. These phosphorylation events were detectable immediately and sustained for as long as the cells were kept exposed to IFN γ treatment (Fig. 9C). Since S727 phosphorylation requires nuclear translocation and chromatin-binding of pSTAT1-Y701 (10), these results indicate robust IFN γ -induced STAT1 activation response in melanocytes. Interestingly, STAT3 also exhibited sustained phosphorylation (pSTAT3-Y705) in response to IFN γ in HEMn-MP cells (Fig. 9C). Strong activation of IRF1 expression was also confirmed (Fig. 9C).

In order to determine which of the transcription factors (STAT1, STAT3, or IRF1) is primarily responsible for IFN γ -induced CTLA4 transactivation, we generated siRNA-mediated knockdowns (KD) of STAT1, STAT3, and IRF1 in the UACC1273 melanoma cell line. Two siRNAs were used for each of the three knockdowns, with >90% reduction in expression, along with parental cells (C) and scrambled (Scr) siRNA-transfected cells as controls (Fig. 9D). All of the KD cells were treated with IFN γ for 7 days, and then analyzed for intracellular CTLA4 expression by flow cytometry. While the UACC1273 cells with STAT3-KD and IRF1-KD exhibited significant increase in CTLA4 protein expression in response to IFN γ treatment, it was completely inhibited in the STAT1-KD cells (Fig. 9E). These results clearly indicate that STAT1 is the principal transcription factor responsible for mediating the IFN γ -induced CTLA4 expression in

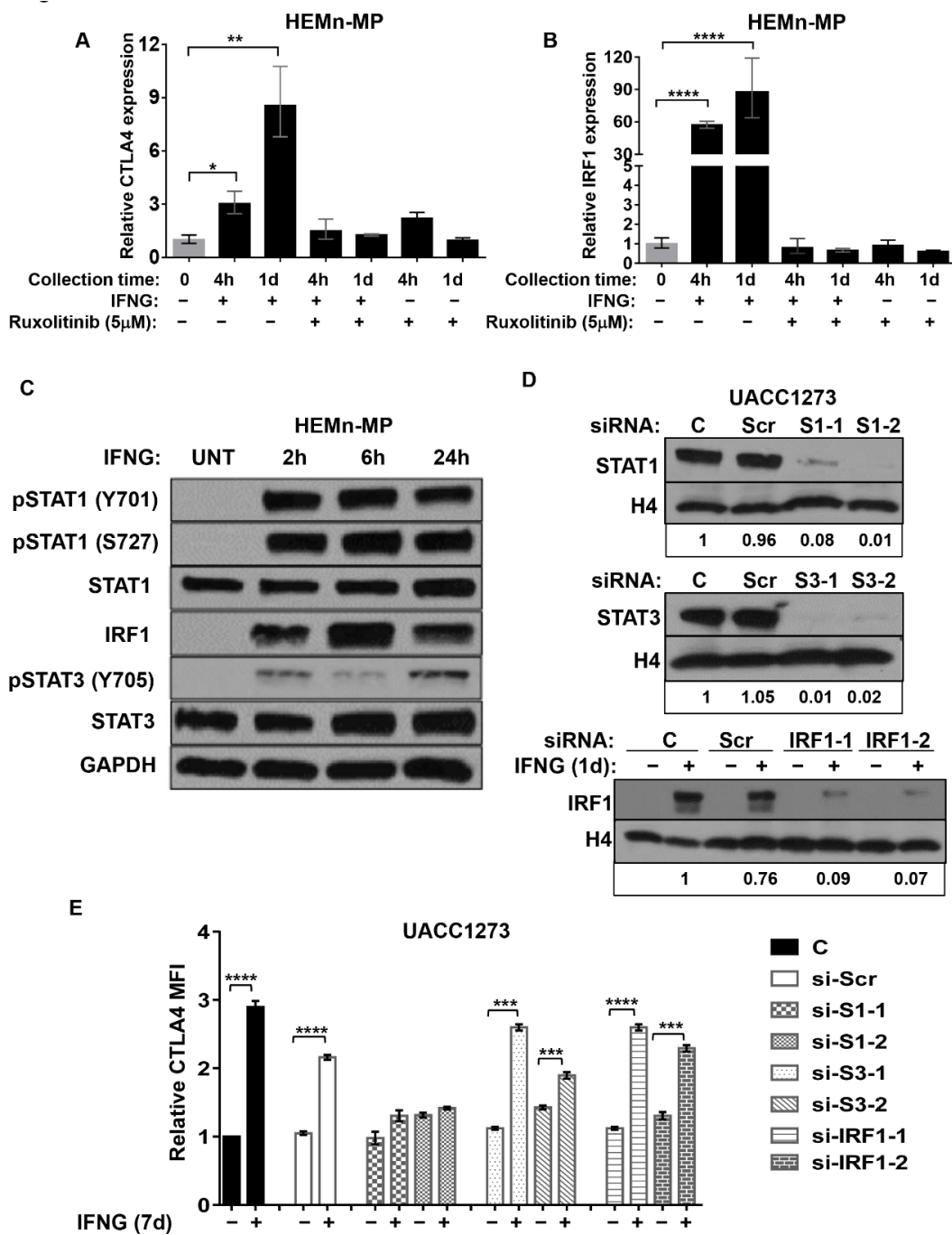


Figure 9. IFN γ -induced CTLA4 expression is mediated by JAK-STAT1 pathway. **A** and **B**, Ruxolitinib treatment blocks IFN γ -induced CTLA4 and IRF1 expression. HEMn-MP cells were pretreated with Ruxolitinib (5 μ M) for 4h before IFN γ treatment. qRT-

PCR analysis of CTLA4 (A) and IRF1 (B) expression in HEMn-MP cells after indicated treatments. Data are presented as mean \pm SEM of three biological replicates. *P<0.05; **P<0.01 compared to both IFN γ and Ruxolitinib-untreated groups. **C**, Western blot analysis of activation of pSTAT1, pSTAT3, and IRF1 by IFN γ treatment in human melanocyte. HEMn-MP cells were cultured in the presence or absence of 10 ng/ml IFN γ for indicated time intervals, then pSTAT1 (Y701), pSTAT1 (Y727), total STAT1, IRF1, pSTAT3 (Y705), total STAT3 and GAPDH expression by western blot. **D**, siRNA-mediated knockdown of STAT1, STAT3, and IRF1 in UACC1273 melanoma cell line with either scrambled siRNA (Scr), si-STAT1 (S1-1, S1-2, two different siRNA-mediated KD), si-STAT3 (S3-1, S3-2, two different siRNAs), or si-IRF1 (IRF1-1 and IRF1-2, two different siRNAs) for 2d, then assessed for STAT1, STAT3, or IRF1 protein levels by western blotting. Histone 4 (H4) protein was used as loading control. Densitometry-based calculations of fold changes, normalized to control group, are shown at the bottom of the blot images. Band intensities of Tiff images were quantified by Image J. Immunoblotting images are representative of 2 independent experiments. **E**, UACC1273 cells were transfected with indicated siRNA for 2d, then cultured in the presence or absence of 10 ng/ml IFN γ treated for 7d before measuring CTLA4 protein expression by flow cytometry. Y axis, fold change of CTLA4 mean MFI compared to no-siRNA control (C) cells without IFN γ treatment. ***P<0.001; ****P<0.0001. The histogram represents MFI \pm SEM of three biological replicates.

melanocytes and melanoma cells, and that CTLA4 is one of the primary response genes downstream of IFN γ signaling pathway.

CTLA4 Promoter is Transcriptionally Active in Melanocytes and Melanoma Cells

To determine the chromatin characteristics of the CTLA4 gene promoter, we inspected the cell type-specific DNase I hypersensitivity of this DNA region through the ENCODE Project (National Human Genome Research Institute, National Institutes of Health) (124). As expected, T cells, CD4⁺ helper T cells, and CD8⁺ $\alpha\beta$ T cells showed DNase I hypersensitivity peaks in the CTLA4 promoter region (Fig. 10A, solid box). Interestingly, human foreskin epidermal melanocytes and melanoma cell lines (SK-MEL-5, MEL-2183, and COLO829) exhibited DNase I hypersensitivity peaks of similar intensity. In contrast, RPMI8226 myeloma cell line, human foreskin keratinocytes and fibroblasts, mammary epithelial cells, PC-3 prostate cancer cell line, MG63 osteosarcoma cell line, and RKO colon carcinoma cell line did not show DNase I hypersensitivity in this region (Fig. 10A, dotted box). These results are consistent with a transcriptionally active open chromatin (euchromatin) configuration in the CTLA4-expressing T cells and melanocyte/melanoma cells, but a heterochromatic (repressive) chromatin in the CTLA4 promoter regions of CTLA4-non-expresser cell types. Concordantly, ENCODE RNA-seq analysis of human foreskin melanocytes showed a good correlation of CTLA4 transcriptional profile with that of the DNase I hypersensitivity in the CTLA4 promoter region (Fig. 10B, solid box).

Histone modifications play a dominant role in the regulation of chromatin architecture, with specific modifications closely associated with transcriptionally active

or inactive chromatin. In this context, two of the most common histone modifications linked with active chromatin within 1 kilobases (-1 kb) of the promoter transcription start sites (TSS) are histone 3 lysine 4 trimethylation (H3K4me3) and histone 3 lysine 27 acetylation (H3K27ac) (125). The ENCODE ChIP-seq data (126) showed high levels of H3K4me3 and H3K27Ac enrichment in the CTLA4 promoter region in both human T cells and foreskin melanocytes, but not in foreskin keratinocytes (Fig. 10B). In contrast, the most common repressive histone mark associated with inactive chromatin, H3K27me3 (27), showed no or low enrichment in the CTLA4 promoter region in T cells and melanocytes, but high enrichment in keratinocytes (Fig. 10B). Altogether, the results obtained from the ENCODE analysis of chromatin state at the CTLA4 promoter locus in different cell types are in congruence with their respective CTLA4 expression patterns, and clearly indicate that CTLA4 promoter harbors a transcriptionally active chromatin configuration in melanocytes and melanoma cells. We next inspected the human CTLA4 gene sequence upstream and downstream the TSS and found four putative GAS motifs (127). To determine the validity of these putative GAS sites and their contribution to IFN γ -induced activation of CTLA4 expression, we generated reporter constructs with CTLA4 promoter (-1kb to TSS) driving firefly luciferase (pCTLA4-Luc), with four different variants that individually harbored deletions of the four putative GAS motifs (pCTLA4-Luc-del1-4) (Fig. 10C). These five constructs were transiently transfected in HEMn-MP cells, along with the control Renilla luciferase construct, and their luciferase activities were tested following 7d of IFN γ treatment. The construct with wildtype CTLA4 promoter (pCTLA4-Luc) showed robust and significant luciferase activity in

response to IFN γ treatment (Fig. 10C). The constructs with the deletion of the most distal putative GAS site (pCTLA4-Luc-del1), and two proximal GAS deletions (pCTLA4-Luc-del3 and -del4) activated intermediate but significant levels of luciferase activity. In contrast, deletion of the second putative GAS site (GAS2 at approximately -850 bp from TSS) (pCTLA4-Luc-del2) completely abolished induction of luciferase in response to IFN γ treatment, clearly identifying this particular site as the principal IFN γ -responsive GAS motif in the CTLA4 promoter region (Fig. 10C).

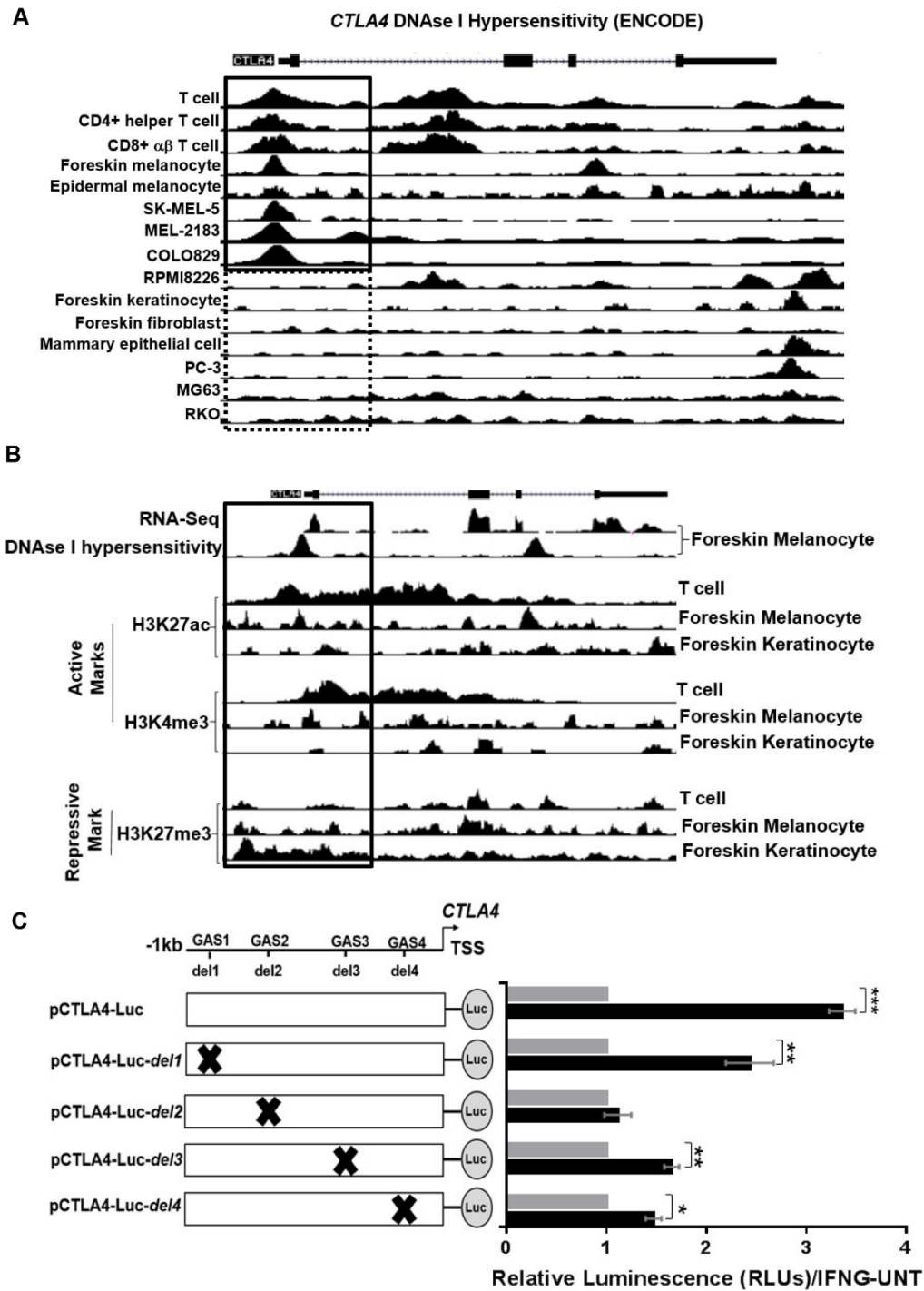


Figure 10. Promoter analysis of human *CTLA4*. A, UCSC genome browser view shows the hu-man *CTLA4* locus (GRCh37/hg19). DNase I hypersensitivity by DNase-seq

analysis for human T cells, CD4⁺ helper T cell, CD8⁺ αβ T cells, foreskin melanocytes, epidermal melanocytes, SK-MEL-5, MEL-2183, COLO829, RPMI8226, foreskin keratinocytes, foreskin fibroblasts, mammary epithelial cells, PC-3, MG63 and RKO were generated by ENCODE Project. Boxes indicate the CTLA4 promoter area. **B**, UCSC genome browser view shows RNA-seq of foreskin melanocytes plus strand signal, DNase-seq signal of foreskin melanocytes and the ChIP-seq fold change signals over control for active promoter marks (H3K27ac, H3K4me3) and repressive mark H3K27me3 in the human T cells, foreskin melanocyte and foreskin keratinocyte and the promoter region around CTLA4 (GRCh37/hg19). **C**, Left: diagrams of firefly luciferase constructs containing putative GAS sites in -1021 bp upstream of TSS. pCTLA4-Luc contains all four putative GAS sites (-1021 bp-TSS), whereas pCTLA4-Luc-del constructs contain single GAS deletions (e.g. del1 for GAS1 deletion) by site-directed mutagenesis. Right: dual luciferase assays were performed in HEMn-MP cells co-transfected with indicated firefly luciferase and Renilla luciferase constructs for 2 d, then cultured in the presence or absence of IFN γ for 7 d. Renilla luciferase activity was used as transfection control. Data are shown as the fold-change of luciferase activity in cells transfected with indicated constructs and treated with IFN γ for 7 d to that of untreated transfected cells. Data represent mean \pm SEM of three biological replicates. *P < 0.05; **P < 0.01; ***P < 0.001.

IFN γ Signaling Recruits the Transcriptional Machinery to the CTLA4 Promoter

We next sought to characterize the recruitment of the IFN γ -induced transcriptional machinery onto the CTLA4 promoter region in melanocytes. Guided by the results of the DNase I hypersensitivity analysis and the promoter analysis above, we designed primer sets to test, by ChIP-qPCR, recruitment of pSTAT1 to three different regions of the CTLA4 promoter and a region downstream of the TSS (Regions R1-4) (Fig. 11A). These regions were strategically selected in regard to the localization of DNase I hypersensitivity and modified histone markers, expected fragmentation size of sonicated DNA, and optimum detection of pSTAT1 recruitment to the CTLA4 TSS. ChIP-qPCR assays with pSTAT1-specific antibody confirmed robust recruitment of pSTAT1 to CTLA4 promoter in an IFN γ -dependent manner (Fig. 11B).

Histone acetylation mediated by histone acetyltransferase CREB-binding protein (CBP)/p300 has been shown to be necessary for transcriptional activation by pSTAT1 (11). Therefore, we assessed the recruitment of CBP/p300 to CTLA4 promoter by ChIP-qPCR analysis, and found that indeed CBP/p300 was recruited there in an IFN γ -dependent fashion (Fig. 11C).

Pretreatment of melanocytes with two different CBP/p300 inhibitors (SGC-CBP30 and PF-CBP1) completely abolished IFN γ -induced CTLA4 expression in HEMn-DP cells (Fig. 11D). Both inhibitor drugs also blocked expression of another CBP/p300-dependent gene, NR4A3, in melanocytes (Fig. 11E). However, they did not affect expression of the housekeeping gene GAPDH, which is not dependent on CBP/p300, and

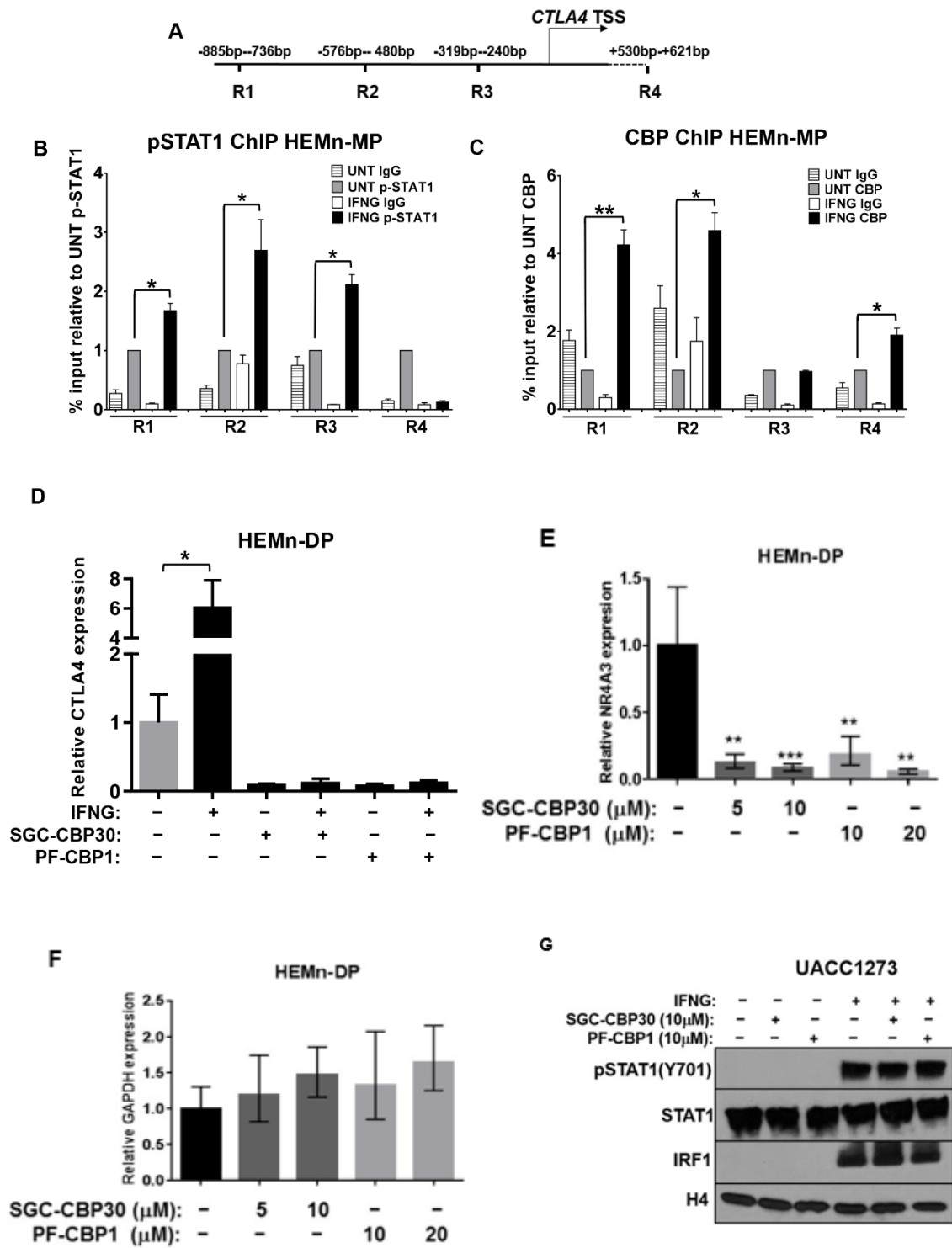


Figure 11. IFN γ /pSTAT1-mediated recruitment of CBP/p300 to the *CTLA4* promoter and accompanied acetylation of histone 3 (H3) and histone 4 (H4). **A**, Schematic representation of primer sets used to detect the *CTLA4* promoter regions (R1-R4). HEMn-MP cells were cultured in the presence or absence of IFN γ for 7 d before being subjected to chromatin immunoprecipitation (ChIP) and qRT-PCR assay with **B**, anti-pSTAT1 (Y705), and **C**, anti-CBP antibodies to measure recruitment to the *CTLA4* promoter. Sonicated nuclear extracts before treatment with antibody were used as input. Relative abundance was calculated as % input and compared to the IFN γ -untreated (UNT) cells. **D**, HEMn-DP cells were pretreated with CBP inhibitors SGC-CBP30 (10 μ M) and PF-CBP1 (20 μ M) for 4 h before IFN γ treatment for 1 d. qRT-PCR analysis of *CTLA4* mRNA expression in HEMn-DP cells after indicated treatments is shown with the data presented as mean \pm SEM of three biological replicates. **E**, qRT-PCR analysis showed that the CBP inhibitors SGC-CBP30 and PF-CBP1 inhibit expression of a known CBP target gene *NR4A3* in HEMn-DP melanocytes after 1 d of treatment, but **(F)** do not affect the expression of the housekeeping gene *GAPDH*. **P < 0.01; ***P < 0.001. **G**, CBP inhibitor treatment does not affect IFN γ signaling, as they failed to block phosphorylation of STAT1 and expression of *IRF1* in response to IFN γ treatment of UACC1273 melanoma cells. UACC1273 cells were pre-treated with either SGC-CBP30 (10 μ M) or PF-CBP1 (10 μ M) for 4 h, then cultured in the presence or absence of IFN γ for 4 h before assessment of pSTAT1, total STAT1, and *IRF1* expression levels by western blot. H4 was used as loading control.

IFN γ -induced STAT1 phosphorylation or IRF1 expression, indicating lack of cellular toxicity (Fig. 11F,G).

IFN γ Signaling Induces Histone Acetylation at CTLA4 Promoter

IFN γ -mediated recruitment of pSTAT1/CBP complex to the *CTLA4* promoter and consequent transcriptional activation in melanocytes was accompanied by enrichment of acetylation of both histones 3 and 4 (AcH3 and AcH4), as shown by ChIP-qPCR analysis with AcH3- and AcH4-specific antibodies (Fig. 12A,B). These results raised the question whether the IFN γ -induced histone acetylation was regional or global. Histone acetylation at the GAPDH locus was found to be unaffected by treatment of melanocytes with IFN γ , indicating that the effect is selective, regional, and perhaps promoter-specific (Fig. 12C). Indeed, global H3 and H4 acetylation were also unaffected by IFN γ treatment of melanocytes, as determined by western blot analysis (Fig. 12D, E, F).

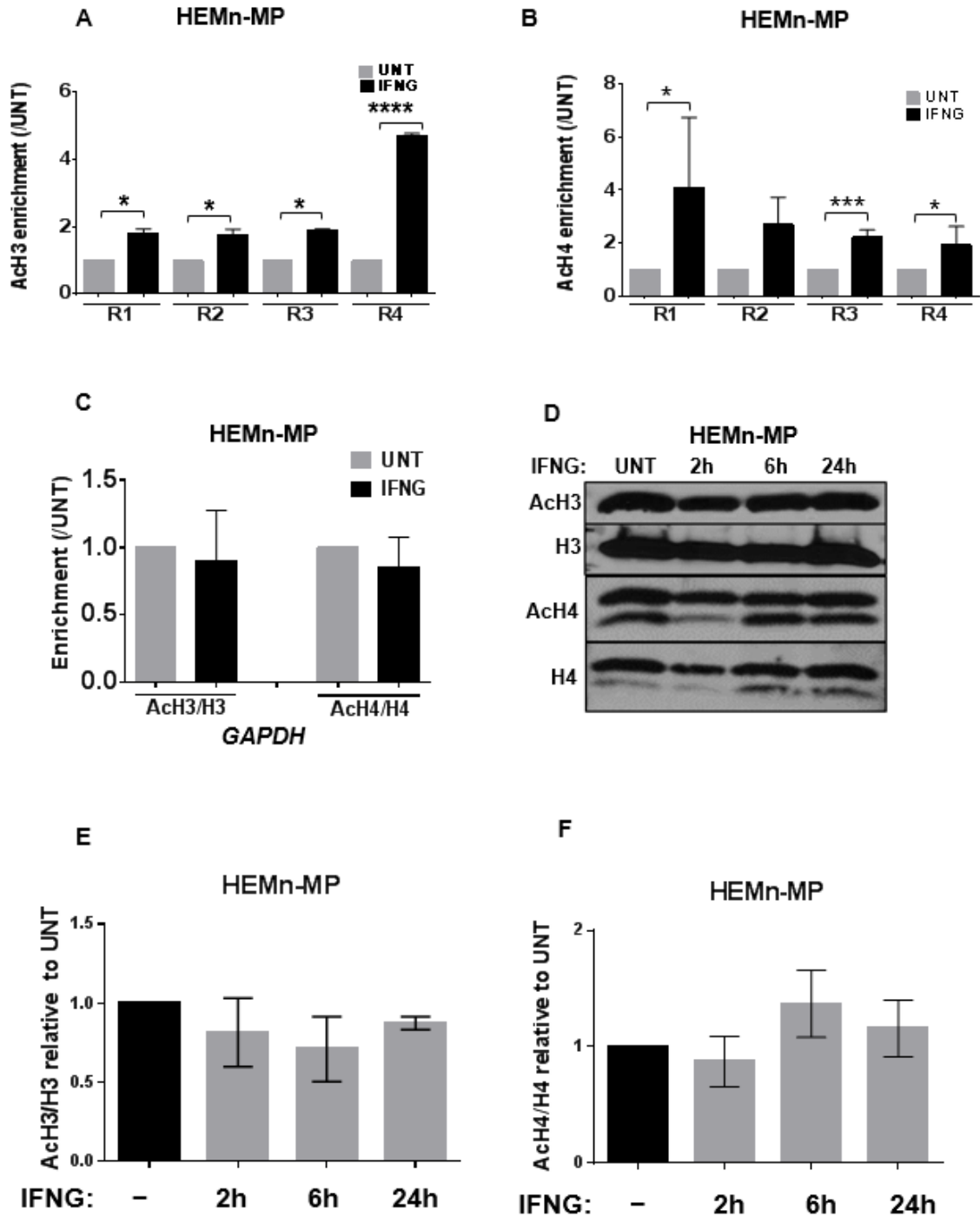


Fig. 12. IFN γ signaling induces histone acetylation at *CTLA4* promoter. A and B, Enrichment of AcH3 and AcH4 around *CTLA4* promoter. C, Enrichments of AcH3 and

AcH4 at the promoter of GAPDH. The enrichment of acetylated histones was normalized to total histone and compared to the IFN γ -UNT cells. **D**, The effect of IFN γ on global levels of AcH3 and AcH4. HEMn-MP cells were cultured in the presence or absence of IFN γ for indicated time, then the global AcH3 and AcH4 levels were detected by western blotting. Immunoblotting images are representative of 3 independent experiments. *P < 0.05; **P < 0.01; ***P<0.001. **E, F**, Quantification of western blotting in D as mean \pm SEM of three independent experiments. Ratios of A, AcH3/H3 to untreated controls and B, AcH4/H4 to untreated controls.

Overexpression of CTLA4 in Melanoma Cell Lines is Regulated by MAPK Pathway

While human melanoma cell lines overexpressed CTLA4, it was unclear whether this overexpression was a result of aberrant activation of the IFN γ pathway. Inhibition of the IFN γ pathway by ruxolitinib treatment did not affect CTLA4 expression in human melanoma cell lines with high baseline CTLA4 expression (Fig. 13A). The baseline expression of other known IFN γ target genes also remained unaffected by ruxolitinib, indicating that these melanoma cell lines do not have an intrinsic upregulation of the IFN γ pathway (Supplementary Fig. 13B-D).

We next asked whether the constitutive activation of the MAPK pathway, driven by oncogenic mutations of BRAF or NRAS, was responsible for the baseline overexpression of CTLA4 in human melanoma cell lines. We utilized the BRAFV600E-specific inhibitor drug vemurafenib (BRAFi) and the MEK inhibitor (MEKi) drug PD0325901 (128). While both vemurafenib and PD0325901 inhibited CTLA4 expression in the BRAFV600E mutant cell lines (but WT for NRAS), only PD0325901 inhibited CTLA4 expression in cell lines carrying mutant NRASQ61K (but either BRAFWT or BRAFN581K) (Fig. 13E). On the other hand, both drugs did not affect the low baseline CTLA4 expression levels of cell lines that did not harbor either BRAFV600E or NRAS mutations (Fig. 13E). Interestingly, the BRAFV600E or NRAS-mutant cell lines expressed CTLA4 at a much greater (40-fold on average) levels than the cell lines wild type for BRAFV600 and NRAS (Fig. 13F). These results clearly indicate that constitutive

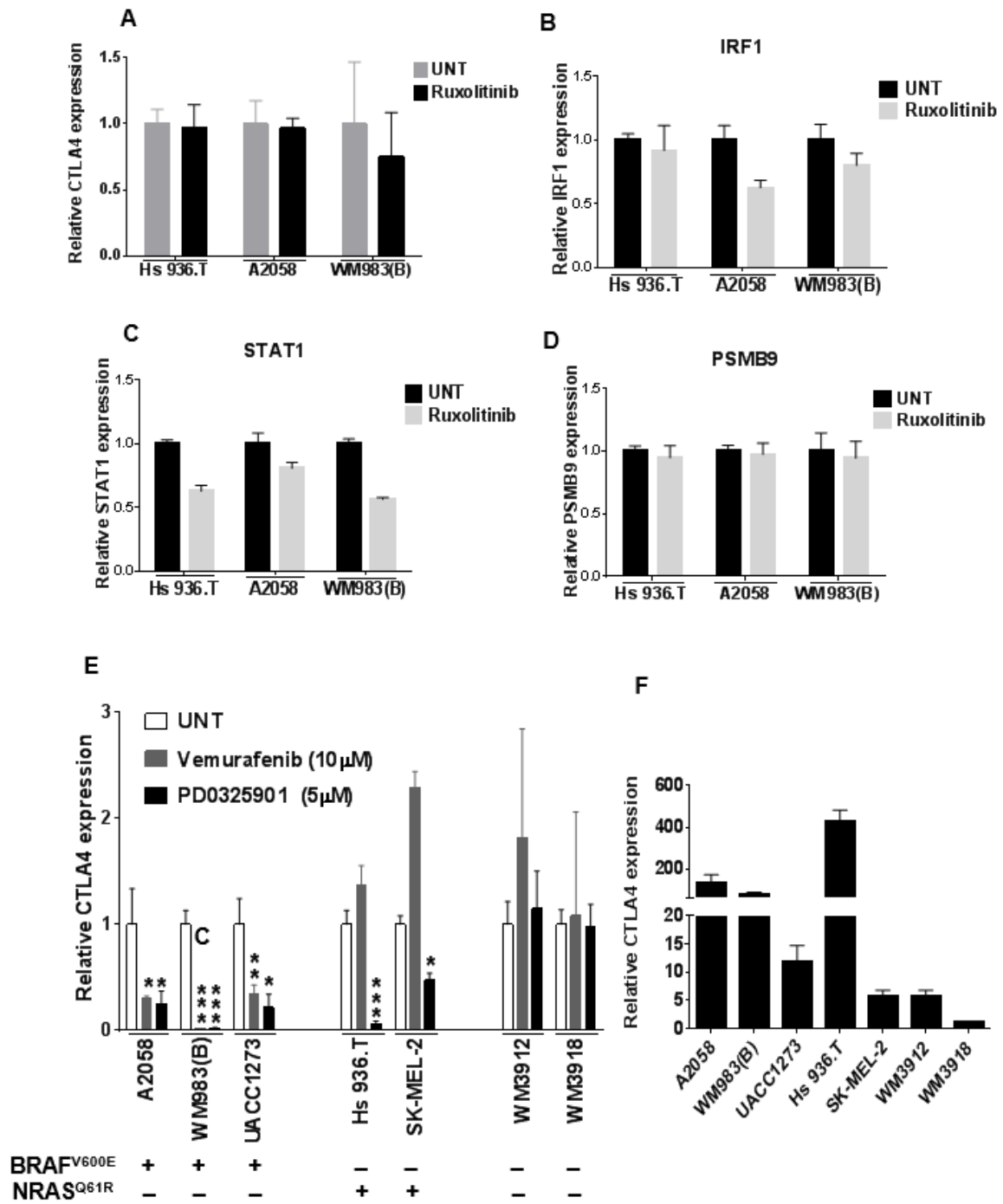


Figure 13. MAPK pathway regulates basal CTLA4 expression in human melanoma cells. A, Ruxolitinib treatment does not affect CTLA4 expression in human melanoma cell lines. The indicated cell lines were treated with Ruxolitinib (5 μM) for 1d and qRT-

PCR analysis of CTLA4 expression was performed. UNT, untreated. **B**, *IRF1*, **C**, *STAT1* and **D**, *PSMB9* expression after indicated treatments. **E**, The indicated cells were treated with either BRAFV600E inhibitor vemurafenib or MEK inhibitor PD0325901 at indicated concentration for 1 d and CTLA4 expression was measured by qRT-PCR. Data presented as mean±SEM of three biological replicates. *P<0.05; **P<0.01; ***P<0.001 over untreated group. The mutational status of each cell line for BRAFV600E and NRASQ61R is given below; +, mutation present; -, mutation ab-sent. **F**, The basal expression of CTLA4 in human melanoma cell lines. Data presented as mean±SEM of three biological replicates for each.

upregulation of the MAPK pathway in melanoma cells enhances CTLA4 expression independent of the IFN γ pathway.

IFN γ -induced Gene Signature in Melanoma Correlates with Response to Ipilimumab

Having determined that CTLA4 is a bona-fide primary IFN γ -responsive gene in melanocytes and melanoma cells, we asked the question whether its expression correlated with that of other known IFN γ target genes in melanoma. We analyzed RNA-seq transcriptome data of melanoma tissues obtained from 20 patients, previously reported by Snyder et al. and Chiappinelli et al. (113, 114). This cohort of 20 patients was part of a larger cohort that had received ipilimumab treatment, and showed either long-term benefit (8 patients with stable disease or better for >6 mo), or no/minimal benefit (12 patients with stable disease for <6 mo or disease progression) (113). Analysis of the transcriptome of these whole melanoma tissues showed that indeed CTLA4 expression significantly correlated with known classical IFN γ target genes, such as STAT1, IRF1, TAP2, GBP2, and HLA-DRB5 (Fig. 14A). Interestingly, CTLA4 expression was also significantly associated with expression of melanoma-associated antigen 11 (MAGEA11), and other immune checkpoints PD-L1, TIM-3 and LAG-3 (Fig. 14A). Intriguingly, clustering of gene expression data of these patients with respect to IFN γ responsive gene expression signature (129) showed that high expression of the IFN γ response signature, including CTLA4, in whole tumor tissue was associated with long-term benefit from ipilimumab treatment (Fig. 14B). In fact, the patients that showed long-

term survival benefit from ipilimumab treatment expressed CTLA4 at significantly higher levels than the non-responders (Fig. 14C, D).

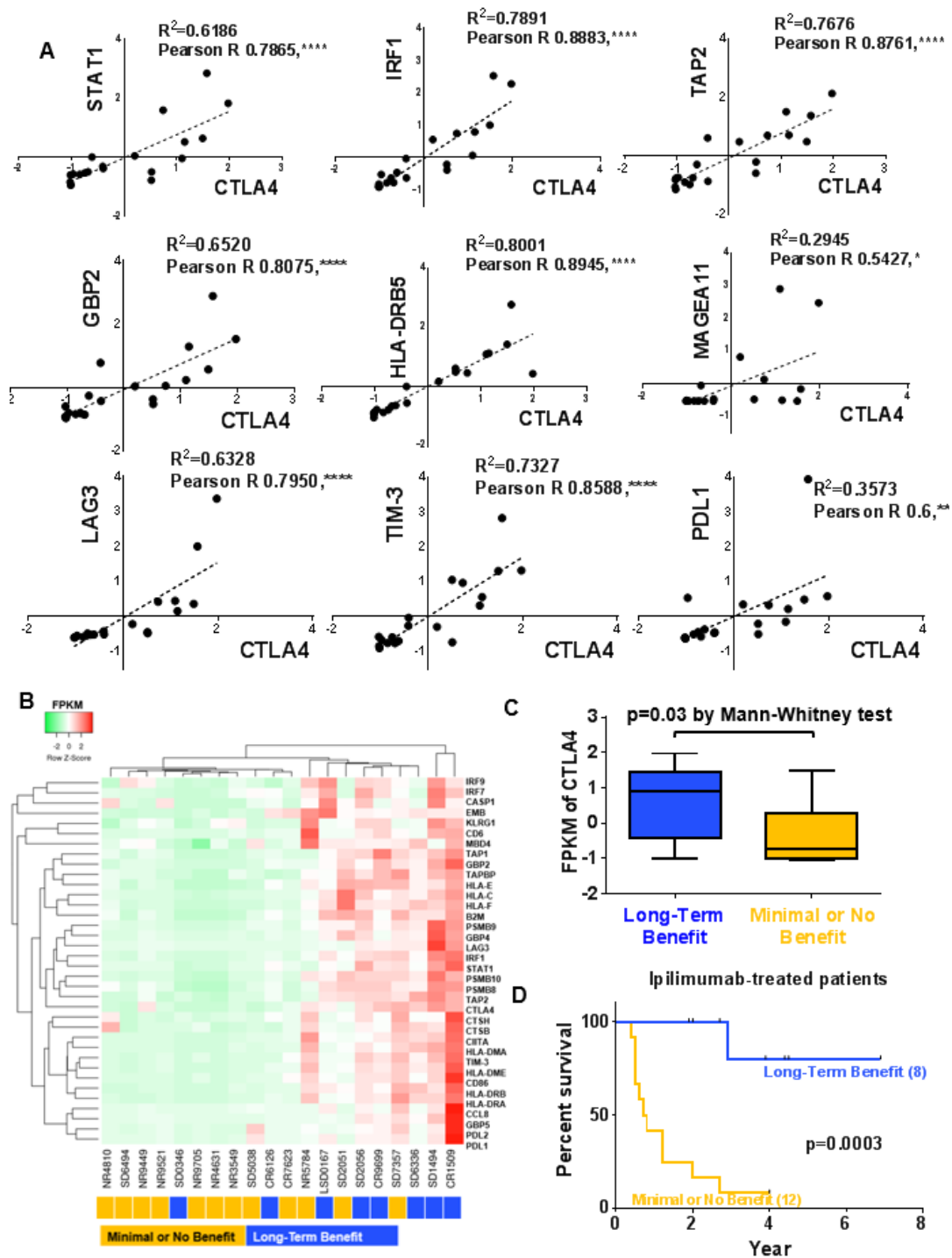


Figure 14. Relationship between CTLA4 expression in melanoma cells and response to anti-CTLA4 immunotherapy. A, Correlation of CTLA4 expression with IFN γ -

response genes STAT1, IRF1, TAP2, GBP2, and HLA-DRB5, a melanoma-specific antigen MAGEA11 and other immune checkpoints TIM-3, LAG3 and PDL1 in human melanoma tumors. X, Y axis, FPKM values of indicated genes. Spearman correlation coefficients (R2), Pearson correlation R, and P values are listed. *P < 0.05; **P < 0.01; ****P < 0.0001. **B**, Clustering analysis was performed on IFN γ -regulated genes and other immune inhibitory receptors TIM-3, LAG3 and PDL1 from anti-CTLA4-treated metastatic melanoma patients with either long-term benefit (blue; n=8) or no/minimal benefit (orange; n=12). **C**, CTLA4 expression in tumor tissues of patients with long-term benefit (blue; n=8) or no/minimal benefit (orange; n=12). **D**, Kaplan-Meier overall survival analysis between metastatic melanoma patients with long-term benefit from anti-CTLA4 immunotherapy treatment and no/minimal benefit patients. P is via log-rank test.

CHAPTER 4

THE ROLE OF CTLA4 IN MEDIATING MELANOMA IMMUNOEVASION

Materials and Methods

Cell Culture

Mouse melanoma cell lines B16, B16N (a subclone cell line of B16 generated at National Cancer Institute), B2903 and B2905A (generated by UV irradiation of *Hgf* transgenic C57BL/6 mice) were cultured in Dulbecco's Modified Eagle Medium (DMEM) supplemented with 10% fetal bovine serum (FBS), L-alanyl-L-Glutamine (2mM) and Gentamycin (50ug/ml) at 5% CO₂.

Mouse Imaging and Quantification of Bioluminescent Signal

All C57BL/6 and NOD scid gamma (NSG) mice used for tumor experiments are 6 to 7-weeks old female mice purchased from The Jackson Laboratory. To establish the B16N or B2905A tail vein tumor model, we inoculated 1.25×10^5 tumor cells into either C57BL/6 or NSG mice through tail-vein (t.v.) injection. To establish the B2905A subcutaneous tumor model, we inoculated 5×10^5 tumor cells into C57BL/6 by subcutaneous (s.c.) injection. To assess the bioluminescent intensity, tumor-bearing mice were administrated 200 μ l of D-Luciferin (15mg/ml, Caliper) by intraperitoneal (i.p.) injection and imaged for luminescent signal by IVIS Imaging System after 10 min post i.p. injection. The bioluminescence signal was recorded as total flux (p/s/cm²/sr) in indicated regions.

Histology

The lung tissues and other organs were harvested and preserved in 10% formalin for 1 d at room temperature and then transferred to 70% ethanol in PBS. All staining of tissues and histological counting of lung nodules were blindly and independently performed by histopathology facility at Fox Chase Cancer Center.

Lentivirus Production and Transduction

Mouse *Ctla4* construct was subcloned into pLVX-IRES-zGreens lentiviral vector (Clontech). Lentiviruses were packaged in and produced by Lenti-X 293T cells (Clontech). B2905A-Luc+, B16N-Luc+ and B2903 mouse melanoma cells were transduced with lentiviruses encoding either *Ctla4* or empty vector. GFP+ cells were sorted by Influx cell sorter a week after transduction.

Flow Cytometry

For intracellular staining, T cells and mouse melanoma cells were fixed and permeabilized by BD Fixation/Permeabilization Solution Kit, followed by manufacture's protocol. Mouse melanoma cells and T cells were stained with antibodies for 30 min at 4°C.

For surface staining, T cells and melanoma cells were blocked in PBS containing 2.5% FBS for 15 min at 4°C before stained with antibodies for 30 min at 4°C.

Anti-mouse *Ctla4*-APC (UC10-489, eBiosciences), anti-mouse CD80-APC (16-10A1, BioLegend), anti-mouse CD86-FITC (GL-1, BioLegend), anti-mouse IFN γ -FITC

(XMG1.2, BioLegend) and isotype control antibodies were used. Cells were then washed and analyzed on a BD FACSCalibur. The data were analyzed using FlowJo software.

CD8+ T Cell Isolation, Activation and Culture in Vitro

CD8⁺ T cells were isolated from mouse spleen and lymph nodes by CD8a (Ly-2) Microbeads (Miltenyi Biotec). T Cells were maintained in Iscove's Modified Dulbecco's Medium (IMDM) medium supplemented with 10% fetal bovine serum (FBS) at 37°C in humidified atmosphere containing 5% CO₂. For *in vitro* stimulation, isolated CD8 T cells were cultured with 10ng/ml mouse IL2 and anti-CD28 antibody (37.51, 1-5µg/ml, BioLegend) at a density of 1-2*10⁵ cells/well in 96-well round-bottom plates coated with anti-CD3 antibody (17A2, 1-5µg/ml, BioLegend).

CFSE Labeling

Isolated CD8 T cells from *Pmel-1* transgenic mice were stained with 5µM CFSE (Life Technology) in PBS containing 2.5% FBS for 20 min. CFSE labeled T cells were cultured and activated as described, and in the presence or absence of anti-CD80 antibody (16-10A1, 10µg/ml, BioLegend) or anti-CD86 antibody (GL1, 10µg/ml, BioLegend). CFSE staining was determined by Flow cytometry at indicated time points.

Co-culture Assay

B2903 melanoma cells were seeded at 2×10^4 cells/well in 96 round-bottom plates and cultured with or without activated Pmel-1 CD8⁺ T cells that were activated for 4 d. The survival of melanoma cells was determined by WST-1 cell viability assay after 24 h of co-culture. The T cells were assessed IFN γ production by Flow cytometry.

Results

Ctla4 Expression Enhances Melanomagenesis in Vivo

Mouse melanoma cell lines (B16N, B2905A, and B2903) expressed very low to zero levels of Ctla4. We first generated ectopic expression of Ctla4 in mouse melanoma cell lines B2905A-Luc which expressed firefly luciferase. Flow cytometry analysis showed that we successfully generated B2905A-Luc cells expressing both intracellular and surface Ctla4 (Fig. 15A). To assess the effect of ectopic expression of Ctla4 in melanomagenesis, we inoculated either B2905A-Luc+-empty vector (EV) or B2905A-Luc+-Ctla4 over-expressed (Ctla4-OE) cells in immunocompetent and syngeneic C57BL/6 mice via tail vein injection and monitored tumor growth by measuring bioluminescent signal on day 0, 7, 11, 18, 21, 25 and 31 using IVIS system. Luminescent intensity in lungs of tumor-bearing mice after 31 d post-injection showed that most of the tumor cells injected grew in the lung, except for a small percentage of mice that developed micro-metastases (Fig. 15B). The luminescent intensity in the lungs of Ctla4 OE group was higher than the control EV group (Fig. 15B). Interestingly, the tumor burden of Ctla4-expressing B2905A cells was indistinguishable from control EV cells before day 18 (Fig. 15C). Beyond time point of day 18, the growth of the control EV cells reached a stationary phase. In contrast, Ctla4-expressing had continual rapid growth (Fig. 15C). This suggests that mice may develop anti-tumor immunity to restrain the growth of the controls tumor cells after day 18. But Ctla4 expression protected melanoma cells from the immune system. In addition, we observed micro-metastases in lower abdomen of some mice in both groups (2 out of 7 in EV group, 4 out of 7 in Ctla4 OE group). The

micro-metastases in #5 of the CTLA4-OE group was confirmed as bladder metastases by histological analysis. The Ctla4-OE group had higher luminescent intensity than the control group, but it did not reach statistical significance, probably due to a low number of samples (Fig. 15D). This suggests that Ctla4 expression may enhance melanoma cells metastasize to secondary organs. Lung tissues of tumor-bearing mice were harvested at d 31 post-injection. Images of lung tissues showed that Ctla4-OE group had more surface metastases (Fig. 15E) as confirmed by histological counts (Fig. 15F). Strikingly, histological analysis of lung tissues showed that lung nodules in control group were heavily infiltrated by lymphocytes and few melanoma cells remained, which were only seen in a few mice in Ctla4-OE group. This may explain the stationary growth phase in mice injected with the control cells.

To assess whether Ctla4-enhanced melanomagenesis was tumor cell-specific, we overexpressed Ctla4 in another melanoma cell line B16N. Flow cytometry showed that B16N-Ctla4 OE cells highly expressed both surface and intracellular Ctla4, but not B16N-Empty Vector (EV) cells (Fig. 16A). To confirm the effect of ectopic expression of Ctla4 expression in melanomagenesis, we administered either B16N-EV or B16N-Ctla4 OE cells in C57BL/6 mice via tail-vein injection. B16N cells grew more aggressively than B2905A cells and we harvested lung tissues at d 20 post-injection. Images of the lung tissues confirmed the results observed in B2905A cells, that expression of Ctla4 in B16N increased tumor growth in the lung (Fig. 16B), as well as by histological counts (Fig. 16C).

Taken together, these results demonstrate that the ectopic expression of CIta4 in melanoma cells promotes tumor growth in lung *in vivo*. CIta4-enhanced melanomagenesis is potentially mediated by inhibition of host anti-tumor immunity.

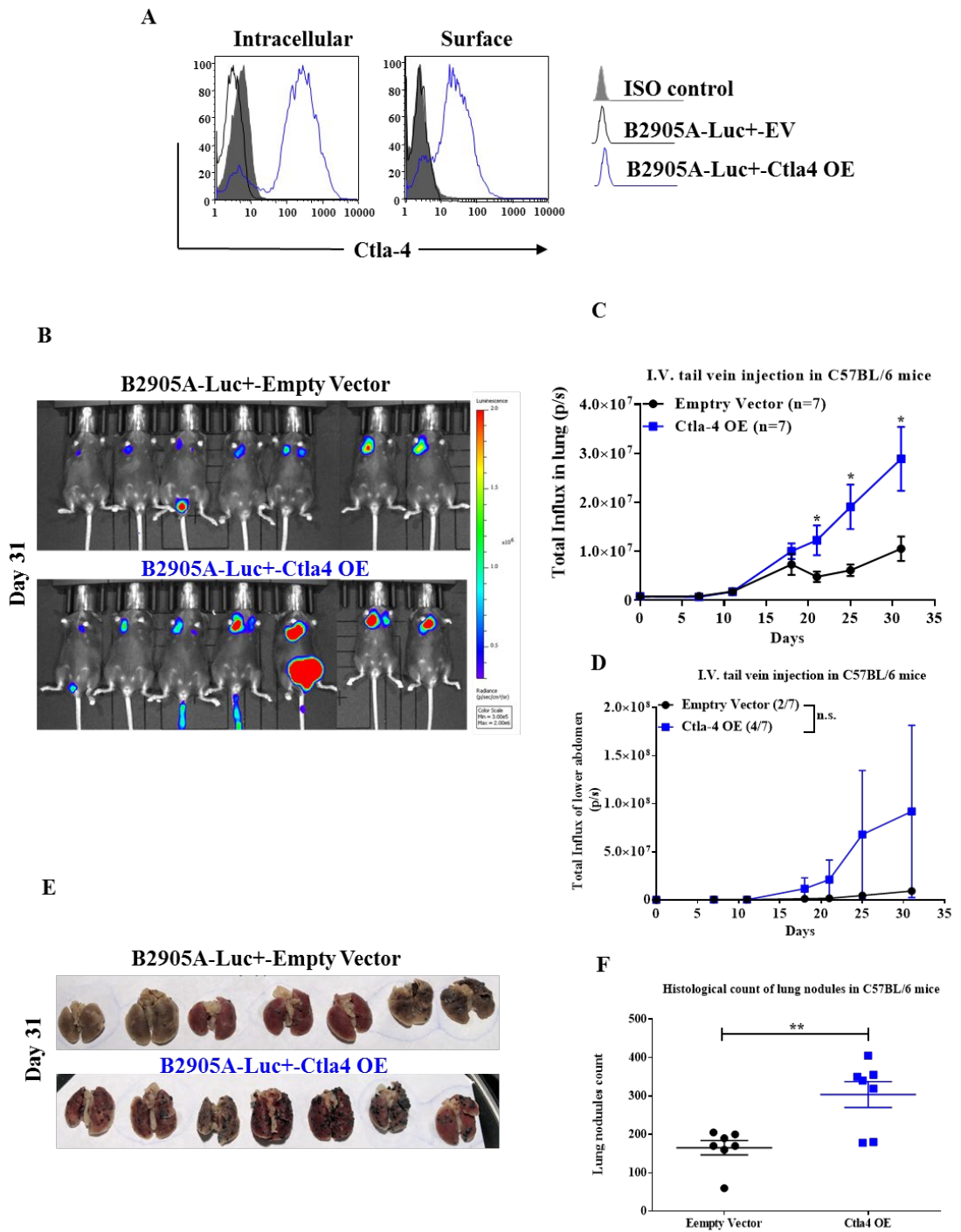


Figure 15. Effects of ectopic expression of CtlA4 in melanomagenesis of B2905A. A, B2905A-Luc+ (encoding luciferase) mouse melanoma cells were transduced with either

empty lentiviral vector (pLVX-IRES-zGreens) or lentiviral vector encoding mouse Ctla4. Flow cytometry analysis of surface and intracellular Ctla4 expression. **B**, B2905A-Luc+ EV or B2905A-Luc+-Ctla4 OE cells were injected via tail-vein injection in C57BL/6 mice. (n=7 per group). *In vivo* luminescent image of mice bearing either B2905A-Luc+ EV or B2905A-Luc+-Ctla4 OE cells at d 31 post-injection. **C**, Luminescent signals (Y-axis, total flux, p/s/cm²/sr) of lung tissues were monitored from d 0 to d 31 post-injection. The data represents as the mean±SEM of seven mice of each group. **D**, Luminescent signals (Y-axis, total flux, p/s/cm²/sr) of micro-metastasis in the lower abdomen were monitored from d 0 to d 31 post-injection. The data represents the mean±SEM of two mice in EV group and four mice in Ctla4-OE group. **E**, Image of lung tissues harvested at d 31 post-injection. **F**, Histological counts of lung nodules were compared between EV group and Ctla4 OE group. *P<0.05; **P<0.01.

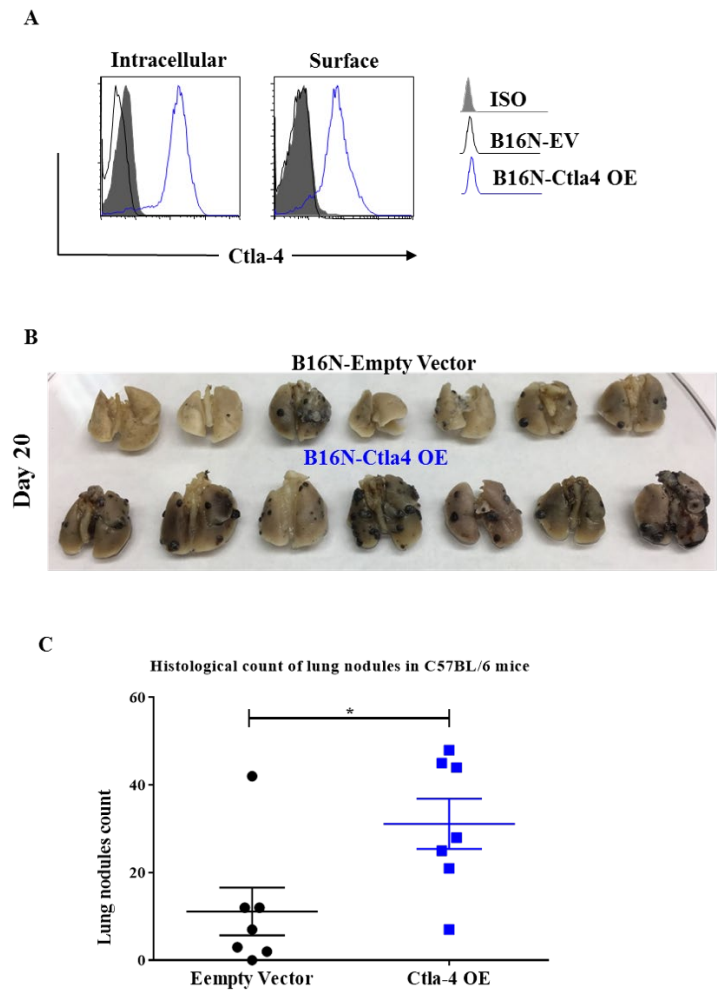


Figure 16. Effects of ectopic expression of Ctla4 in melanomagenesis of B16N. **A**, B16N mouse melanoma cells were transduced with either empty lentiviral vector (pLVX-IRES-zGreens) or lentiviral vector encoding mouse Ctla4. Flow cytometry analysis both of surface and intracellular Ctla4 expression. **B**, B16N-EV or B16N-Ctla4 OE cells were injected via tail-vein injection in C57BL/6 mice (n=7 for each group). Image of lung tissues harvested at d 20 post-injection. **C**, Histological counts of lung nodules were compared between EV group and Ctla4 OE group. *P<0.05.

Ctla4-enhanced Melanomagenesis is Mediated by Inhibition of the Immune System

To evaluate the role of the immune system in Ctla4-enhanced melanomagenesis, we inoculated either B2905A-EV or B2905A-Ctla4 OE into immunodeficient NSG mice via tail vein injection. NSG mouse is deficient in mature lymphocytes and serum immunoglobulin (Ig), and lacks of functional NK cells. Tumor growth curves showed that both the control group and the Ctla4-OE group grew exponentially in NSG mice, and there was no difference of tumor burden in the lung (Fig. 17A, B). This was also confirmed by the histological count of lung nodules (Fig. 17C). Interestingly, we observed no stationary growth phase of B2905A-EV cells in NSG mice, which we saw in C57BL/6 mice at 18 d post-injection. It suggested that halt in proliferation of B2905A-EV cells in C57BL/6 mic, was due to the host immune system. Additionally, Ctla4 OE group had higher luminescent signals in micro-metastases than control group in NSG mice (Fig. 17D), which was similar to what we observed in C57BL/6 mice. This reveals that the expression Ctla4 in melanoma cells may have intrinsic effects on secondary metastasis, which is independent in the immune system.

We also inoculated B2905A-EV or B2905A-Ctla4 OE cells into C57BL/6 mice via subcutaneous injection. The tumor growth curves showed that tumorigenesis did not differ significantly between those two groups (Fig. 17E, F). Differences in tumorigenesis between subcutaneous model and tail vein model have been observed in numerous studies (130, 131). Subcutaneous tumor is poor at angiogenesis, which leads to limit accesses to immune system (132). It is also possible that Ctla4-enhanced melanomagenesis is dependent on the lung microenvironment.

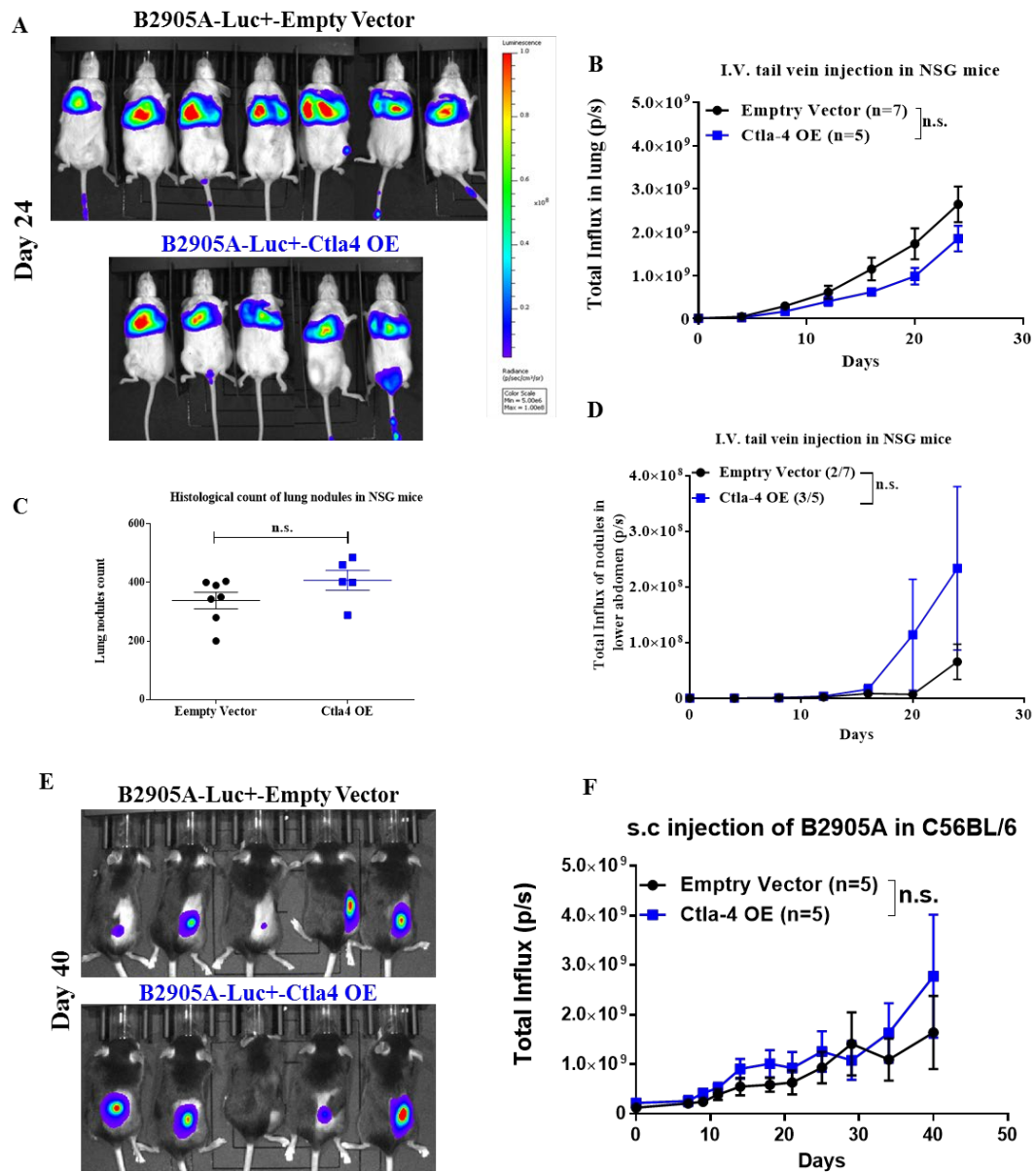


Figure 17. Role of the immune system in Ctla4-enhanced melanomagenesis. (A-D)

Melanoma cells were inoculated via tail vein injection in NSG mice (B2905A-Luc+-EV, n=7; B2905A-Luc+-Ctla4 OE, n=5). **A**, *In vivo* luminescent images of mice bearing either B2905A-Luc+-EV or B2905A-Luc+-Ctla4 OE cells at 24 d post injection. **B**, **D**, Luminescent intensity (Y axis, total flux, p/s/cm²/sr) of lung nodules were monitored

from d 0 to d 24. **C**, Histological count of lung nodules was compared between the EV group and Ctl4-OE group. (**E-F**) Melanoma cells were inoculated via s.c. injection in C56BL/6 mice (n=5 for both groups). **E**, *In vivo* luminescent image of mice bearing either B2905A-Luc+-EV or B2905A-Luc+-Ctl4 OE cells at 40 d post-injection. **F**, Luminescent intensity (Y axis, total flux, p/s/cm²/sr) of the tumor burden was monitored from d 0 to d 40. The data represents the mean±SEM of five mice per group. n.s. not significant.

Ligation of CD86 in T Cells Inhibits CD8 T Cells Proliferation in Vitro, but not CD80 Ligation

The Ctla4 ligands, CD80 (B7.1) and CD86 (B7.2) are expressed on APCs, mostly dendritic cells and B cells. CD80 and CD86 expressed on APCs play an important role in T cell activation during priming phase. The ligation of CD80 and CD86 with CD28 expressed on T cell provides important co-stimulatory signal to fully activate T cell. Thus, the function of CD80 and CD86 on APCs is well studied and elucidated. Interestingly, it has been reported that expression of CD80 and CD86 on both mouse and human T cells (133, 134). But the expression and functions of these ligands on T cells are largely unclear.

We first tested if CD8 T cells express CD80 and CD86 by flow cytometry. Indeed, activated CD8 T cells robustly expressed surface CD80 and CD86. Interestingly, only a small percentage of activated CD8 T cells were double positive for CD80 and CD86 (Fig. 18A). To test the effect of CD80 or CD86 ligation in CD8 T cell proliferation, we labeled freshly isolated CD8 T cells with CFSE, and then activated with anti-CD3/CD28 antibodies and IL2 in the presence or absence of either anti-CD80 or anti-CD86 antibodies. Surprisingly, treatment of anti-CD86 antibody dramatically suppressed CD8 T cell proliferation as early as 2 d, and the inhibitory effect was lasting as long as 6 d. In contrast, treatment of anti-CD80 antibody alone did not affect CD8 T cell proliferation (Fig. 18B, C). This data reveals that ligation of CD86 delivered negative signals to CD8 T cell proliferation during activation *in vitro*.

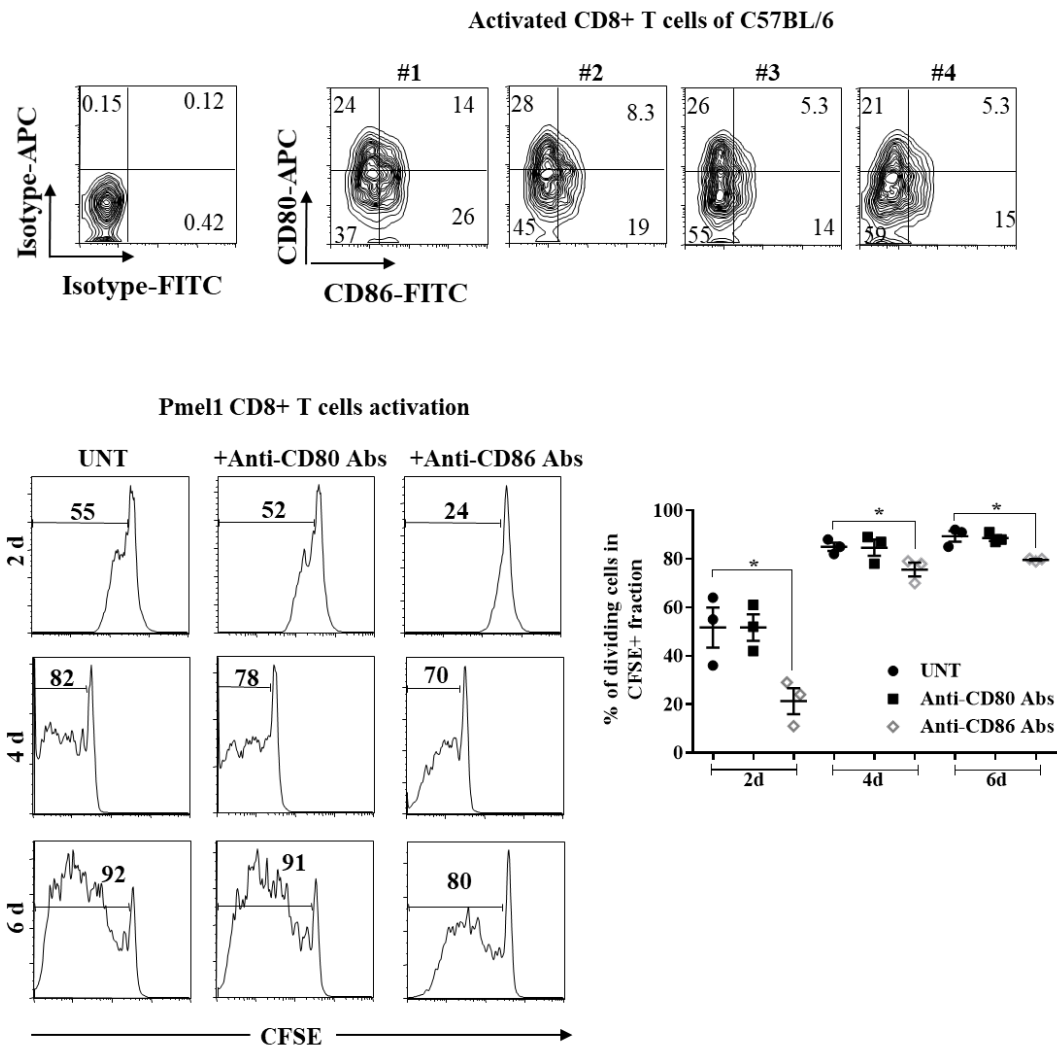


Figure 18. The role of CD80 and CD86 in regulation of the activation and proliferation of CD8 T cells. **A**, CD8+ T lymphocytes were isolated from spleen and lymph nodes of C57BL/6 mice. T cells were activated by culturing with anti-CD3/CD28 antibodies and IL2 for 6 d. Flow cytometry analysis of expression CD80 (B7-1) and CD86 (B7-2) on the surface of activated CD8+ T cells, a total of four mice were used. **B**, CFSE-labeled CD8+ T cells isolated from Pmel-1 mice were activated by culturing with anti-CD3/CD28 antibodies and IL2 for indicated the time-points in the presence or

absence of either anti-CD80 antibody (10 μ g/ml) or anti-CD86 antibody (10 μ g/ml).

Percentage is the proportion of cells that proliferated. **C**, Quantification in **B**. The data represents the mean \pm SEM of T cells isolated from three Pmel1 mice. *P<0.05.

Expression of Ctl4 in Melanoma Cells is Resistant to CD8 T Cell Cytotoxicity in Vitro

To evaluate whether Ctl4 expression in melanoma cells is protective against CD8 T cell cytotoxicity, we co-cultured either B2903-EV or B2903-Ctl4 cells with varying ratios of gp100-specific CD8 T cells (were activated for 4 d *in vitro*) for 1 d. Ctl4-expressing cells exhibited complete protection from CD8 T cells-mediated cytotoxicity when co-cultured in 1:1 or 1:3 (melanoma cell: T cell) ratio (Fig. 19A). Interestingly, the survival of Ctl4-expressing cells dramatically decreased when co-cultured in 1:5 ratio suggested that the excessive number of T cells had overcome the protective effect mediated by Ctl4. IFN γ production is important for cytotoxicity of CD8 T cells. IFN γ production in Pmel-1 CD8 T cells was significantly lower when co-cultured with Ctl4-expressing melanoma cells compared to the control cells (Fig. 19B, C).

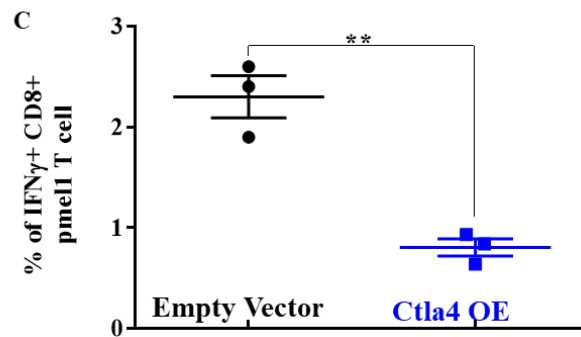
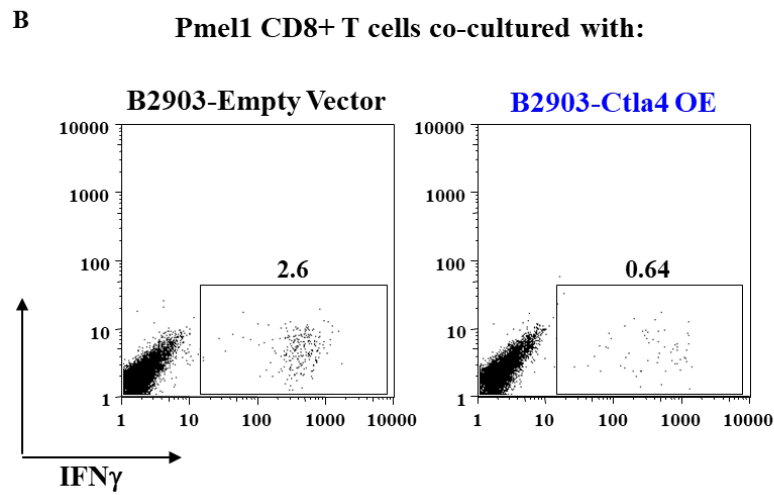
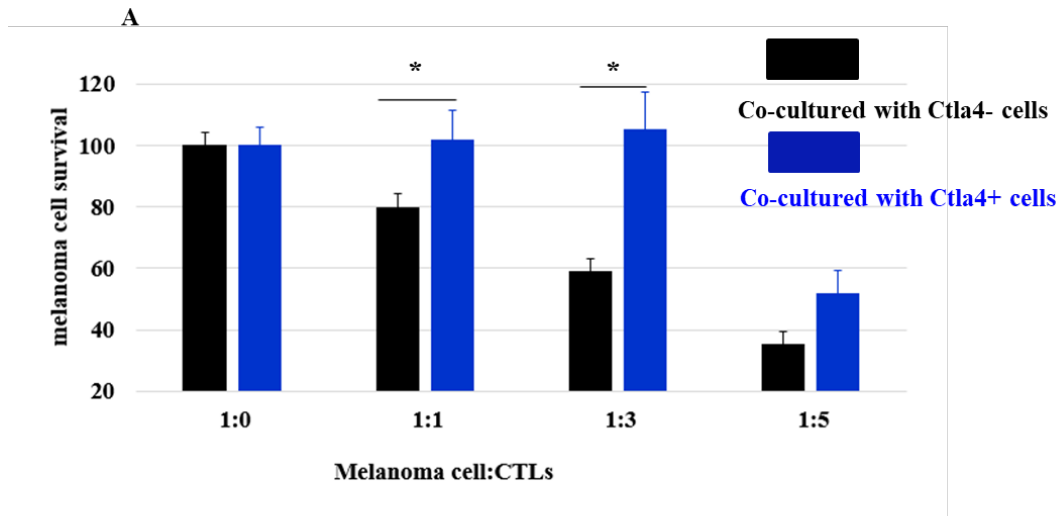


Figure 19. Role of Ctla4 in inhibition of CD8 T cell cytotoxicity. A, B2903-EV and B2903-Ctla4 OE melanoma cells were co-cultured with CD8+ T cells expressing anti-

gp100 TCR isolated from Pmel-1 mice at the indicated ratios. The data represents as the mean \pm SEM of four independent co-cultures, relative to survival of melanoma cells without T cells. *P<0.05. **B**, Representative flow cytometry analysis of IFN γ production CD8⁺ T cells after co-culture with melanoma cells for 1 d. **C**, Quantification of the percentage of IFN γ producing CD8⁺ T cells isolated from mice after co-culture with either Ctl4-expressing or control cells. Each dots represent one mice used for T cell isolation. *P<0.05; **P<0.01.

CHAPTER 5

DISCUSSION

Part I: Interferon Gamma Regulates Melanogenesis in Mouse Melanoma Cells

We demonstrated that accumulation of fully glycosylated, mature tyrosinase in B16 and B16N cells cultured with IFN γ was mediated by Jak1/2-Stat1 axis in a temporal manner. Treatment of IFN γ rapidly activated pStat1 as early as 20 min, but we did not observe increasing melanogenesis until 3 d of treatment. Interestingly, continual treatment of IFN γ was not required. Type I interferon, IFN α 2 activates the formation and activation of Stat1-Stat2-Irf9 complexes, leading to initial transcription of genes with IFN-stimulated response elements (ISREs). IFN α 2 also initiates and activates the formation of Stat1-Stat1 homodimers (3). However, IFN α 2 treatment did not increase melanogenesis, which suggested another indirect signaling pathway was activated by IFN γ contributed to melanin synthesis.

Mitf was rapidly upregulated by α MSH via activation and phosphorylation of Creb as early as 2 h, which resulted in elevating the expressions of Tyr and Tyrp1, and increasing melanin synthesis for 1 d of treatment. In contrast, we only observed upregulation of Mitf by IFN γ for 1 d of treatment. Additionally, Knock-out Stat1 abolished upregulation of Mitf by IFN γ . This data indicates that IFN γ /Jak1/2/Stat1 indirectly increases the expression of Mitf, but the molecular mechanisms of regulating Mitf transcriptional expression need to be further investigated.

Numerous evidence has shown the role of Mitf in initiating and maintaining the transcription of *Tyr*, *Tyrp1* and *Dct* in melanocytes and melanoma cells. Unexpectedly, IFN γ did not increase mRNA expression of *Tyr*, *Tyrp1* and *Dct* despite that it increased Mitf expression. In contrast, upregulation of Mitf by α MSH dramatically elevated mRNA expression of *Tyr* and *Tyrp1*. One possible explanation is that IFN γ potentially induced factors negatively cooperated with Mitf in regulating transcription levels of *Tyr* and *Tyrp1*. It has been reported that Mitf-induced transcription of *Tyr*, *Tyrp1* and *Dct* is dependent on other transcriptional factors, such as Sox10. MITF cannot induce the transcription of *TYR* and *TYRP2* in absence of SOX10 (135-137). IFN γ decreased *Sox10* expression (data not shown), which might explain why mRNA expression of *Tyr* was unresponsive to upregulation of Mitf. However, we observed elevation of Tyr protein levels by IFN γ treatment for 4 d, which suggested that IFN γ upregulated Tyr protein expression via post-transcriptional mechanisms. This also explained the lag in induction of melanin biosynthesis between treatment of IFN γ or α MSH. Newton et al. have also reported that the elevation of MITF expression only increases tyrosinase protein expression, but not its mRNA expression in human melanocytes by treatment of forskolin, a melanogenesis inducer (102). Taken together, MITF regulates melanogenesis via both directly transcriptional regulation of melanin synthesis enzymes, or indirect post-translational modulation of melanosome biosynthesis including maturation and trafficking of melanogenesis-related enzymes.

The role of IFN γ in regulation of vascular pH is largely unknown and warranted further investigation. Khalkhali-Ellis et al. have reported that IFN γ decreased vacuolar

pH via Stat1 signaling pathway in mammary epithelial cells and breast cancer cell lines (138). Indeed, we have found that vacuolar-type H⁺-ATPase genes that are responsible for acidification of vacuole were upregulated upon IFN γ treatment by RNA-seq analysis. However, melanosomal pH, especially in stage I and stage II melanosomes, were alkalized by IFN γ via upregulation of *Oca2* expression that was melanocyte/melanoma-specific. This suggests that the regulation of pH by IFN γ may be cell-specific to fulfill different functions via various mediators. In melanocytes/melanoma cells, the alkalization of early-stage melanosomes facilitated melanosome maturation, results in increasing trafficking and accumulation of mature tyrosinase. Our data suggests that *Mitf* can potentially induce *Oca2* expression to regulate melanogenesis independently transcriptional initiation of melanogenesis-related genes.

Wang et al. showed that IFN γ enhances melanin content in normal human melanocytes as well as upregulation of melanogenesis-related genes (139). Additionally, Bae et al. have observed hyperpigmentation of tail skin, where epidermal melanocytes are present, in *ARE-Del*^{-/-} mice that have chronic circulating serum IFN γ (140). They suggested that skin hyperpigmentation was the consequence of primary biliary cholangitis (140). However, we propose that the hyperpigmented tail skin in those mice most likely results from the chronic exposure to IFN γ in tail skin microenvironment. In some contexts, Natarajan et al. and Son et al. have shown that IFN γ signaling causes hypopigmentation and reduces α -MSH-induced melanin synthesis in B16 cell (141, 142). One possible explanation was that the B16 cells used in these papers had a saturated pigmentation level and the treatment of IFN γ was not long enough to observe increasing

melanin synthesis. They also proposed that *IFNG*^{-/-} mice in C57BL/6 background presented hyperpigmented tail phenotype. Nonetheless, we did not observe the same phenotype in our in house IFN γ -null C57BL/6 mice. The contradictory results suggest that IFN γ -induced melanogenesis may be in a cell-type specific manner.

Interestingly, Yang et al. have proposed that constitutive activation of Stat3 in B16 cells was important for tyrosinase expression (12). They mutated the phosphorylation site of Stat3 at Y705, which resulted in loss of transcriptional activity. The overexpression of mutated Stat3 (dominant-negative Stat3) in B16 cells decreases tyrosinase expression, which leads to melanin synthesis inhibition (12). Yet, we did not observe reduction of tyrosinase expression and melanin synthesis in Stat3-KO clones we generated by CRISPR-Cas9. Additionally, we have shown that IFN γ -induced hyperpigmentation was mediated by Stat1 signaling axis, but not Stat3 signaling axis. These results suggest that depigmentation effect mediated by Stat3-DN is due to unidentified mechanisms, rather than disruption of transcription function of Stat3. Indeed, Liu et al. have recently demonstrated an unexpected role of STAT3 in regulating lysosomal pH (143). STAT3 decreases lysosomal pH via enhancement of lysosomal vascular H⁺-ATPase activity by association that is dependent on coiled-coil domain of STAT3 and independent on phosphorylation of either Tyr705 or Ser727 (143). It implies that the overexpression of Stat3-DN in B16 cells may acidify melanosomal lumen via enhancing H⁺-ATPase activity from extra cytosolic Stat3 protein, which sequentially results in the loss of pigmentation. This highlights the importance of melanosomal pH in regulation of melanogenesis.

Clinical Implication

The Postinflammatory hyperpigmentation (PIH) is a normal skin response to cutaneous inflammatory stimulations such as skin wounding process, especially in dark-skinned individuals (144). In the wounding site, hyperpigmentation is due to an increasing production and secretion of melanin by melanocytes (145). PIH significantly impaired quality of life of those patients because it lasts months to years. However, the molecular mechanisms of PIH are not well understood. Many epidemiological studies have shown that PIH is among the most common reasons for darker-skinned individuals seeking dermatological consultation (144). The treatment options include topical tyrosinase inhibitors and other depigmentation agents, but remain limited (144). Prevention of PIH is also considered as one of valuable treatment options. However, the lack of prevention strategies is due to the complex unknown pathogenesis of PIH. The skin wounding process recruits robust cytokines-secreted inflammatory cells that are responsible for clearing debris and infections. It has been reported that IFN γ plays an important role in wound healing process and pathogenesis of PIH (146). We have demonstrated that IFN γ induces hyperpigmentation. Thus, it potentially serves as a positive mediator of PIH. Administration of anti-IFN γ antibody or JAK1/2 inhibitor at the wounding sites have potential to prevent or at least attenuate PIH in patients. However, further studies are needed to fully elucidate the role of IFN γ in the pathogenesis of PIH and clinically evaluate the efficacy of IFN γ blockade for treatment of PIH.

Part II: The Role of Interferon Gamma-induced CTLA4 in Tumor Immunoavoidance

It is conventionally thought that CTLA4 is predominantly expressed in immune lineages, mainly T cells. Here we show that CTLA4 is expressed in human primary melanocytes and is highly overexpressed in melanoma cell lines, but not in non-melanoma tumor cell lines. Concordantly, we have found that the promoter region of CTLA4 exhibits open chromatin configuration in melanocytes and melanoma cells, akin to T cells, but not in other cell types. Most interestingly, we have identified CTLA4 as a novel downstream target gene of IFN γ signaling via activation of STAT1-mediated signaling, which recruits CBP and POLII to the *CTLA4* promoter and modulates histone acetylation. An analysis of previously published RNA-seq datasets of melanoma patients treated with ipilimumab showed that patients that exhibited an IFN γ -responsive gene expression signature, including overexpression of CTLA4, demonstrated better clinical response than those that did not express this signature.

The overexpression of CTLA4 is driven by the constitutively activated MAPK pathway in human melanoma cell lines that harbor activating BRAF or NRAS mutations. This intriguing finding reveals that oncogenic mutations also play a vital role in mediating the crosstalk between tumor cells and immune system, other than regulating proliferation, apoptosis and migration of tumor cells. Our findings shed a light on the possibility of combining MAPK inhibitors and anti-CTLA4 antibody to improve response, persistence and resistance for metastatic melanoma treatment.

The most studied and widely accepted primary function of CTLA4 is to competitively antagonize CD28 on naïve T cells by virtue of its greater affinity for the

mutual ligands CD80/CD86, which prevents T cell activation and induces anergy. However, our data highlights the novel and unrecognized functions of CTLA4 in melanoma cells that aids their survival, immunoevasion and tumorigenic capabilities. The melanoma-CTLA4-mediated inhibitory function provides an unconventional reverse inhibitory signal via CD86 into CTLs.

B2905A cells grew slowly in syngeneic mice *in vivo*, and lung nodules harvested from tumor-bearing mice inoculated cells by tail vein injection, were heavily infiltrated by lymphocytes. This suggests that B2905A is a highly immunogenic melanoma cell line and potentially a great model for studying crosstalk between the immune system and tumor cells, especially for testing checkpoint blockades in mouse model.

The expression of Ctl4 on melanoma cells enhanced tumorigenesis *in vivo* by enabling melanoma cells to escape from anti-tumor immunity. Strikingly, the lung nodules harvested from mice bearing B2905A-Ctl4 OE tumors were not as heavily infiltrated by lymphocytes as the control group. The tumor growth curves between B2905A-Ctl4 OE cells and B2905A-EV cells were indistinguishable at early phase (before d 18 post-injection), which suggested the overexpression of Ctl4 did not alter tumor growth *in vivo*. This was consistent with tumor proliferation *in vitro* (data not shown). The diverged tumor growth curves between those groups showed after d 18 post-injection were potentially due to Ctl4-induced tumor immunoevasion, resulted in rapid tumor growth. Indeed, the tumorigenesis of B2905A-Ctl4 OE cells and B2905A-EV cells had no difference in NSG mice that lack of T cells, B cells and functional NK cells. This data confirms that the immune system, especially the adaptive immune system is

essential in mediating Ctla4-enhanced melanomagenesis. It is well known that CD8 T cells are the guardian and first-line fighters against the tumor growth. We speculated that Ctla4 expression inhibited CD8 T cell cytotoxicity that was responsible for diverged tumor growth. Indeed, the expression of Ctla4 protected melanoma cells from CD8 T cells attack and inhibited IFN γ production in T cells by co-culture assay *in vitro*. To narrow down which lymphocytes or immune components are essential for Ctla4-mediated tumor immunoevasion, we will profile the lymphocytes infiltrated into lung nodules of mice injected either B2905A-EV or B2905A-Ctla4 OE by flow cytometry and immunohistochemistry (IHC) with our collaborators at Fox Chase Cancer Center.

CD80 and CD86 are predominantly expressed on APCs, such as dendritic cells and macrophages, to co-stimulate T cell activation. We have confirmed that CD80 and CD86 are also expressed in naïve and activated mouse CD8 T cells in our system, which is consistent with previously findings (147, 148). However, the regulation of CD80 and CD86 and its functional role in T cells are poorly understood. Interestingly, we showed that ligation of CD86, but not CD80, inhibited CD8 T cell proliferation during activation via anti-CD86 antibody. However, whether the ligation of Ctla4-CD86 delivers the same inhibitory signal to CD8 lymphocytes remains unclear. We will also delineate whether CD86 delivers inhibitory signals to T cells *in vivo*. Fascinatingly, it has been shown that PDL1/CD80 interaction is required for the induction and maintenance of peripheral T-cell tolerance (149, 150). This supports that CTLA4/CD86 interaction may have a role in mediating T-cell function *in vivo* as well. It has been shown that CD8 T cells expressing CD86 was detected in high amounts in peripheral blood of patients with systemic Lupus

Erythematosus and other autoimmune diseases, and was associated with clinical features (151, 152). This suggests that CD86-mediated inhibitory signals in T cells has important clinical implications other than in tumor biology, which needs to be further investigated.

Although we did not observe significant differences in tumor burden between B2905A-EV and B2905A-Ctla4 OE cells in NSG mice, H&E staining of lung tissues showed that the lung nodules of B2905A-Ctla4 OE cells were larger than B2905A-EV cells. The immunodeficient NSG mice still have detectable and functional neutrophils and monocytes. It has been reported that both of neutrophils and monocytes have either pro-tumorigenic or anti-tumorigenic roles, depending on specific tumor microenvironments (153-157). One possible explanation is that the expression of Ctla4 recruits more neutrophils or monocytes into lung nodules via unidentified mechanisms and the contribution of these infiltrated immune cells to tumorigenesis was limited. Indeed, infiltrating neutrophil has been shown to be mere bystanders in many types of tumors (158). To elucidate the potential mechanisms and its role in tumorigenesis, we have to examine all these types of cells in tumor microenvironment of lung nodules by IHC and flow cytometry. The role of Ctla4 expression on tumor cells might have an unanticipated role in modulating components of tumor microenvironment.

The high expression of CTLA4 in human melanoma cells and its regulation by the IFNG/JAK/STAT1-mediated signaling pathway may have important functional consequences in the clinical response to anti-CTLA4 immunotherapy of melanoma. These findings have potential implications for the conventional and prototypical roles of the IFN γ signaling pathway and CTLA4 in tumor immunosurveillance and tumor

immuno-evasion. Interferons are cytokines best known for their regulation of immune responses involved in host defense against viral and bacterial infections, and have long been associated with cytostatic/cytotoxic and antitumor immune surveillance (159). IFN γ has been postulated to be intimately involved in the elimination stage of the immunoediting paradigm (39, 160). However, we have previously suggested that it may also be important at the equilibrium and/or evasion stages, in potential roles that are pro-melanomagenic (95, 110, 161). If so, what are the molecular mechanisms for these counter-dogmatic roles? One clue may be in its homeostatic function. While IFN γ activates an inflammatory cascade, it also plays a crucial role in limiting the destruction of tissues in the aftermath of inflammation. IFN γ signaling can plausibly act to protect normal cells from the collateral damage associated with inflammation-associated tissue remodeling. Concomitantly, these same mechanisms may allow cells harboring oncogenic mutations to evade destruction and survive in a state of equilibrium until they become transformed. In effect, IFN γ -mediated inflammation may lead to an immunosuppressive and tolerogenic tissue or tumor microenvironment, which may be mechanistically achieved by IFN γ -induced enhancement of immune checkpoints, mediated by molecules like CTLA4, PD1 and PDL1 in the tissue/tumor microenvironment. Indeed, PDL1 is a known downstream target gene of IFN γ in many tumor types, including melanoma, and contributes to T cell inhibition by interacting with B7-1 (CD80) (150, 162, 163). Melanocytes are built for enhanced survival, to withstand both UVR exposure ensuring the continued synthesis of melanin, and the chemical stresses associated with the presence of melanin itself. Expression of immuno-evasive

molecules like CTLA4 and PD-L1 could be a complementary survival mechanism in the aftermath of UVR assault. These immunoevasive elements may play an integral role in further protecting melanocytes from eradication by the UVB-induced inflammatory response, which is otherwise designed to remodel all damaged portions of the skin. Melanoma could then be branded as an opportunistic cancer taking advantage of this built-in circuitry to develop into one of the most immunoevasive cancers. The fact that this circuitry converges on $IFN\gamma$ epitomizes the importance of this signaling pathway to melanocytic survival mechanisms and provides a novel perspective regarding its dual role in melanomagenesis, and perhaps in tumorigenesis in general.

Clinical Implication

New Mechanism of Anti-CTLA4 Immunotherapy

The anti-CTLA4 monoclonal antibody (Ipilimumab) immunotherapy is thought to bind and sequester CTLA4 on CTLs, restoring B7:CD28 interactions and reactivating CTL activity. Here we have reported significant correlation of CTLA4 expression with those of the immune checkpoints PD-L1, TIM-3, and LAG-3. It is plausible that IFN γ -induced CTLA4 expression in melanocytes and melanoma cells contributes to microenvironmental immunosuppression by direct melanocyte/melanoma cell-mediated inhibition of T cell cytotoxicity, which would aid melanomagenesis. It challenges the current paradigm of the route of action of anti-CTLA4 immunotherapy. It is possible that the mechanism of action of anti-CTLA4 immunotherapy, at least partially, depends upon inhibition of CTLA4 expressed by the melanoma cells, which would interfere with a melanoma cell-mediated T cell deactivation. Further mechanistic studies will be required to delineate such a melanoma cell-T cell inhibitory crosstalk.

Biomarkers for Anti-CTLA4 Immunotherapy

Anti-CTLA4 checkpoint blockade has dramatically improved clinical outcomes and deeply reshaped the treatments for melanoma patients. However, the clinical responses occur in only a small subset of patients. It is urgent to identify appropriate predictive and prognostic biomarkers to create a clinical platform which can be used to predict the response to CTLA4 blockade in melanoma patients. We have also identified an IFN γ -response gene expression signature in human melanoma tissues, including

CTLA4, as a potential biomarker for response to anti-CTLA4 immunotherapy. However, there are two important caveats with these conclusions. First, these results are based on a very small cohort of 20 patients, and warrant further larger-scale studies to verify clinical applicability. Secondly, the gene expression data were derived from whole tumor tissues, which leaves open the possibility that the source of the differential expression of IFN γ signature and CTLA4 is the difference in tumor-associated immune cells, e.g. tumor infiltrating lymphocytes (TILs) and macrophages. Snyder et al. had reported that in this cohort of patient tissues, there was no difference between the responders and non-responders with respect to tumor-associated CD45+ leukocytes, CD8+ T cells, and FOXP3+ Treg cells, which seemingly rules out a quantitative difference in immune cell infiltrate as an explanation for this finding (113). However, qualitative differences in the immune infiltrate cannot be ruled out. For example, we have previously reported that 70% of human melanomas harbor macrophages that secrete IFN γ (95), which would explain the different levels of IFN γ in the tumor microenvironment and the consequent IFN γ -responsive signature in the tumor tissues. The functional status of TILs in melanoma tissues remains poorly characterized and their relative contribution to therapeutic response is poorly understood (164). Therefore, whether it is the CTLA4 expression in melanoma cells or tumor-associated immune cells that is the defining factor in patient response to ipilimumab remains an open question. The latter seems to be the most likely explanation, especially in light of our results that show concordance of CTLA4 expression with other immune checkpoints. However, overexpression of CTLA4 in melanoma cell lines suggests that it may be a plausible alternative or complementary

target of ipilimumab. Further studies will be required to assess the effects of melanocytic expression of immune checkpoints on the TIL function in the tumor microenvironment and response to immune checkpoint inhibitors.

Combination Therapy of MAPKi and Anti-CTLA4 Antibody

We have shown evidence that the overexpression of CTLA4 in human melanoma cell lines is driven by the constitutively activated MAPK/ERK pathway, as targeted inhibitors of BRAFV600E and MEK were able to abolish CTLA4 overexpression, specifically in the cell lines harboring activating BRAF or NRAS mutations. These intriguing results add to the complexity of the crosstalk between the mutational landscape of melanoma cells and the immune profile of the tumor microenvironment. There is currently considerable interest in potential therapeutic strategies combining the molecularly targeted inhibitors of MAPK pathway and immunotherapies. Several ongoing clinical trials are exploring the efficacy of concomitant treatment of advanced melanoma with BRAF and MEK inhibitors, anti-CTLA4 and/or anti-PD-1 antibodies (e.g. NCT02224781, NCT01940809). It has been suggested that BRAF/MEK inhibition can enhance T cell infiltration and immune recognition of melanoma cells by increasing the expression levels of melanoma-specific antigens, which would in turn enhance efficacy of anti-melanoma immunotherapy (165-167). Activated MAPK-driven CTLA4 expression within melanoma cells may play a substantial role in determining the responses to such combination therapeutic regimens. These potential molecular circuits warrant further investigation.

Taken together, the results from these experiments will potentially be informative for fully understanding CTLA4 function and its role in UV-induced melanogenesis. More importantly, it will benefit cancer patients numerously with further evaluation of the role of CTLA in checkpoint blockades.

REFERENCE CITED

1. Eshleman EM, Lenz LL. Type I interferons in bacterial infections: taming of myeloid cells and possible implications for autoimmunity. *Front Immunol.* 2014;5:431.
2. de Weerd NA, Samarajiwa SA, Hertzog PJ. Type I interferon receptors: biochemistry and biological functions. *J Biol Chem.* 2007;282(28):20053-7.
3. Plataniias LC. Mechanisms of type-I- and type-II-interferon-mediated signalling. *Nat Rev Immunol.* 2005;5(5):375-86.
4. Donnelly RP, Kotenko SV. Interferon-lambda: a new addition to an old family. *J Interferon Cytokine Res.* 2010;30(8):555-64.
5. Hall JC, Rosen A. Type I interferons: crucial participants in disease amplification in autoimmunity. *Nat Rev Rheumatol.* 2010;6(1):40-9.
6. Hegde S, Fox L, Wang X, Gumperz JE. Autoreactive natural killer T cells: promoting immune protection and immune tolerance through varied interactions with myeloid antigen-presenting cells. *Immunology.* 2010;130(4):471-83.
7. Castro F, Cardoso AP, Goncalves RM, Serre K, Oliveira MJ. Interferon-Gamma at the Crossroads of Tumor Immune Surveillance or Evasion. *Front Immunol.* 2018;9:847.
8. Haring JS, Corbin GA, Harty JT. Dynamic regulation of IFN-gamma signaling in antigen-specific CD8+ T cells responding to infection. *J Immunol.* 2005;174(11):6791-802.

9. Wenta N, Strauss H, Meyer S, Vinkemeier U. Tyrosine phosphorylation regulates the partitioning of STAT1 between different dimer conformations. *Proc Natl Acad Sci U S A*. 2008;105(27):9238-43.
10. Sadzak I, Schiff M, Gattermeier I, Glinitzer R, Sauer I, Saalmuller A, et al. Recruitment of Stat1 to chromatin is required for interferon-induced serine phosphorylation of Stat1 transactivation domain. *Proc Natl Acad Sci U S A*. 2008;105(26):8944-9.
11. Zhang JJ, Vinkemeier U, Gu W, Chakravarti D, Horvath CM, Darnell JE, Jr. Two contact regions between Stat1 and CBP/p300 in interferon gamma signaling. *Proc Natl Acad Sci U S A*. 1996;93(26):15092-6.
12. Yang CH, Fan M, Slominski AT, Yue J, Pfeffer LM. The role of constitutively activated STAT3 in B16 melanoma cells. *Int J Interferon Cytokine Mediat Res*. 2010;2010(2):1-7.
13. Choi H, Choi H, Han J, Jin SH, Park JY, Shin DW, et al. IL-4 inhibits the melanogenesis of normal human melanocytes through the JAK2-STAT6 signaling pathway. *J Invest Dermatol*. 2013;133(2):528-36.
14. Rottman M, Catherinot E, Hochedez P, Emile JF, Casanova JL, Gaillard JL, et al. Importance of T cells, gamma interferon, and tumor necrosis factor in immune control of the rapid grower *Mycobacterium abscessus* in C57BL/6 mice. *Infect Immun*. 2007;75(12):5898-907.

15. Shrestha B, Wang T, Samuel MA, Whitby K, Craft J, Fikrig E, et al. Gamma interferon plays a crucial early antiviral role in protection against West Nile virus infection. *J Virol.* 2006;80(11):5338-48.
16. Ikeda H, Old LJ, Schreiber RD. The roles of IFN gamma in protection against tumor development and cancer immunoediting. *Cytokine Growth Factor Rev.* 2002;13(2):95-109.
17. Vojdani A, Pollard KM, Campbell AW. Environmental triggers and autoimmunity. *Autoimmune Dis.* 2014;2014:798029.
18. Sharma P, Kumar P, Sharma R. Natural Killer Cells - Their Role in Tumour Immunosurveillance. *J Clin Diagn Res.* 2017;11(8):BE01-BE5.
19. Street D, Kaufmann AM, Vaughan A, Fisher SG, Hunter M, Schreckenberger C, et al. Interferon-gamma enhances susceptibility of cervical cancer cells to lysis by tumor-specific cytotoxic T cells. *Gynecol Oncol.* 1997;65(2):265-72.
20. Aquino-Lopez A, Senyukov VV, Vlastic Z, Kleinerman ES, Lee DA. Interferon Gamma Induces Changes in Natural Killer (NK) Cell Ligand Expression and Alters NK Cell-Mediated Lysis of Pediatric Cancer Cell Lines. *Front Immunol.* 2017;8:391.
21. Takeda K, Nakayama M, Sakaki M, Hayakawa Y, Imawari M, Ogasawara K, et al. IFN-gamma production by lung NK cells is critical for the natural resistance to pulmonary metastasis of B16 melanoma in mice. *J Leukoc Biol.* 2011;90(4):777-85.

22. Burkholder B, Huang RY, Burgess R, Luo S, Jones VS, Zhang W, et al. Tumor-induced perturbations of cytokines and immune cell networks. *Biochim Biophys Acta*. 2014;1845(2):182-201.
23. Mandai M, Hamanishi J, Abiko K, Matsumura N, Baba T, Konishi I. Dual Faces of IFN γ in Cancer Progression: A Role of PD-L1 Induction in the Determination of Pro- and Antitumor Immunity. *Clin Cancer Res*. 2016;22(10):2329-34.
24. Bhat P, Bergot AS, Waterhouse N, Frazer IH. Human papillomavirus E7 oncoprotein expression by keratinocytes alters the cytotoxic mechanisms used by CD8 T cells. *Oncotarget*. 2018;9(5):6015-27.
25. Hollenbaugh JA, Dutton RW. IFN- γ regulates donor CD8 T cell expansion, migration, and leads to apoptosis of cells of a solid tumor. *J Immunol*. 2006;177(5):3004-11.
26. Townsend PA, Scarabelli TM, Davidson SM, Knight RA, Latchman DS, Stephanou A. STAT-1 interacts with p53 to enhance DNA damage-induced apoptosis. *J Biol Chem*. 2004;279(7):5811-20.
27. Pearce EJ, C MK, Sun J, J JT, McKee AS, Cervi L. Th2 response polarization during infection with the helminth parasite *Schistosoma mansoni*. *Immunol Rev*. 2004;201:117-26.
28. Rakshit S, Chandrasekar BS, Saha B, Victor ES, Majumdar S, Nandi D. Interferon- γ induced cell death: Regulation and contributions of nitric oxide, cJun N-terminal kinase, reactive oxygen species and peroxynitrite. *Biochim Biophys Acta*. 2014;1843(11):2645-61.

29. Pereira RA, Tschärke DC, Simmons A. Upregulation of class I major histocompatibility complex gene expression in primary sensory neurons, satellite cells, and Schwann cells of mice in response to acute but not latent herpes simplex virus infection in vivo. *J Exp Med*. 1994;180(3):841-50.
30. Ma W, Lehner PJ, Cresswell P, Pober JS, Johnson DR. Interferon-gamma rapidly increases peptide transporter (TAP) subunit expression and peptide transport capacity in endothelial cells. *J Biol Chem*. 1997;272(26):16585-90.
31. Arellano-Garcia ME, Misuno K, Tran SD, Hu S. Interferon-gamma induces immunoproteasomes and the presentation of MHC I-associated peptides on human salivary gland cells. *PLoS One*. 2014;9(8):e102878.
32. Santambrogio L, Sato AK, Fischer FR, Dorf ME, Stern LJ. Abundant empty class II MHC molecules on the surface of immature dendritic cells. *Proc Natl Acad Sci U S A*. 1999;96(26):15050-5.
33. Schiller JH, Pugh M, Kirkwood JM, Karp D, Larson M, Borden E. Eastern cooperative group trial of interferon gamma in metastatic melanoma: an innovative study design. *Clin Cancer Res*. 1996;2(1):29-36.
34. Meyskens FL, Jr., Kopecky K, Samson M, Hersh E, Macdonald J, Jaffe H, et al. Recombinant human interferon gamma: adverse effects in high-risk stage I and II cutaneous malignant melanoma. *J Natl Cancer Inst*. 1990;82(12):1071.
35. Meyskens FL, Jr., Kopecky KJ, Taylor CW, Noyes RD, Tuthill RJ, Hersh EM, et al. Randomized trial of adjuvant human interferon gamma versus observation in

high-risk cutaneous melanoma: a Southwest Oncology Group study. *J Natl Cancer Inst.* 1995;87(22):1710-3.

36. Alberts DS, Marth C, Alvarez RD, Johnson G, Bidzinski M, Kardatzke DR, et al. Randomized phase 3 trial of interferon gamma-1b plus standard carboplatin/paclitaxel versus carboplatin/paclitaxel alone for first-line treatment of advanced ovarian and primary peritoneal carcinomas: results from a prospectively designed analysis of progression-free survival. *Gynecol Oncol.* 2008;109(2):174-81.

37. Wiesenfeld M, O'Connell MJ, Wieand HS, Gonchoroff NJ, Donohue JH, Fitzgibbons RJ, Jr., et al. Controlled clinical trial of interferon-gamma as postoperative surgical adjuvant therapy for colon cancer. *J Clin Oncol.* 1995;13(9):2324-9.

38. Dunn GP, Ikeda H, Bruce AT, Koebel C, Uppaluri R, Bui J, et al. Interferon-gamma and cancer immunoediting. *Immunol Res.* 2005;32(1-3):231-45.

39. Dunn GP, Koebel CM, Schreiber RD. Interferons, immunity and cancer immunoediting. *Nat Rev Immunol.* 2006;6(11):836-48.

40. Dunn GP, Old LJ, Schreiber RD. The three Es of cancer immunoediting. *Annu Rev Immunol.* 2004;22:329-60.

41. O'Sullivan T, Saddawi-Konefka R, Vermi W, Koebel CM, Arthur C, White JM, et al. Cancer immunoediting by the innate immune system in the absence of adaptive immunity. *J Exp Med.* 2012;209(10):1869-82.

42. Mojic M, Takeda K, Hayakawa Y. The Dark Side of IFN-gamma: Its Role in Promoting Cancer Immuno-evasion. *Int J Mol Sci.* 2017;19(1).

43. Morel E, Bellon T. HLA class I molecules regulate IFN-gamma production induced in NK cells by target cells, viral products, or immature dendritic cells through the inhibitory receptor ILT2/CD85j. *J Immunol.* 2008;181(4):2368-81.
44. Zhang ZN, Zhu ML, Chen YH, Fu YJ, Zhang TW, Jiang YJ, et al. Elevation of Tim-3 and PD-1 expression on T cells appears early in HIV infection, and differential Tim-3 and PD-1 expression patterns can be induced by common gamma - chain cytokines. *Biomed Res Int.* 2015;2015:916936.
45. Cho H, Kang H, Lee HH, Kim CW. Programmed Cell Death 1 (PD-1) and Cytotoxic T Lymphocyte-Associated Antigen 4 (CTLA-4) in Viral Hepatitis. *Int J Mol Sci.* 2017;18(7).
46. Ribas A. Tumor immunotherapy directed at PD-1. *N Engl J Med.* 2012;366(26):2517-9.
47. Lee V, Le DT. Efficacy of PD-1 blockade in tumors with MMR deficiency. *Immunotherapy.* 2016;8(1):1-3.
48. Nowicki TS, Akiyama R, Huang RR, Shintaku IP, Wang X, Tumeh PC, et al. Infiltration of CD8 T Cells and Expression of PD-1 and PD-L1 in Synovial Sarcoma. *Cancer Immunol Res.* 2017;5(2):118-26.
49. Eroglu Z, Zaretsky JM, Hu-Lieskovan S, Kim DW, Algazi A, Johnson DB, et al. High response rate to PD-1 blockade in desmoplastic melanomas. *Nature.* 2018;553(7688):347-50.
50. Lin SY, Yang CY, Liao BC, Ho CC, Liao WY, Chen KY, et al. Tumor PD-L1 Expression and Clinical Outcomes in Advanced-stage Non-Small Cell Lung

Cancer Patients Treated with Nivolumab or Pembrolizumab: Real-World Data in Taiwan. *J Cancer*. 2018;9(10):1813-20.

51. M L, P PV, T K, M P, E S, J P, et al. Essential role of HDAC6 in the regulation of PD-L1 in melanoma. *Molecular oncology*. 2016;10(5):735-50.

52. Riella LV, Paterson AM, Sharpe AH, Chandraker A. Role of the PD-1 pathway in the immune response. *Am J Transplant*. 2012;12(10):2575-87.

53. Mbongue JC, Nicholas DA, Torrez TW, Kim NS, Firek AF, Langridge WH. The Role of Indoleamine 2, 3-Dioxygenase in Immune Suppression and Autoimmunity. *Vaccines (Basel)*. 2015;3(3):703-29.

54. Katz JB, Muller AJ, Prendergast GC. Indoleamine 2,3-dioxygenase in T-cell tolerance and tumoral immune escape. *Immunol Rev*. 2008;222:206-21.

55. Prendergast GC. Immune escape as a fundamental trait of cancer: focus on IDO. *Oncogene*. 2008;27(28):3889-900.

56. Sucker A, Zhao F, Pieper N, Heeke C, Maltaner R, Stadtler N, et al. Acquired IFN γ resistance impairs anti-tumor immunity and gives rise to T-cell-resistant melanoma lesions. *Nat Commun*. 2017;8:15440.

57. Campbell MT, Siefker-Radtke AO, Gao J. The State of Immune Checkpoint Inhibition in Urothelial Carcinoma: Current Evidence and Future Areas of Exploration. *Cancer J*. 2016;22(2):96-100.

58. Khattri R, Auger JA, Griffin MD, Sharpe AH, Bluestone JA. Lymphoproliferative disorder in CTLA-4 knockout mice is characterized by CD28-regulated activation of Th2 responses. *J Immunol*. 1999;162(10):5784-91.

59. Chen L, Flies DB. Molecular mechanisms of T cell co-stimulation and co-inhibition. *Nat Rev Immunol.* 2013;13(4):227-42.
60. Facciabene A, Motz GT, Coukos G. T-regulatory cells: key players in tumor immune escape and angiogenesis. *Cancer Res.* 2012;72(9):2162-71.
61. Callahan MK, Postow MA, Wolchok JD. CTLA-4 and PD-1 Pathway Blockade: Combinations in the Clinic. *Frontiers in oncology.* 2014;4:385.
62. Wolchok JD, Saenger Y. The mechanism of anti-CTLA-4 activity and the negative regulation of T-cell activation. *The oncologist.* 2008;13 Suppl 4:2-9.
63. Contardi E, Palmisano GL, Tazzari PL, Martelli AM, Fala F, Fabbi M, et al. CTLA-4 is constitutively expressed on tumor cells and can trigger apoptosis upon ligand interaction. *Int J Cancer.* 2005;117(4):538-50.
64. Pistillo MP, Tazzari PL, Palmisano GL, Pierri I, Bolognesi A, Ferlito F, et al. CTLA-4 is not restricted to the lymphoid cell lineage and can function as a target molecule for apoptosis induction of leukemic cells. *Blood.* 2003;101(1):202-9.
65. Egen JG, Kuhns MS, Allison JP. CTLA-4: new insights into its biological function and use in tumor immunotherapy. *Nat Immunol.* 2002;3(7):611-8.
66. Attia P, Phan GQ, Maker AV, Robinson MR, Quezado MM, Yang JC, et al. Autoimmunity correlates with tumor regression in patients with metastatic melanoma treated with anti-cytotoxic T-lymphocyte antigen-4. *J Clin Oncol.* 2005;23(25):6043-53.
67. Shah KV, Chien AJ, Yee C, Moon RT. CTLA-4 is a direct target of Wnt/beta-catenin signaling and is expressed in human melanoma tumors. *J Invest Dermatol.* 2008;128(12):2870-9.

68. Weber JS. Tumor evasion may occur via expression of regulatory molecules: a case for CTLA-4 in melanoma. *J Invest Dermatol.* 2008;128(12):2750-2.
69. Chen H, Weng QY, Fisher DE. UV signaling pathways within the skin. *J Invest Dermatol.* 2014;134(8):2080-5.
70. Wang CQF, Akalu YT, Suarez-Farinas M, Gonzalez J, Mitsui H, Lowes MA, et al. IL-17 and TNF synergistically modulate cytokine expression while suppressing melanogenesis: potential relevance to psoriasis. *J Invest Dermatol.* 2013;133(12):2741-52.
71. Kawakami A, Fisher DE. The master role of microphthalmia-associated transcription factor in melanocyte and melanoma biology. *Lab Invest.* 2017;97(6):649-56.
72. Sturm RA. A golden age of human pigmentation genetics. *Trends Genet.* 2006;22(9):464-8.
73. Chang TS. An updated review of tyrosinase inhibitors. *Int J Mol Sci.* 2009;10(6):2440-75.
74. Slominski A, Tobin DJ, Shibahara S, Wortsman J. Melanin pigmentation in mammalian skin and its hormonal regulation. *Physiol Rev.* 2004;84(4):1155-228.
75. Jagirdar K, Smit DJ, Ainger SA, Lee KJ, Brown DL, Chapman B, et al. Molecular analysis of common polymorphisms within the human Tyrosinase locus and genetic association with pigmentation traits. *Pigment Cell Melanoma Res.* 2014;27(4):552-64.

76. Wang R, Tang P, Wang P, Boissy RE, Zheng H. Regulation of tyrosinase trafficking and processing by presenilins: partial loss of function by familial Alzheimer's disease mutation. *Proc Natl Acad Sci U S A*. 2006;103(2):353-8.
77. Halaban R, Cheng E, Zhang Y, Moellmann G, Hanlon D, Michalak M, et al. Aberrant retention of tyrosinase in the endoplasmic reticulum mediates accelerated degradation of the enzyme and contributes to the dedifferentiated phenotype of amelanotic melanoma cells. *Proc Natl Acad Sci U S A*. 1997;94(12):6210-5.
78. Branza-Nichita N, Negroiu G, Petrescu AJ, Garman EF, Platt FM, Wormald MR, et al. Mutations at critical N-glycosylation sites reduce tyrosinase activity by altering folding and quality control. *J Biol Chem*. 2000;275(11):8169-75.
79. Ancans J, Tobin DJ, Hoogduijn MJ, Smit NP, Wakamatsu K, Thody AJ. Melanosomal pH controls rate of melanogenesis, eumelanin/phaeomelanin ratio and melanosome maturation in melanocytes and melanoma cells. *Experimental cell research*. 2001;268(1):26-35.
80. Ando H, Kondoh H, Ichihashi M, Hearing VJ. Approaches to identify inhibitors of melanin biosynthesis via the quality control of tyrosinase. *J Invest Dermatol*. 2007;127(4):751-61.
81. Raposo G, Marks MS. Melanosomes--dark organelles enlighten endosomal membrane transport. *Nat Rev Mol Cell Biol*. 2007;8(10):786-97.
82. Recchi C, Chavrier P. V-ATPase: a potential pH sensor. *Nat Cell Biol*. 2006;8(2):107-9.

83. Chen K, Minwalla L, Ni L, Orlow SJ. Correction of defective early tyrosinase processing by bafilomycin A1 and monensin in pink-eyed dilution melanocytes. *Pigment Cell Res.* 2004;17(1):36-42.
84. Ancans J, Hoogduijn MJ, Thody AJ. Melanosomal pH, pink locus protein and their roles in melanogenesis. *J Invest Dermatol.* 2001;117(1):158-9.
85. Zeng H, Harashima A, Kato K, Gu L, Motomura Y, Otsuka R, et al. Degradation of Tyrosinase by Melanosomal pH Change and a New Mechanism of Whitening with Propylparaben. *Cosmetics.* 2017;4(4):43.
86. Cheli Y, Luciani F, Khaled M, Beuret L, Bille K, Gounon P, et al. α -MSH and Cyclic AMP elevating agents control melanosome pH through a protein kinase A-independent mechanism. *J Biol Chem.* 2009;284(28):18699-706.
87. Watabe H, Valencia JC, Yasumoto K, Kushimoto T, Ando H, Muller J, et al. Regulation of tyrosinase processing and trafficking by organellar pH and by proteasome activity. *J Biol Chem.* 2004;279(9):7971-81.
88. Ramsay M, Colman MA, Stevens G, Zwane E, Kromberg J, Farrall M, et al. The tyrosinase-positive oculocutaneous albinism locus maps to chromosome 15q11.2-q12. *Am J Hum Genet.* 1992;51(4):879-84.
89. Sitaram A, Piccirillo R, Palmisano I, Harper DC, Dell'Angelica EC, Schiaffino MV, et al. Localization to mature melanosomes by virtue of cytoplasmic dileucine motifs is required for human OCA2 function. *Mol Biol Cell.* 2009;20(5):1464-77.

90. Gardner JM, Nakatsu Y, Gondo Y, Lee S, Lyon MF, King RA, et al. The mouse pink-eyed dilution gene: association with human Prader-Willi and Angelman syndromes. *Science*. 1992;257(5073):1121-4.
91. Mauri L, Barone L, Al Oum M, Del Longo A, Piozzi E, Manfredini E, et al. SLC45A2 mutation frequency in Oculocutaneous Albinism Italian patients doesn't differ from other European studies. *Gene*. 2014;533(1):398-402.
92. Bin BH, Bhin J, Yang SH, Shin M, Nam YJ, Choi DH, et al. Membrane-Associated Transporter Protein (MATP) Regulates Melanosomal pH and Influences Tyrosinase Activity. *PLoS One*. 2015;10(6):e0129273.
93. Lamason RL, Mohideen MA, Mest JR, Wong AC, Norton HL, Aros MC, et al. SLC24A5, a putative cation exchanger, affects pigmentation in zebrafish and humans. *Science*. 2005;310(5755):1782-6.
94. Morice-Picard F, Lasseaux E, Francois S, Simon D, Rooryck C, Bieth E, et al. SLC24A5 mutations are associated with non-syndromic oculocutaneous albinism. *J Invest Dermatol*. 2014;134(2):568-71.
95. Zaidi MR, Davis S, Noonan FP, Graff-Cherry C, Hawley TS, Walker RL, et al. Interferon-gamma links ultraviolet radiation to melanomagenesis in mice. *Nature*. 2011;469(7331):548-53.
96. Ran FA, Hsu PD, Wright J, Agarwala V, Scott DA, Zhang F. Genome engineering using the CRISPR-Cas9 system. *Nature protocols*. 2013;8(11):2281-308.
97. Levy C, Khaled M, Fisher DE. MITF: master regulator of melanocyte development and melanoma oncogene. *Trends Mol Med*. 2006;12(9):406-14.

98. Wang Y, Radfar S, Liu S, Riker AI, Khong HT. Mitf-Mdel, a novel melanocyte/melanoma-specific isoform of microphthalmia-associated transcription factor-M, as a candidate biomarker for melanoma. *BMC Med.* 2010;8:14.
99. Pierrat MJ, Marsaud V, Mauviel A, Javelaud D. Expression of microphthalmia-associated transcription factor (MITF), which is critical for melanoma progression, is inhibited by both transcription factor GLI2 and transforming growth factor-beta. *J Biol Chem.* 2012;287(22):17996-8004.
100. Wellbrock C, Marais R. Elevated expression of MITF counteracts B-RAF-stimulated melanocyte and melanoma cell proliferation. *J Cell Biol.* 2005;170(5):703-8.
101. Bhatnagar V, Srirangam A, Abburi R. In vitro modulation of proliferation and melanization of melanoma cells by citrate. *Mol Cell Biochem.* 1998;187(1-2):57-65.
102. Newton RA, Cook AL, Roberts DW, Leonard JH, Sturm RA. Post-transcriptional regulation of melanin biosynthetic enzymes by cAMP and resveratrol in human melanocytes. *J Invest Dermatol.* 2007;127(9):2216-27.
103. Ando H, Wen ZM, Kim HY, Valencia JC, Costin GE, Watabe H, et al. Intracellular composition of fatty acid affects the processing and function of tyrosinase through the ubiquitin-proteasome pathway. *Biochem J.* 2006;394(Pt 1):43-50.
104. Ando H, Watabe H, Valencia JC, Yasumoto K, Furumura M, Funasaka Y, et al. Fatty acids regulate pigmentation via proteasomal degradation of tyrosinase: a new aspect of ubiquitin-proteasome function. *J Biol Chem.* 2004;279(15):15427-33.

105. Ambrosio AL, Boyle JA, Aradi AE, Christian KA, Di Pietro SM. TPC2 controls pigmentation by regulating melanosome pH and size. *Proc Natl Acad Sci U S A*. 2016;113(20):5622-7.
106. Ancans J, Thody AJ. Activation of melanogenesis by vacuolar type H(+)-ATPase inhibitors in amelanotic, tyrosinase positive human and mouse melanoma cells. *FEBS Lett*. 2000;478(1-2):57-60.
107. Bellono NW, Escobar IE, Lefkovith AJ, Marks MS, Oancea E. An intracellular anion channel critical for pigmentation. *Elife*. 2014;3:e04543.
108. Chen K, Manga P, Orlow SJ. Pink-eyed dilution protein controls the processing of tyrosinase. *Mol Biol Cell*. 2002;13(6):1953-64.
109. Bellono NW, Escobar IE, Oancea E. A melanosomal two-pore sodium channel regulates pigmentation. *Sci Rep*. 2016;6:26570.
110. Zaidi MR, Merlino G. The two faces of interferon-gamma in cancer. *Clin Cancer Res*. 2011;17(19):6118-24.
111. Qing Y, Stark GR. Alternative activation of STAT1 and STAT3 in response to interferon-gamma. *J Biol Chem*. 2004;279(40):41679-85.
112. Martin KA, Lupey LN, Tempera I. Epstein-Barr Virus Oncoprotein LMP1 Mediates Epigenetic Changes in Host Gene Expression through PARP1. *J Virol*. 2016;90(19):8520-30.
113. Snyder A, Makarov V, Merghoub T, Yuan J, Zaretsky JM, Desrichard A, et al. Genetic basis for clinical response to CTLA-4 blockade in melanoma. *N Engl J Med*. 2014;371(23):2189-99.

114. Chiappinelli KB, Strissel PL, Desrichard A, Li H, Henke C, Akman B, et al. Inhibiting DNA Methylation Causes an Interferon Response in Cancer via dsRNA Including Endogenous Retroviruses. *Cell*. 2015;162(5):974-86.
115. Barretina J, Caponigro G, Stransky N, Venkatesan K, Margolin AA, Kim S, et al. The Cancer Cell Line Encyclopedia enables predictive modelling of anticancer drug sensitivity. *Nature*. 2012;483(7391):603-7.
116. Cancer Cell Line Encyclopedia C, Genomics of Drug Sensitivity in Cancer C. Pharmacogenomic agreement between two cancer cell line data sets. *Nature*. 2015;528(7580):84-7.
117. Qureshi OS, Kaur S, Hou TZ, Jeffery LE, Poulter NS, Briggs Z, et al. Constitutive clathrin-mediated endocytosis of CTLA-4 persists during T cell activation. *J Biol Chem*. 2012;287(12):9429-40.
118. Leung HT, Bradshaw J, Cleaveland JS, Linsley PS. Cytotoxic T lymphocyte-associated molecule-4, a high-avidity receptor for CD80 and CD86, contains an intracellular localization motif in its cytoplasmic tail. *J Biol Chem*. 1995;270(42):25107-14.
119. Mead KI, Zheng Y, Manzotti CN, Perry LC, Liu MK, Burke F, et al. Exocytosis of CTLA-4 is dependent on phospholipase D and ADP ribosylation factor-1 and stimulated during activation of regulatory T cells. *J Immunol*. 2005;174(8):4803-11.
120. Valk E, Leung R, Kang H, Kaneko K, Rudd CE, Schneider H. T cell receptor-interacting molecule acts as a chaperone to modulate surface expression of the CTLA-4 coreceptor. *Immunity*. 2006;25(5):807-21.

121. Boehm U, Klamp T, Groot M, Howard JC. Cellular responses to interferon-gamma. *Annu Rev Immunol.* 1997;15:749-95.
122. Caldenhoven E, Buitenhuis M, van Dijk TB, Raaijmakers JA, Lammers JW, Koenderman L, et al. Lineage-specific activation of STAT3 by interferon-gamma in human neutrophils. *J Leukoc Biol.* 1999;65(3):391-6.
123. Mesa RA, Yasothan U, Kirkpatrick P. Ruxolitinib. *Nat Rev Drug Discov.* 2012;11(2):103-4.
124. Bernstein BE, Birney E, Dunham I, Green ED, Gunter C, Snyder M. An integrated encyclopedia of DNA elements in the human genome. *Nature.* 2012;489(7414):57-74.
125. Shlyueva D, Stampfel G, Stark A. Transcriptional enhancers: from properties to genome-wide predictions. *Nat Rev Genet.* 2014;15(4):272-86.
126. Thurman RE, Rynes E, Humbert R, Vierstra J, Maurano MT, Haugen E, et al. The accessible chromatin landscape of the human genome. *Nature.* 2012;489(7414):75-82.
127. Begitt A, Droscher M, Meyer T, Schmid CD, Baker M, Antunes F, et al. STAT1-cooperative DNA binding distinguishes type 1 from type 2 interferon signaling. *Nat Immunol.* 2014;15(2):168-76.
128. Boussemart L, Malka-Mahieu H, Girault I, Allard D, Hemmingsson O, Tomasic G, et al. eIF4F is a nexus of resistance to anti-BRAF and anti-MEK cancer therapies. *Nature.* 2014;513(7516):105-9.

129. Schroder K, Hertzog PJ, Ravasi T, Hume DA. Interferon-gamma: an overview of signals, mechanisms and functions. *J Leukoc Biol.* 2004;75(2):163-89.
130. van Deventer HW, Serody JS, McKinnon KP, Clements C, Brickey WJ, Ting JP. Transfection of macrophage inflammatory protein 1 alpha into B16 F10 melanoma cells inhibits growth of pulmonary metastases but not subcutaneous tumors. *J Immunol.* 2002;169(3):1634-9.
131. Criscuoli ML, Nguyen M, Eliceiri BP. Tumor metastasis but not tumor growth is dependent on Src-mediated vascular permeability. *Blood.* 2005;105(4):1508-14.
132. Zhang Y, Toneri M, Ma H, Yang Z, Bouvet M, Goto Y, et al. Real-Time GFP Intravital Imaging of the Differences in Cellular and Angiogenic Behavior of Subcutaneous and Orthotopic Nude-Mouse Models of Human PC-3 Prostate Cancer. *Journal of cellular biochemistry.* 2016;117(11):2546-51.
133. Elloso MM, Scott P. Expression and contribution of B7-1 (CD80) and B7-2 (CD86) in the early immune response to *Leishmania major* infection. *J Immunol.* 1999;162(11):6708-15.
134. Taylor PA, Lees CJ, Fournier S, Allison JP, Sharpe AH, Blazar BR. B7 expression on T cells down-regulates immune responses through CTLA-4 ligation via T-T interactions [corrections]. *J Immunol.* 2004;172(1):34-9.
135. Jager M, Queinnec E, Houliston E, Manuel M. Expansion of the SOX gene family predated the emergence of the Bilateria. *Mol Phylogenet Evol.* 2006;39(2):468-77.

136. Potterf SB, Mollaaghababa R, Hou L, Southard-Smith EM, Hornyak TJ, Arnheiter H, et al. Analysis of SOX10 function in neural crest-derived melanocyte development: SOX10-dependent transcriptional control of dopachrome tautomerase. *Dev Biol.* 2001;237(2):245-57.
137. D'Mello SA, Finlay GJ, Baguley BC, Askarian-Amiri ME. Signaling Pathways in Melanogenesis. *Int J Mol Sci.* 2016;17(7).
138. Khalkhali-Ellis Z, Abbott DE, Bailey CM, Goossens W, Margaryan NV, Gluck SL, et al. IFN-gamma regulation of vacuolar pH, cathepsin D processing and autophagy in mammary epithelial cells. *Journal of cellular biochemistry.* 2008;105(1):208-18.
139. Wang S, Zhou M, Lin F, Liu D, Hong W, Lu L, et al. Interferon-gamma induces senescence in normal human melanocytes. *PLoS One.* 2014;9(3):e93232.
140. Bae HR, Leung PS, Tsuneyama K, Valencia JC, Hodge DL, Kim S, et al. Chronic expression of interferon-gamma leads to murine autoimmune cholangitis with a female predominance. *Hepatology.* 2016;64(4):1189-201.
141. Son J, Kim M, Jou I, Park KC, Kang HY. IFN-gamma inhibits basal and alpha-MSH-induced melanogenesis. *Pigment Cell Melanoma Res.* 2014;27(2):201-8.
142. Natarajan VT, Ganju P, Singh A, Vijayan V, Kirty K, Yadav S, et al. IFN-gamma signaling maintains skin pigmentation homeostasis through regulation of melanosome maturation. *Proc Natl Acad Sci U S A.* 2014;111(6):2301-6.

143. Liu B, Palmfeldt J, Lin L, Colaco A, Clemmensen KKB, Huang J, et al. STAT3 associates with vacuolar H(+)-ATPase and regulates cytosolic and lysosomal pH. *Cell Res.* 2018.
144. Davis EC, Callender VD. Postinflammatory hyperpigmentation: a review of the epidemiology, clinical features, and treatment options in skin of color. *J Clin Aesthet Dermatol.* 2010;3(7):20-31.
145. Costin GE, Hearing VJ. Human skin pigmentation: melanocytes modulate skin color in response to stress. *FASEB J.* 2007;21(4):976-94.
146. Harmon AC, Cornelius DC, Amaral LM, Faulkner JL, Cunningham MW, Jr., Wallace K, et al. The role of inflammation in the pathology of preeclampsia. *Clin Sci (Lond).* 2016;130(6):409-19.
147. Jeannin P, Herbault N, Delneste Y, Magistrelli G, Lecoanet-Henchoz S, Caron G, et al. Human effector memory T cells express CD86: a functional role in naive T cell priming. *J Immunol.* 1999;162(4):2044-8.
148. Paine A, Kirchner H, Immenschuh S, Oelke M, Blasczyk R, Eiz-Vesper B. IL-2 upregulates CD86 expression on human CD4(+) and CD8(+) T cells. *J Immunol.* 2012;188(4):1620-9.
149. Drenkard C, G GB, Lewis TT, Pobiner B, J JP, Lim SS. Physician-patient interactions in African American patients with systemic lupus erythematosus: Demographic characteristics and relationship with disease activity and depression. *Semin Arthritis Rheum.* 2018.

150. Butte MJ, Keir ME, Phamduy TB, Sharpe AH, Freeman GJ. Programmed death-1 ligand 1 interacts specifically with the B7-1 costimulatory molecule to inhibit T cell responses. *Immunity*. 2007;27(1):111-22.
151. Goronzy JJ, Weyand CM. T-cell co-stimulatory pathways in autoimmunity. *Arthritis Res Ther*. 2008;10 Suppl 1:S3.
152. Abe K, Takasaki Y, Ushiyama C, Asakawa J, Fukazawa T, Seki M, et al. Expression of CD80 and CD86 on peripheral blood T lymphocytes in patients with systemic lupus erythematosus. *J Clin Immunol*. 1999;19(1):58-66.
153. Hagerling C, Casbon AJ, Werb Z. Balancing the innate immune system in tumor development. *Trends Cell Biol*. 2015;25(4):214-20.
154. Liu Y, Zeng G. Cancer and innate immune system interactions: translational potentials for cancer immunotherapy. *J Immunother*. 2012;35(4):299-308.
155. Juric V, Ruffell B, Evason KJ, Hu J, Che L, Wang L, et al. Monocytes promote liver carcinogenesis in an oncogene-specific manner. *J Hepatol*. 2016;64(4):881-90.
156. Cassetta L, Pollard JW. Cancer immunosurveillance: role of patrolling monocytes. *Cell Res*. 2016;26(1):3-4.
157. Ocana A, Nieto-Jimenez C, Pandiella A, Templeton AJ. Neutrophils in cancer: prognostic role and therapeutic strategies. *Mol Cancer*. 2017;16(1):137.
158. Uribe-Querol E, Rosales C. Neutrophils in Cancer: Two Sides of the Same Coin. *J Immunol Res*. 2015;2015:983698.

159. Brown TJ, Lioubin MN, Marquardt H. Purification and characterization of cytostatic lymphokines produced by activated human T lymphocytes. Synergistic antiproliferative activity of transforming growth factor beta 1, interferon-gamma, and oncostatin M for human melanoma cells. *J Immunol.* 1987;139(9):2977-83.
160. Schreiber RD, Old LJ, Smyth MJ. Cancer immunoediting: integrating immunity's roles in cancer suppression and promotion. *Science.* 2011;331(6024):1565-70.
161. Zaidi MR, Hornyak TJ, Merlino G. A genetically engineered mouse model with inducible GFP expression in melanocytes. *Pigment Cell Melanoma Res.* 2011;24(2):393-4.
162. Ritprajak P, Azuma M. Intrinsic and extrinsic control of expression of the immunoregulatory molecule PD-L1 in epithelial cells and squamous cell carcinoma. *Oral oncology.* 2015;51(3):221-8.
163. Garcia-Diaz A, Shin DS, Moreno BH, Saco J, Escuin-Ordinas H, Rodriguez GA, et al. Interferon Receptor Signaling Pathways Regulating PD-L1 and PD-L2 Expression. *Cell Rep.* 2017;19(6):1189-201.
164. Luke JJ, Flaherty KT, Ribas A, Long GV. Targeted agents and immunotherapies: optimizing outcomes in melanoma. *Nat Rev Clin Oncol.* 2017;14(8):463-82.
165. Frederick DT, Piris A, Cogdill AP, Cooper ZA, Lezcano C, Ferrone CR, et al. BRAF inhibition is associated with enhanced melanoma antigen expression and a

more favorable tumor microenvironment in patients with metastatic melanoma. *Clin Cancer Res.* 2013;19(5):1225-31.

166. Hu-Lieskovan S, Mok S, Homet Moreno B, Tsoi J, Robert L, Goedert L, et al. Improved antitumor activity of immunotherapy with BRAF and MEK inhibitors in BRAF(V600E) melanoma. *Sci Transl Med.* 2015;7(279):279ra41.

167. Wilmott JS, Long GV, Howle JR, Haydu LE, Sharma RN, Thompson JF, et al. Selective BRAF inhibitors induce marked T-cell infiltration into human metastatic melanoma. *Clin Cancer Res.* 2012;18(5):1386-94.